nature climate change

LETTERS

PUBLISHED ONLINE: 22 SEPTEMBER 2013 | DOI: 10.1038/NCLIMATE2009

Co-benefits of mitigating global greenhouse gas emissions for future air quality and human health

J. Jason West[1]*, Steven J. Smith[2], Raquel A. Silva[1], Vaishali Naik[3], Yuqiang Zhang[1], Zachariah Adelman[1], Meridith M. Fry[1], Susan Anenberg[4], Larry W. Horowitz[5] and Jean-Francois Lamarque[6]

Actions to reduce greenhouse gas (GHG) emissions often reduce co-emitted air pollutants, bringing co-benefits for air quality and human health. Past studies[1–6] typically evaluated near-term and local co-benefits, neglecting the long-range transport of air pollutants[7–9], long-term demographic changes, and the influence of climate change on air quality[10–12]. Here we simulate the co-benefits of global GHG reductions on air quality and human health using a global atmospheric model and consistent future scenarios, via two mechanisms: reducing co-emitted air pollutants, and slowing climate change and its effect on air quality. We use new relationships between chronic mortality and exposure to fine particulate matter[13] and ozone[14], global modelling methods[15] and new future scenarios[16]. Relative to a reference scenario, global GHG mitigation avoids 0.5±0.2, 1.3±0.5 and 2.2±0.8 million premature deaths in 2030, 2050 and 2100. Global average marginal co-benefits of avoided mortality are US$50–380 per tonne of CO_2, which exceed previous estimates, exceed marginal abatement costs in 2030 and 2050, and are within the low range of costs in 2100. East Asian co-benefits are 10–70 times the marginal cost in 2030. Air quality and health co-benefits, especially as they are mainly local and near-term, provide strong additional motivation for transitioning to a low-carbon future.

Past studies have estimated that the human health co-benefits of GHG mitigation, by reducing co-emitted air pollutants, can be substantial[1,2], and when monetized, range across many studies from a small fraction of GHG mitigation costs to exceeding them[3–6]. Here we estimate the co-benefits of global GHG reductions for air quality and human health using a global atmospheric model and future scenarios. We account for the influence of international air pollutant transport on health[9], the effect of methane on global ozone[8], increases in population and susceptibility to air pollution[17], and economic growth that increases valuation. In addition to direct co-benefits of reduced co-emitted air pollutants (mainly local and immediate), we account for a second co-benefits mechanism, not previously quantified, in which slowing climate change decreases its effects on air quality (global and long-term). Climate change has been shown to increase ozone in the US and Europe (although the magnitude and patterns differ among studies), for example, through increased photochemical reaction rates and biogenic emissions, and meteorological changes, but decrease ozone in remote areas. Fine particulate matter ($PM_{2.5}$) may also increase in polluted regions, but the net effect of several influences of climate change is less clear[10–12].

Global GHG emission reductions are modelled in the Representative Concentration Pathway 4.5 (RCP4.5) scenario[18]. The four RCP scenarios represent a range of global GHG emissions[16], but as these scenarios were developed by different groups, their projections of future air pollutant emissions are inconsistent with one another[19]. Rather than comparing different RCP scenarios, we compare RCP4.5 with its associated reference scenario (REF). REF is a self-consistent representation of the future development of energy and land use, assuming an intermediate pathway for economic development and population growth, and assuming no climate policy. Regionally specific air pollutant emissions in REF were developed such that air pollutant concentrations in each world region are consistent with the assumed future economic development to 2100 (ref. 20).

Relative to REF, RCP4.5 applies a global carbon price across all economic sectors including terrestrial carbon through an efficient market, such that the 2100 CO_2 concentration decreases from 760 to 525 ppm, and anthropogenic radiative forcing stabilizes at $4.5\ W\ m^{-2}$. Air pollutant emission controls in REF are assumed to stay in place as the climate policy is implemented in RCP4.5. REF and RCP4.5 are therefore entirely consistent in their underlying assumptions, allowing differences in air pollutant emissions to be attributed uniquely to the RCP4.5 climate policy. RCP4.5 reduces GHG emissions by decreasing fossil fuel use substantially (replacing it with nuclear and renewable energy, primarily wind) and energy demand modestly, and by increasing forest cover and biofuels. Carbon capture and geologic storage grows such that it applies to nearly all electricity generation from fossil fuels and biofuels by 2100 (ref. 18).

In REF, worldwide population-weighted metrics of ozone and $PM_{2.5}$ in Fig. 1 decrease in 2100 relative to 2000. Industrialized regions reduce emissions and improve air quality throughout the century, whereas many developing regions have worse air quality in 2030 and/or 2050, before improving. Relative to REF, abating GHG emissions in RCP4.5 causes substantial reductions in ozone (8.1 ppb) and $PM_{2.5}$ ($2.4\ \mu g\ m^{-3}$) in 2100. The 2100 ozone reduction is largely (89%) due to co-emitted air pollutants, with only 11% from the change in meteorology due to climate change, and is strongly influenced by the large decrease in methane emissions in RCP4.5. Changes in meteorology produce a small increase in global average $PM_{2.5}$ relative to REF. In Fig. 2, meteorological changes in 2100 cause regional increases or decreases in $PM_{2.5}$ that are small compared with the direct effect of co-emitted air pollutants. Slowing climate change decreases ozone in some polluted regions

[1]University of North Carolina at Chapel Hill, Chapel Hill, North Carolina 27599, USA, [2]Joint Global Change Research Institute, Pacific Northwest National Laboratory, College Park, Maryland 20740, USA, [3]UCAR/NOAA Geophysical Fluid Dynamics Laboratory, Princeton, New Jersey 08540, USA, [4]US Environmental Protection Agency, Washington DC 20004, USA, [5]NOAA Geophysical Fluid Dynamics Laboratory, Princeton, New Jersey 08540, USA, [6]National Center for Atmospheric Research, Boulder, Colorado 80301, USA. *e-mail: jasonwest@unc.edu

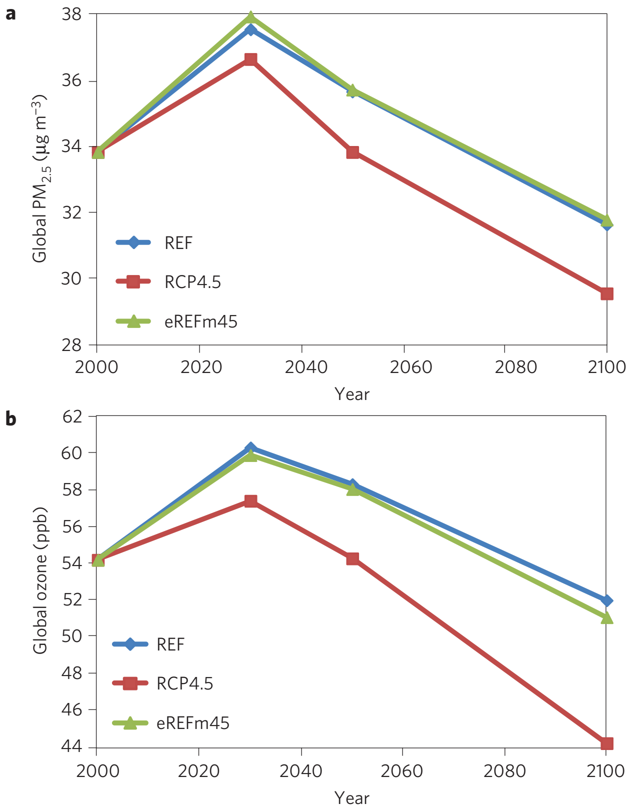

Figure 1 | Global population-weighted indicators of air quality. a, Surface annual average PM2.5. **b**, 6-month ozone-season average of 1-h daily maximum ozone. Concentrations are averaged over four model years, for the reference scenario (REF), the GHG abatement scenario (RCP4.5), and a simulation with REF emissions and RCP4.5 meteorology (eREFm45).

and over the Amazon where the increase in biogenic volatile organic compound (VOC) emissions slows; it increases ozone in many remote areas, as it slows the increase of absolute humidity and HO_x radicals that destroy ozone[10].

In REF, global air-pollution-related mortality increases in 2030 and then decreases, for both ozone and $PM_{2.5}$ (Fig. 3). In North America, mortality decreases throughout the century, whereas mortality peaks in 2030 in East Asia and in 2050 in South Asia given that air pollution controls are implemented more aggressively as economies grow. In Africa, $PM_{2.5}$ mortality peaks in 2050, but ozone mortality grows to 2100. The global co-benefits of GHG mitigation, estimated as the difference between REF and RCP4.5, total 0.4 ± 0.2, 1.1 ± 0.5 and 1.5 ± 0.6 million avoided deaths per year in 2030, 2050 and 2100 for $PM_{2.5}$, and 0.09 ± 0.06, 0.2 ± 0.1 and 0.7 ± 0.5 million for ozone. In 2030, two-thirds of the global co-benefits occur in China (Fig. 4), as it has a large population and severe energy-related air pollution; the climate policy incentivizes changes away from conventional coal for electricity and industrial heat. In South Asia, there are little co-benefits in 2030 because of a shift towards biomass combustion in RCP4.5, and local $PM_{2.5}$ increases in India due to climate change-induced meteorological changes associated with the monsoon. However, co-benefits are substantial in this region in 2050 and 2100 (0.5 ± 0.2 and 1.1 ± 0.4 million avoided deaths) as energy shifts away from fossil fuels and populations grow. In Africa, air pollution mortality increases in 2100 in REF, relative to 2000 concentrations, but deaths decrease in RCP4.5.

Co-benefits of avoided air pollution mortality are monetized using high and low values of a statistical life (VSLs), and are compared with the marginal costs of GHG reductions (the global carbon price) from 13 models meeting a $4.5\,W\,m^{-2}$ target[21]. In 2030, the monetized mortality co-benefits exceed the median carbon price in all regions but Australia; in East Asia, co-benefits are 10–70 times the median cost (Fig. 5). In 2050, global average co-benefits exceed the carbon price at both VSLs. By 2100, GHG reductions and costs increase markedly, as more expensive reduction measures are implemented, and co-benefits are within the low range of the carbon price. In 2050 and 2100, marginal co-benefits (assumed equal to the average co-benefit) are greatest in South Asia and East Asia. Marginal co-benefits are largest in regions with a high population affected by air pollution decreases, but also high in North America and Europe, reflecting high VSLs. Marginal co-benefits also do not vary strongly among time periods, but are highest in 2030 in more industrialized regions (including East Asia), because near-term reductions in air pollutant emissions leave less opportunity for co-benefits later. In less industrialized regions (for example, South Asia, Africa), co-benefits are highest in 2050 or 2100, reflecting rapid population and economic growth (increasing VSLs).

Monetized co-benefit estimates are US\$50–380 per tonne of CO_2 for the worldwide average, US\$30–600 for the US and Western Europe, US\$70–840 for China and US\$-20–400 for India (range includes differences over three years, high and low VSLs, and uncertainty in the concentration–response functions (CRFs)). These are higher than previous estimates of US\$1–128 for the US and Western Europe, and US\$6–196 for developing nations[3–5], as we use new relationships for chronic mortality, account for ozone as well as $PM_{2.5}$, model international air pollution transport and changes in global ozone from methane, and evaluate future scenarios in which population, susceptibility to air pollution, and VSLs grow. In a sensitivity analysis (Supplementary Information), we show that estimated future $PM_{2.5}$ mortality co-benefits may be substantially lower under assumptions of a log-linear CRF or a high-concentration threshold. We also show that future demographic changes (population growth, baseline mortality rates, and VSLs) have strong influences on the monetized co-benefits, particularly in 2100, and are probably an important factor in the higher co-benefits estimated here than in previous studies (Supplementary Information).

Monetized co-benefits could alternatively be evaluated as an avoided cost of air pollution controls, which would be lower than our estimates where the benefits of pollution controls exceed the costs. This approach could be estimated as the avoided air pollution controls needed to achieve air quality standards or air pollutant emission targets[22,23]. However, future air quality standards are unknown and this approach would neglect substantial health improvements from reductions below relevant standards. Future work should evaluate global co-benefits as avoided air pollution control costs, or as a combination of health benefits and avoided costs where both are evaluated relative to standards or emission targets. For example, global climate mitigation has been shown to avoid US\$100–600 billion per year in air pollution control and energy security expenditures in 2030 (ref. 24).

Co-benefits may be underestimated because we neglect people younger than 30, including effects on children and neonatal effects, and the benefits of avoided morbidity outcomes and ecosystem effects from reduced air pollution. Future work should quantify these additional air pollution co-benefits. In addition, the coarse spatial resolution of MOZART-4 probably underestimates $PM_{2.5}$ exposure in cities, and the RCP emissions omit primary inorganic $PM_{2.5}$ (fly ash), which is greatest in developing nations. We likewise neglect indoor air pollution, particularly from residential solid fuels[25], which would be alleviated by some measures in RCP4.5. We caution that applying CRFs from the US globally and into the future entails large uncertainties. Co-benefits via the effects of climate change on air quality are small compared with the reduction of co-emitted air pollutants, but we neglect effects on fires and dust, which

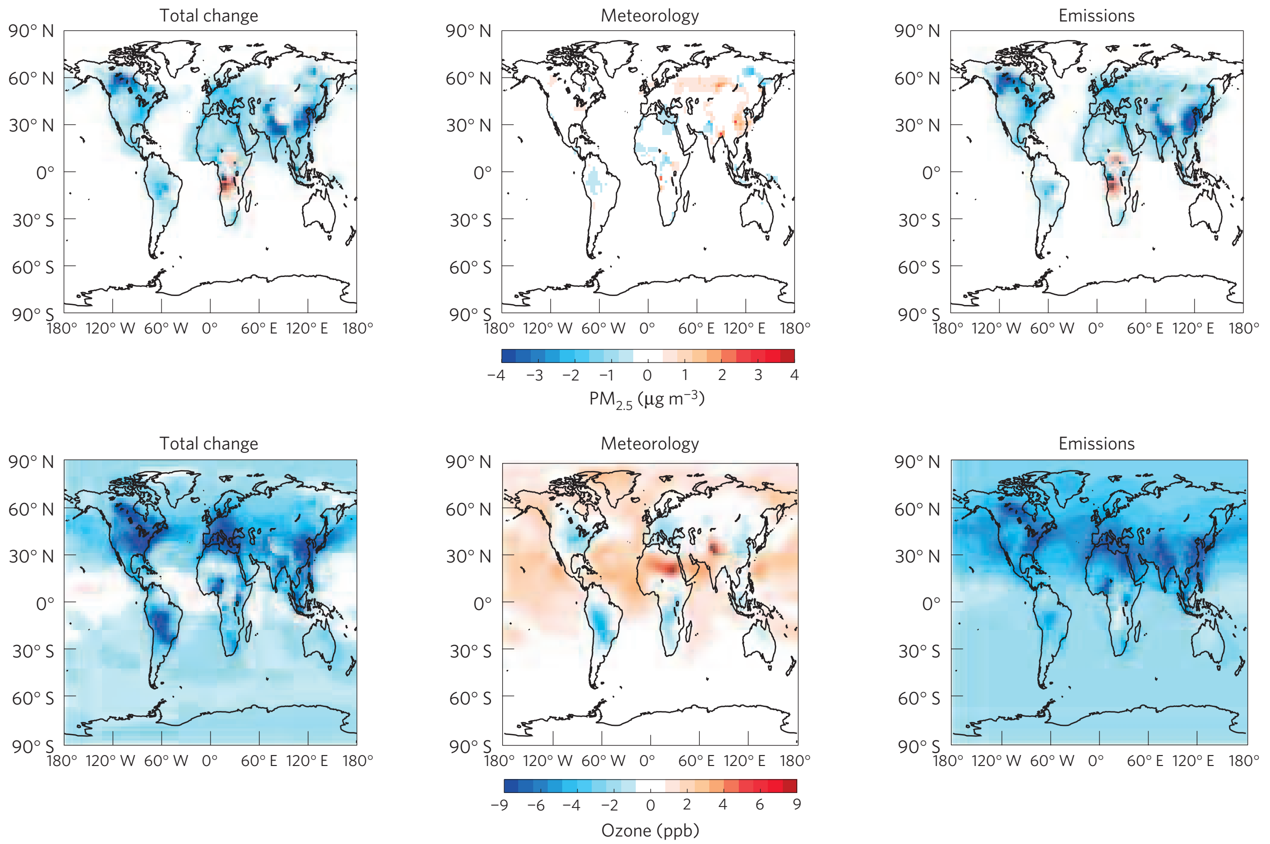

Figure 2 | Effects of GHG mitigation on annual average $PM_{2.5}$ and the 6-month ozone-season average of daily 1-h maximum ozone in 2100. Concentrations are averaged over four model years, for the total change (RCP4.5 — REF), and components due to changes in meteorology from climate change (eREFm45 — REF), and emissions (RCP4.5 — eREFm45).

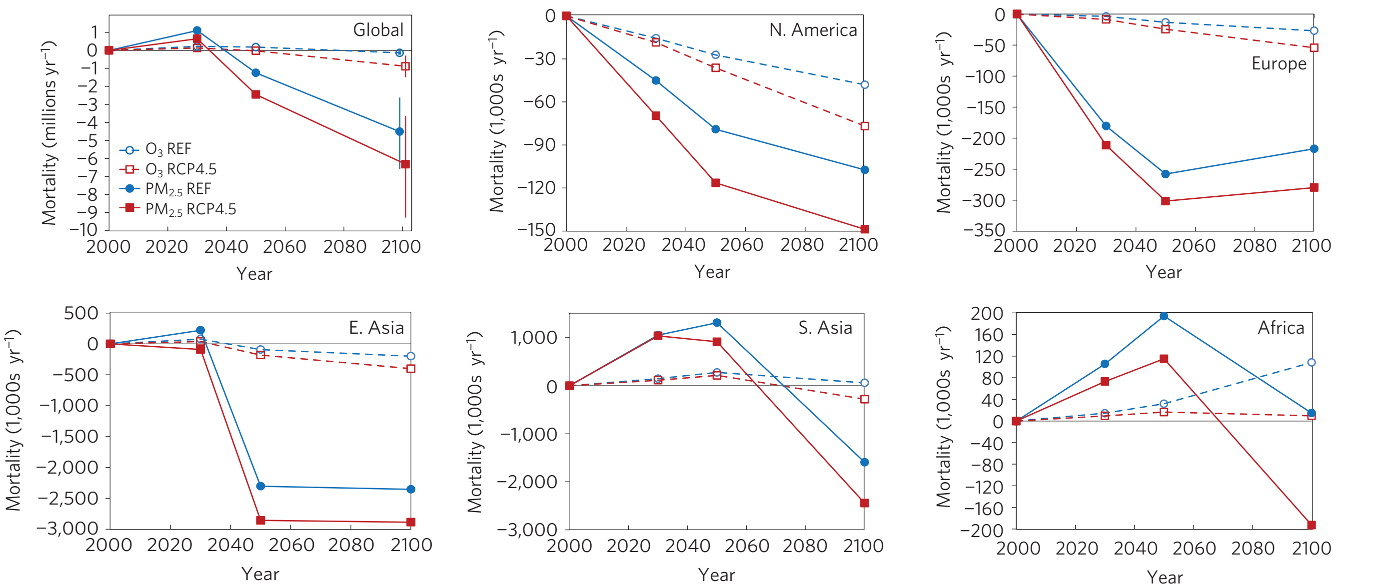

Figure 3 | Premature mortality from $PM_{2.5}$ (CPD plus lung cancer) and ozone (respiratory), evaluated for future concentrations relative to 2000 levels, in the REF and RCP4.5 scenarios, globally and in selected world regions. Co-benefits can be estimated as the difference between REF and RCP4.5. In the global panel, points in 2100 are offset horizontally to show uncertainty bars, which reflect the 95% confidence intervals on the CRFs and neglect other uncertainties.

may be substantial[26]. Co-benefits are presented for the specific reference and GHG abatement scenarios modelled here, and would differ for other scenarios. In particular, if the air pollution controls built into REF were less aggressive, there would be greater potential for co-benefits. On the other hand, REF may not be consistent with recent decreases in SO_2 emissions in China[27], which could cause an overestimate of co-benefits. Co-benefits also depend on mitigation technology choices and national participation; where lower income

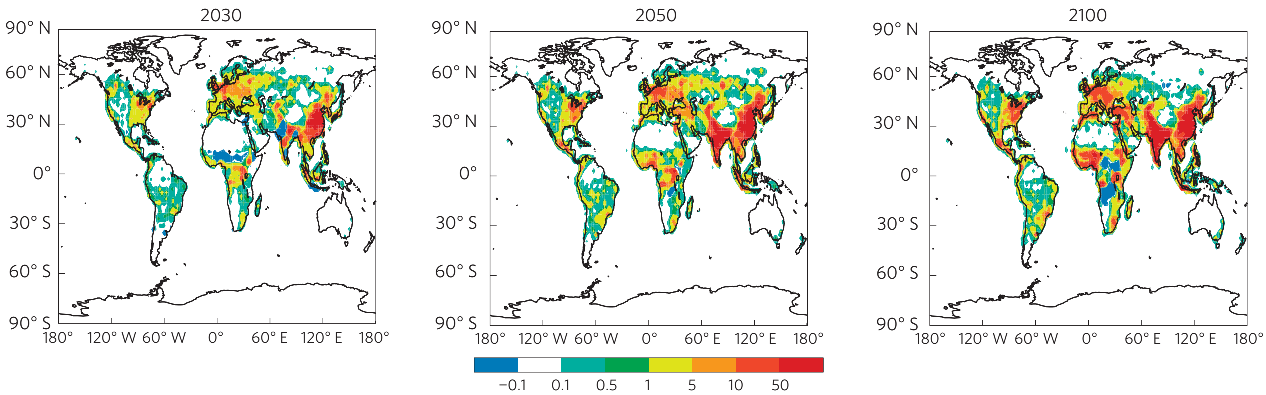

Figure 4 | Co-benefits of avoided premature mortality from $PM_{2.5}$ (CPD plus lung cancer) and ozone (respiratory) in 2030, 2050 and 2100 (deaths per year per 1,000 km^2, colour scale).

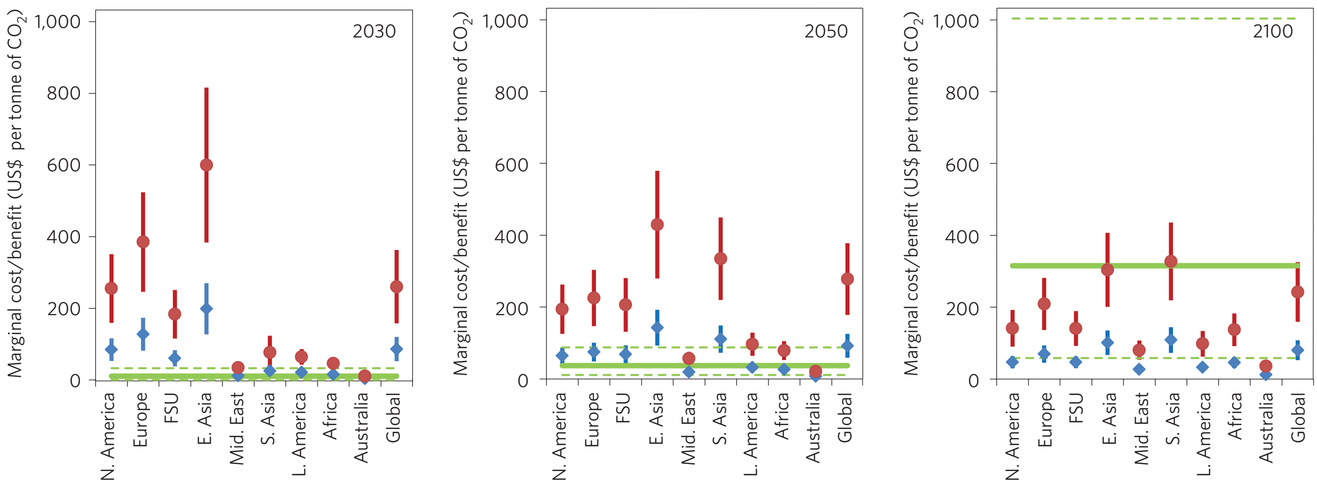

Figure 5 | Regional marginal co-benefits of avoided mortality under high (red) and low (blue) VSLs, and global marginal abatement costs (the carbon price), as the median (solid green line) and range (dashed green lines) of 13 models[21]. Marginal benefits are the total benefits (sum of ozone respiratory, $PM_{2.5}$ CPD and $PM_{2.5}$ lung cancer mortality) divided by the total CO_2 reduction, in each year under RCP4.5 relative to REF. Uncertainty in benefits reflects 95% confidence intervals on the CRFs. FSU, Former Soviet Union.

countries delay entry into a climate policy, their co-benefits would probably decrease, while overall mitigation costs increase[21].

In the global average and in many individual world regions, the co-benefits of avoided air pollution mortality can justify substantial reductions in GHG emissions, apart from other benefits of slowing global climate change. These results reflect the high premium that society places on avoiding death, through the VSLs used here. Decisions to mitigate GHG emissions should be motivated primarily by the benefits of slowing climate change, and air pollutant emission reductions by the benefits of improving air quality. However, decisions should also account for the full costs and benefits of proposed actions, as these results show the substantial air quality and health benefits of pursuing a low-carbon future. As these co-benefits occur mainly locally, in the near term, and with high certainty, they contrast with the long-term distributed global benefits of slowing climate change, and therefore may be attractive to nations considering GHG reductions. Not all individual measures would bring such co-benefits. Therefore, there is a need to investigate the air quality co-benefits of specific alternatives in specific regions, while accounting for the international impacts of air pollution and long-term effects via methane and climate change. For policy, there is a need to better coordinate actions on air quality and climate change. By addressing both problems simultaneously, they may be managed more effectively, at less cost, and with greater overall benefits.

Methods

The MOZART-4 global chemical transport model[28] is used to simulate ozone and $PM_{2.5}$ air quality in 2000, 2030, 2050 and 2100. Anthropogenic emissions inputs of many species for REF were processed through the same steps as RCP4.5, which include speciating VOCs to MOZART-4 species by matching similar species, adding monthly emissions distributions to the annual total emissions, and regridding to a $2^\circ \times 2.5^\circ$ horizontal grid used for the MOZART-4 simulations. Biogenic VOC emissions are calculated online within MOZART-4, and therefore respond to changing climate conditions. Other natural emissions are from ref. 28 and are assumed static, such that we neglect possible influences of climate change on emissions of dust, sea salt and pollutants from fires.

Meteorological inputs are from global general circulation model simulations of RCP4.5 and RCP8.5 (ref. 29) using the AM3 model. RCP8.5 climate is used as a proxy for REF climate because no climate simulations have been conducted for REF. The estimated global mean temperature change under REF is 3.6 °C in 2095 (relative to the pre-industrial), whereas it is 4.5° for RCP8.5 and 2.3° for RCP4.5, using the MAGICC climate model. Co-benefits resulting from slowing future climate change are therefore biased high, but because these co-benefits are shown to be small (Figs 1 and 2), this bias is of little importance. By simulating REF emissions with meteorology from RCP4.5 (eREFm45), we separate the influences of changes in co-emitted air pollutants from those caused by climate change. For each scenario–year combination, five meteorological years are simulated with the first used as a spinup, and the average of four years is reported here to reduce the effects of meteorological variability.

Model performance relative to observations of ozone and $PM_{2.5}$ species is comparable to other global models (Supplementary Information). Large contributions of dust made $PM_{2.5}$ estimates unrealistically large in arid regions, and so modelled dust concentrations were divided by 5 globally to roughly agree with the global surface concentrations of ref. 30. We forced dust and sea salt concentrations to be the same in all simulations as we lack confidence in the modelled responses to changes in climate for these species; this choice does not influence our mortality estimates because mortality is based on the difference in $PM_{2.5}$ between simulations. We also compared our simulated changes in regional and global average ozone and $PM_{2.5}$ concentrations in RCP4.5 in future years relative to 2000 against an ensemble of models, finding that our simulations are comparable (Supplementary Information). Concentrations in the lowest vertical coordinate are taken to represent ground-level exposure.

Premature human mortality is estimated from modelled air pollutant concentrations using the methods of ref. 15, and using CRFs based on the American Cancer Society study for chronic mortality from cardiopulmonary disease (CPD) and lung cancer for exposure to $PM_{2.5}$ (ref. 13), and chronic respiratory mortality for exposure to ozone[14]. Consistent with these studies, we evaluate premature mortality from chronic exposures for adults (30 years and older) using the annual average $PM_{2.5}$ and the six-month ozone season average of 1-h daily maximum ozone. These CRFs for cause-specific mortality are assumed to apply globally and into the future. Future population and baseline mortality rates are taken from International Futures[17], with global population growing to 9.7 billion in 2100. International Futures accounts for changing causes of baseline mortality, capturing the future increase in the fraction of deaths by respiratory and CPD causes, and therefore increased susceptibility to air pollution. We use International Futures to estimate the population and baseline rates of CPD, lung cancer and respiratory mortality for the population above 30, in each country, which is then gridded to the $2^\circ \times 2.5^\circ$ grid using a geographic information system. For gridded population, we also use the spatial distribution of present-day population at fine resolution to distribute population within each country. Mortality calculations are conducted on the $2^\circ \times 2.5^\circ$ grid used by MOZART-4.

Avoided mortality is monetized using low and high VSLs (based on 2005 VSLs of US\$1.8 million as a low value for Western Europe and US\$7.4 million for the USA), which are adjusted to different world regions and into the future using an income elasticity of 0.5 (yielding 2030 global means of US\$1.2 and US\$3.6 million; Supplementary Information). All monetary values are expressed as 2005 US dollars. As most mortality benefits are from $PM_{2.5}$ and influences of climate change on air quality are small, most avoided deaths result from co-emitted air pollutants in the same year; consequently, we simply compare marginal costs and benefits in the three modelled years, without discounting. The benefit curve with respect to CO_2 reductions is assumed to be flat, as there is little nonlinearity in the global air quality responses to changes in emissions and in the CRFs; marginal co-benefits are therefore estimated as the total co-benefits divided by the CO_2 reduction.

Received 22 April 2013; accepted 16 August 2013; published online 22 September 2013

References

1. Working Group on Public Health and Fossil Fuel Combustion Short-term improvements in public health from global climate policies on fossil fuel combustion: An interim report. *Lancet* **350,** 1341–1349 (1997).
2. Cifuentes, L., Borja-Aburto, V. H., Gouveia, N., Thurston, G. & Davis, D. L. Climate change: Hidden health benefits of greenhouse gas mitigation. *Science* **293,** 1257–1259 (2001).
3. Barker, T. *et al.* in *IPCC Climate Change 2007: Mitigation of Climate Change* (eds Metz, B., Davidson, O. R., Bosch, P. R., Dave, R. & Meyer, L. A.) 619–690 (Cambridge Univ. Press, 2007).
4. Markandya, A. *et al.* Public health benefits of strategies to reduce greenhouse-gas emissions: Low-carbon electricity generation. *Lancet* **374,** 2006–2015 (2009).
5. Nemet, G. F., Holloway, T. & Maier, P. Implications of incorporating air-quality co-benefits into climate change policymaking. *Environ. Res. Lett.* **5,** 014007 (2010).
6. Bell, M. L. *et al.* Ancillary human health benefits of improved air quality resulting from climate change mitigation. *Environ. Health* **7,** 41 (2008).
7. Task Force on Hemispheric Transport of Air Pollution *Hemispheric Transport of Air Pollution 2010, Part A. Ozone and Particulate Matter* (United Nations Economic Commission for Europe, 2010).
8. West, J. J., Fiore, A. M., Horowitz, L. W. & Mauzerall, D. L. Global health benefits of mitigating ozone pollution with methane emission controls. *Proc. Natl Acad. Sci. USA* **103,** 3988–3993 (2006).
9. Anenberg, S. C. *et al.* Intercontinental impacts of ozone pollution on human mortality. *Environ. Sci. Technol.* **43,** 6482–6487 (2009).
10. Jacob, D. J. & Winner, D. A. Effect of climate change on air quality. *Atmos. Environ.* **43,** 51–63 (2009).
11. Weaver, C. P. *et al.* A preliminary synthesis of modeled climate change impacts on US regional ozone concentrations. *Bull. Am. Meteorol. Soc.* **90,** 1843–1863 (2009).
12. Fiore, A. M. *et al.* Global air quality and climate. *Chem. Soc. Rev.* **41,** 6663–6683 (2012).
13. Krewski, D. *et al. Extended Follow-up and Spatial Analysis of the American Cancer Society Study Linking Particulate Air Pollution and Mortality* (Health Effects Institute, 2009).
14. Jerrett, M. *et al.* Long-term ozone exposure and mortality. *N. Engl. J. Med.* **360,** 1085–1095 (2009).
15. Anenberg, S. C., Horowitz, L. W., Tong, D. Q. & West, J. J. An estimate of the global burden of anthropogenic ozone and fine particulate matter on premature human mortality using atmospheric modeling. *Environ. Health Persp.* **118,** 1189–1195 (2010).
16. Moss, R. H. *et al.* Representative concentration pathways: A new approach to scenario development for the IPCC fifth assessment report. *Nature* **463,** 747–756 (2010).
17. Hughes, B. B. *et al.* Projections of global health outcomes from 2005 to 2060 using the International Futures integrated forecasting model. *Bull. World Health Organ.* **89,** 478–486 (2011).
18. Thomson, A. M. *et al.* RCP4.5: A pathway for stabilization of radiative forcing by 2100. *Climatic Change* **109,** 77–94 (2011).
19. Van Vuuren, D. *et al.* The representative concentration pathways: An overview. *Climatic Change* **109,** 5–31 (2011).
20. Smith, S. J., West, J. J. & Kyle, P. Economically consistent long-term scenarios for air pollutant and greenhouse gas emissions. *Climatic Change* **108,** 619–627 (2011).
21. Clarke, L. *et al.* International climate policy architectures: Overview of the EMF 22 International Scenarios. *Energy Econom.* **31,** S64–S81 (2009).
22. Burtraw, D. *et al.* Ancillary benefits of reduced air pollution in the US from moderate greenhouse gas mitigation policies in the electricity sector. *J. Environ. Econ. Manage.* **45,** 650–673 (2003).
23. Van Vuuren, D. P. *et al.* Exploring the ancillary benefits of the Kyoto Protocol for air pollution in Europe. *Energy Policy* **34,** 444–460 (2006).
24. McCollum, D. L. *et al.* Climate policies can help resolve energy security and air pollution challenges. *Climatic Change* **119,** 479–494 (2013).
25. Wilkinson, P. *et al.* Health and climate change 1: Public health benefits of strategies to reduce greenhouse-gas emissions: Household energy. *Lancet* **374,** 1917–1929 (2009).
26. Pechony, O. & Shindell, D. T. Driving forces of global wildfires over the past millennium and the forthcoming century. *Proc. Natl Acad. Sci. USA* **107,** 19167–19170 (2010).
27. Klimont, Z., Smith, S. J. & Cofala, J. The last decade of global anthropogenic sulfur dioxide: 2000-2011 emissions. *Environ. Res. Lett.* **8,** 014003 (2013).
28. Emmons, L. K. *et al.* Description and evaluation of the Model for Ozone and Related chemical Tracers, version 4 (MOZART-4). *Geosci. Model Develop.* **3,** 43–67 (2010).
29. Lamarque, J. F. *et al.* The Atmospheric Chemistry and Climate Model Intercomparison Project (ACCMIP) overview and description of models, simulations and climate diagnostics. *Geosci. Model Develop.* **6,** 179–206 (2013).
30. Brauer, M. *et al.* Exposure assessment for estimation of the global burden of disease attributable to outdoor air pollution. *Environ. Sci. Technol.* **46,** 652–60 (2012).

Acknowledgements

This publication was financially supported by the US Environmental Protection Agency STAR grant #834285, the Integrated Assessment Research Program in the US Department of Energy, Office of Science, the National Institute of Environmental Health Sciences grant #1 R21 ES022600-01, fellowship SFRH/BD/62759/2009 from the Portuguese Foundation for Science and Technology (to R.A.S.), and an EPA STAR Graduate Fellowship (to M.M.F.). Its contents are solely the responsibility of the grantee and do not necessarily represent the official views of the USEPA or other funding sources. USEPA and other funding sources do not endorse the purchase of any commercial products or services mentioned in the publication. NCAR is operated by the University Corporation of Atmospheric Research under sponsorship of the National Science Foundation. We thank the National Oceanographic and Atmospheric Administration for computing resources, L. Emmons for MOZART-4 guidance, and G. Characklis.

Author contributions

J.J.W. and S.J.S. conceived of the study. J.J.W., J-F.L., Z.A. and M.M.F. prepared emissions inputs, and V.N. and L.W.H. prepared meteorological inputs. J.J.W. conducted the MOZART-4 simulations, and J.J.W., Y.Z., Z.A. and M.M.F. analysed MOZART-4 output. R.A.S., J.J.W., S.A. and Y.Z. analysed human mortality. Economic valuation was conducted by J.J.W., S.J.S. and S.A. J.J.W. wrote the paper and all co-authors commented on it.

Additional information

Supplementary information is available in the online version of the paper. Reprints and permissions information is available online at www.nature.com/reprints. Correspondence and requests for materials should be addressed to J.J.W.

Competing financial interests

The authors declare no competing financial interests.

nature climate change
SUPPLEMENTARY INFORMATION
DOI: 10.1038/NCLIMATE2009

Co-benefits of mitigating global greenhouse gas emissions for future air quality and human health

J. Jason West, Steven J. Smith, Raquel A. Silva, Vaishali Naik, Yuqiang Zhang, Zachariah Adelman, Meridith M. Fry, Susan Anenberg, Larry W. Horowitz, Jean-Francois Lamarque

Supplementary Information:
Methods and Additional Results
Figures S1-S34
Tables S1-S13

1. Emission Scenarios

The goal of this work is to estimate the changes in pollutant concentrations and associated health outcomes resulting as a consequence of the pollutant emission reductions that occur as a co-benefit of a climate policy. It is important, therefore, that we use scenarios where the only change between the two scenarios is due to a climate policy. We, therefore, examine two scenarios that were developed by an integrated assessment model, the Global Change Assessment Model (GCAM), and which differ only by the application of a climate policy.

GCAM simulates energy consumption in 14 world regions, disaggregated into general end-use and transformation categories (e.g., buildings, industry, transportation, electric power generation, liquid fuel refining, agricultural crop production, beef and dairy production). Online documentation is provided at http://wiki.umd.edu/gcam/. Details on emissions for the GCAM reference case and RCP4.5 are available at http://www.globalchange.umd.edu/gcamrcp/.

The GCAM reference scenario (REF) represents a self-consistent pathway of socio-economic and technological development over the 21st century. REF represents a world where global incomes increase substantially over the 21st century, with global GDP increasing by a factor of ten[1]. Population increases by 40%, a slight decline after a peak of 9 billion after mid-century, and primary energy use triples. GDP per capita (Figure S1) increases over the century such that most world regions are near current OECD levels by the end of the century. The one exception is Africa, where GDP per capita is still lower than current OECD levels by the end of the century. Africa is starting from a much lower income at present than other world regions, and current economic growth is much lower than, for example, India and China.

REF and RCP4.5 are unique among the RCP scenarios in that global atmospheric modeling (MOZART-2) was used iteratively in the scenario development process to ensure consistency between economic development and air pollutant concentrations among many world regions into the future. This is described by Smith et al.[2], and a brief summary is given here. The GCAM model scenario provides energy consumption by broad technology class, which combined with assumptions for air pollutant emission controls, results in projected air pollutant emissions over time. Air pollutant emissions control assumptions were developed through a general "pseudo-

Kuznets" approach whereby pollutant emissions controls are assumed to increase as a function of income[3-5], although not necessarily with identical assumptions across regions. Smith et al.[2] used the MOZART-2 model to examine the resulting surface pollutant concentrations over time in three snapshot years: 2005, 2050, and 2095. Two rounds of analysis were conducted on preliminary scenarios, and regional pollutant emission coefficients were adjusted, particularly in Asia, so that surface pollutant concentrations were consistent with assumed income levels. Through this procedure, the resulting REF scenario has a consistent, long-term relationship between pollutant concentrations and regional incomes. A detailed description of the aerosol emissions of this REF scenario is also available in Smith and Bond[6].

Air pollutant emissions in the GCAM scenarios represent state of the art long-term emissions projections. Emissions for several species in the two GCAM scenarios used here are compared to results in the literature in Figure S2. These emissions also compare favorably to near-term projections, as addressed in the 2010 HTAP assessment[7]. Emissions are generally lower than emissions in the SRES scenarios, which did not contain, for example, the impact of emission controls for ozone precursor emissions[5].

The RCP4.5 scenario was developed from the REF scenario by applying a global carbon price to all world regions and all sectors including carbon in terrestrial systems. This results in a shift in technology choices away from carbon intensive fuels toward less carbon intensive technologies. These shifts happen throughout the energy system, from energy production and transformation to end-use technologies in buildings, transportation, and industry. Carbon dioxide capture and geologic sequestration (CCS) is utilized as a low carbon energy transformation option. The use of biomass energy together with CCS (BECCS) results in net negative emissions. The carbon price on terrestrial systems incentivizes the preservation and enhancement of carbon in soils and vegetation, including net reforestation globally. These system-wide transformations increase the price of energy, which also causes a small decrease in energy service demands. These scenarios are described in greater detail by Clarke et al.[1], Thomson et al.[8], and references therein.

The RCP4.5 scenario used here is one of four scenarios released in support of community modeling activities. The aim of the RCP process was to provide, over a relatively quick time-frame, a set of four scenarios that span the range of potential future radiative forcing. It is important to note, as discussed by van Vuuren et al.[9], that the RCP scenarios do not form a consistent set relative to each other. The RCP8.5 scenario, for example, is not a reference scenario relative to the other scenarios. The scenarios were developed by different groups, and their projections of future air pollutant emissions are not consistent with one another. Rather than comparing different RCP scenarios, we compare a single RCP scenario (RCP4.5) with its associated reference case (REF), both produced by the same integrated assessment model. Because we focus on the RCP4.5 scenario, we also compare our modeled RCP4.5 global air pollutant concentrations in future years with those from other global atmospheric models.

2. Atmospheric Modeling Methods

2.1. Scenarios and emissions inputs

Anthropogenic emissions for the year 2000 simulation are described by Lamarque et al.[10]. Emissions for RCP4.5 are described by Thomson et al.[8]. Emissions for RCP4.5 were downloaded at 0.5° resolution from the RCP website (http://www.iiasa.ac.at/web-apps/tnt/RcpDb/) for the years 2030, 2050, and 2100. We likewise use RCP4.5 emissions for 2000 in the year 2000 simulation, as 2000 is before emissions start to diverge among the RCP scenarios, and there are only very small differences between the "historical" 2000 emissions and the RCP4.5 year 2000 emissions.

Emissions for REF were prepared for this project following the same steps as the reported emissions for RCP scenarios, including the same resolution, source categories, and speciation of volatile organic compounds (VOCs). Anthropogenic emissions for the 2000, REF, and RCP4.5 simulations include emissions of VOCs, nitrogen oxides (NO_x), sulfur dioxide (SO_2), carbon monoxide (CO), ammonia (NH_3), and primary black carbon (BC) and organic carbon (OC) aerosols. Emissions are reported for each of several anthropogenic emissions categories: surface transportation, shipping, aviation, energy, solvents, waste, industry, residential and commercial, agriculture waste burning, agriculture, savanna burning, and land use change (forest burning).

These emissions were processed by speciating VOCs to MOZART-4 species by matching similar species, and monthly emissions distributions were added to the reported global totals by scaling to the RETRO emissions database, separately for each pollutant, source category, and grid cell, as documented by Fry et al.[11]. Emissions of BC and OC were multiplied by factors of 1.15 and 1.4, respectively, to account for the ratio of $PM_{2.5}$ primary emissions to the PM_1 emissions in the original emissions source[12] used for RCP emissions[10], following Anenberg et al.[13]. Biogenic VOC emissions are calculated online using the MEGAN model[14-16], and respond to future climate change. Other natural emissions are taken from Emmons et al.[16] and are assumed static. MOZART-4 simulations used fixed global methane concentrations corresponding to the time history of emissions (Table S1): the year 2000 was based on direct observations; RCP4.5 used the same values used by RCP (CMIP5) models, and based on MAGICC6[17]; and REF used MAGICC5.3[8]. All emissions were regridded from the original 0.5°x0.5° resolution to the MOZART-4 grid of 2°x2.5°. Global anthropogenic emissions are presented in Table S1. Table S2 shows CO_2 emissions reductions in RCP4.5 relative to REF.

2.2 MOZART-4 simulations

MOZART-4 simulations are conducted at a horizontal resolution of 2°x2.5° and 38 vertical layers extending to 2 mb. Meteorological inputs to MOZART-4 were generated by the NOAA Geophysical Fluid Dynamics Laboratory atmospheric GCM (AM3)[18] simulations of RCP4.5 and RCP8.5 conducted for ACCMIP[19]. RCP8.5 was used as a proxy for REF climate, since no GCM conducted future climate simulations for REF emissions. The AM3 simulations had fixed sea-surface temperature and fixed emissions over several model years, reflecting conditions present in 2000, 2030, 2050, and 2100, and the simulations responded to all anthropogenic forcings including both long-lived greenhouse gases and short-lived forcings such as ozone and aerosols.

MOZART-4 was run for 5 meteorological years for each scenario-year combination, using the first year as a spinup and the average concentrations over four meteorological years are reported here to reduce interannual variability. The lowest modeled level from MOZART-4 (extending to approximately 58 m above the surface) is taken to indicate ground-level concentrations.

$PM_{2.5}$ is calculated from MOZART-4 output as 1.375*SO4 + 1.29*NO3 + BC + 1.4*OC + 0.2*Dust + Sea Salt, where all of SO4, NO3, BC, and OC are assumed to exist in the $PM_{2.5}$ size fraction. SO4 and NO3 are assumed to exist as $(NH_4)_2SO_4$ and NH_4NO_3 (the factors 1.375 and 1.29 account for the NH_4). OC includes both primary OC and secondary organic aerosol, and is multiplied by 1.4 to account for species other than carbon. For dust and sea salt, only the size fractions relevant for $PM_{2.5}$ (size bins 1-3) are used. Dust in desert regions was found to be too high in the model, so global dust concentrations were multiplied by 0.2 to achieve rough consistency with the $PM_{2.5}$ concentrations estimated by Brauer et al.[20]. This correction is done to present plausible $PM_{2.5}$ concentrations in dusty regions, and does not affect the calculation of mortality, which is based on the change in $PM_{2.5}$ between scenarios, for the base mortality estimates. Dust and sea salt are assumed not to change between years and scenarios, neglecting possible influences of climate change or human disturbances on these species. Similarly, we neglect possible changes in fire and wetland emissions due to climate change.

Within MOZART-4, the MEGAN model estimates biogenic VOC emissions, and responds to changes in climate. We assume that forest cover is constant over the period modeled for simplicity. Modeled biogenic emissions therefore do not incorporate the decrease in forest cover in the REF scenario, nor the increase in RCP4.5 relative to REF[8].

For the air pollution mortality estimates, ozone and $PM_{2.5}$ surface concentrations are summarized using metrics consistent with those in the epidemiological studies used here[21,22], as shown in Figure 1 of the main paper. For $PM_{2.5}$, this is the simple annual average. For ozone, it is the 6-month ozone season average of the 1-hr daily maximum ozone concentration. Since ozone seasons vary around the world, we find the ozone season in each grid cell as the highest consecutive 6-month period of 1-hr. daily maximum ozone.

2.3 Experimental design

The experimental design is shown in Table S3. By simulating REF emissions together with meteorology from RCP4.5 (referred to as eREFm45), and by simulating RCP4.5 emissions together with RCP8.5 meteorology (e45m85, only simulated in 2050), we separate the influences on air quality of changes in co-emitted air pollutants from those caused by climate change.

As in Figure 2 of the main paper, the total air quality changes from GHG mitigation are estimated as RCP4.5 minus REF. Changes in air quality due to emissions changes alone are RCP4.5 minus eREFm45. Changes due to meteorological changes (climate change) alone are eREFm45 minus REF. The additional simulation (e45m85) gives another means of identifying the air quality changes due to emissions changes alone (e45m85 minus REF) or due to meteorological changes alone (RCP4.5 minus e45m85). Since the air quality changes due to meteorology are estimated to be small and e45m85 is very similar to RCP4.5, we do not present e45m85 results in the main paper.

3. Atmospheric model performance evaluation

The MOZART-4 simulation for 2000 is compared against selected observations of key pollutants. The performance evaluation overall shows that MOZART-4 performance is comparable to other global atmospheric models. Here the performance of MOZART-4 is limited because the meteorological inputs reflect simulated conditions rather than reconstructions of historical meteorology. We have previously evaluated similar MOZART-4 simulations that use meteorology from the GEOS-5 reanalysis for 2004-2006, and emissions from the RCP8.5 scenario for 2005[11], finding that performance is comparable.

Figures S3 and S4 compare modeled ozone above the surface against ozonesonde observations at nine representative locations[23]. We compare modeled ozone at the surface in the United States with observations from CASTNET (Figure S5), and in Europe with observations from EMEP (Figure S6). The model shows a high bias for ozone in the summer in parts of the US (Great Lakes and Northeast), as has been observed for other global models, and less bias in Europe. Figures S7-S12 show comparisons of surface concentrations of $PM_{2.5}$ species relative to observations from the IMPROVE network in the US and from EMEP in Europe. The comparison shows rather good agreement, but a tendency to overestimate ammonium nitrate. Note that the importance of model biases is reduced in that we focus on differences between the REF and RCP4.5 scenarios.

We also compare the results of our future simulation of RCP4.5 with those from an ensemble of chemistry climate models in ACCMIP, focusing on annual average changes in surface concentrations of ozone and $PM_{2.5}$ with respect to the year 2000, globally and in each of 9 world regions. Fiore et al.[24] reported annual average concentration changes relative to the average of two decades (1980s and 2000s), but we have updated the ACCMIP model results to include more models and to only evaluate relative to the 2000s for better agreement with the 2000 simulation here. Figures S13-S15 show the comparison of our MOZART-4 results relative to the 2000 simulation with the mean and full range of ACCMIP models. For ozone, our simulations are clearly within the range of ACCMIP models, although with greater future decreases relative to 2000 than the ACCMIP multi-model mean. For $PM_{2.5}$, we show results for a comparison with 3 models that report the total $PM_{2.5}$ (each model used its own formula to calculate total $PM_{2.5}$) (Figure S14), and 5 models for which we calculated total $PM_{2.5}$ as a sum of reported species (Figure S15). Results suggest good agreement, and do not indicate that our simulations are an outlier.

4. Modeled pollutant concentrations in future scenarios

Emissions in 2000 and in REF and RCP4.5 are shown in Figures S16-S21. We comment here on a few patterns of emissions changes that may seem contradictory.

1) In India in 2030 and 2050, RCP4.5 has higher emissions of OC and CO than does REF. This is a result of the increased combustion of biomass as a GHG mitigation strategy, in the

residential, industrial, and electricity generation sectors. Beyond 2050, this consumption of biomass shifts to sectors that use CCS, such as electricity generation[25].

2) In Western Canada there is a large increase in emissions of many species (except SO_2) in REF, as a result of forest fires related to deforestation. These emissions are decreased in RCP4.5 as the climate policy slows deforestation to preserve carbon in the forest. This leads to large air quality improvements in this region in RCP4.5 with respect to REF (though with small effects on mortality co-benefits as population is small).

3) Emissions of OC, BC, and CO in Central Africa increase in RCP4.5 relative to REF in 2100. This is a result of decreases in deforestation (and reforestation) in RCP4.5, which decrease emissions from forest burning, but also increase burning in savannas in RCP4.5. The emissions pattern reflects these changes in forest and savanna land.

4) Emissions of NMVOCs in the Middle East increase in RCP4.5 relative to REF in 2100. In REF, much of the low-cost conventional oil reserves have been exploited by 2100, causing oil production to decrease toward 2100. With the climate policy in RCP4.5, oil is exploited more slowly, and consequently, oil production is greater in RCP4.5 in 2100 than in REF, leading to greater NMVOC emissions.

Pollutant concentrations (and health impacts below) are summarized for the 14 world regions used by the GCAM model (Figure S22). Modeled ozone and $PM_{2.5}$ concentrations are shown in Figures S23-S29. Figure S23 reproduces Figure 1 from the main paper, but includes a point in 2050 for the e45m85 simulation. Since the air pollutant changes via changes in climate are small (as estimated from eREFm45 minus REF), and because e45m85 gives results very similar to RCP4.5, we omitted e45m85 from the main paper.

Biogenic VOC emissions are one of the driving forces for changes in air quality due to climate change. Figure S30 shows global isoprene emissions as calculated online by MEGAN within MOZART-4, also including a small component of anthropogenic emissions. In Figure S30, biogenic emissions grow due to future climate change, but are reduced under RCP4.5 relative to REF.

5. Methods for analysis of premature mortality

Global chemical transport models have been used previously to drive several assessments of premature human mortality[26-37]. These methods typically use coarse horizontal grid resolution, which would be expected to underestimate exposure to $PM_{2.5}$ in urban areas, as population and emissions tend to be localized around urban areas that are smaller than the typical grid cell size of global models. While ozone mortality also likely has error because of coarse grid resolution, it is less clear whether this would likely be an under- or overestimate[38].

We focus on premature mortality, as deaths hastened by air pollution typically dominate assessments of the total monetized benefits of actions to reduce air pollution[39]. In doing so, we neglect other effects of air pollution on morbidity outcomes. Following Anenberg et al.[33], we assess premature mortality attributed to outdoor air pollution using relative risk estimates from reanalyses of the American Cancer Society study in the US. For $PM_{2.5}$, the relative risks used for cardiopulmonary and lung cancer mortality are 1.128 (95% C.I.: 1.077–1.182) and 1.142 (95% C.I.: 1.057–1.234), respectively, for a 10 μg m^{-3} increase in $PM_{2.5}$[21], and for ozone, the relative risk for respiratory mortality is 1.040 (95% C.I.: 1.013-1.067) for a 10 ppb increase[22]. To be consistent with these epidemiological studies, we limit our analysis to adults aged 30 and above.

We apply concentration-response functions from the US to the rest of the world, as available studies of the effects of ozone and $PM_{2.5}$ on mortality outside of the US are broadly consistent[40-42], and concentration-response relationships are not strongly dependent on sex, age, or race[21,22,43]. We assume that these relationships also hold in the future. We estimate cause-specific mortality rather than all-cause mortality in order to reduce error when estimating mortality outside of the US or in the future, where the baseline causes of death differ.

Deaths from ozone and $PM_{2.5}$ are added, as was done by Anenberg et al.[36] and Shindell et al.[37], and supported by Krewski et al.[44]. We use relative risks for ozone from Jerrett et al.[22] that control for $PM_{2.5}$, and both Krewski et al.[21] and Jerrett et al.[22] reported that $PM_{2.5}$-related mortality was dominated by cardiovascular mortality while ozone was primarily associated with respiratory mortality. We therefore justify our choice of adding mortality from ozone and $PM_{2.5}$, but in doing so, it is possible that we may be partially double-counting deaths. Finally, we assume that the concentration-response function holds over the full range of possible concentrations, with no high-concentration or low-concentration thresholds. We do not use thresholds in the main paper, as the current epidemiology literature does not provide clear evidence for thresholds[21,22,45,46]. However, we evaluate the sensitivity of our results to a low-concentration threshold, as air pollution decreases in REF to 2100. High concentrations are most important for $PM_{2.5}$, as it is more variable than ozone. For $PM_{2.5}$, the highest concentrations are typically found in dusty regions, and recent research has suggested that the slope of the exposure-response relationship may flatten at higher concentrations[47,48]. If this research is correct, we would overestimate mortality from changes in $PM_{2.5}$ in regions with high concentrations. Later, we evaluate the sensitivity of our results to alternative functions for $PM_{2.5}$ mortality.

Air pollution-related mortality ($\Delta Mort$) is evaluated in each grid cell and year as:

$$\Delta Mort = y_0 \, (1 - exp^{-\beta \Delta X}) \, Pop \qquad (1)$$

Where y_0 is the baseline mortality rate, β is the concentration-response factor (derived from the relative risk as $RR = exp^{\beta \Delta X}$), ΔX is the change in air pollutant concentration for ozone or $PM_{2.5}$ (relative to counterfactual concentrations), and Pop is the population (here, of adults above 30 years of age). In Figure 3 of the main paper, we show results where ΔX is calculated for future years relative to 2000 concentrations. This emphasizes the effects of changes in air pollution through time. For evaluating co-benefits, we estimate ΔX for REF minus RCP4.5 in the same year. Since Equation 1 is slightly nonlinear, the results are slightly different compared to if we had estimated mortality for ΔX =REF-2000 and ΔX =RCP4.5-2000, and then took the difference.

Future global population and baseline incidence of mortality for cardiopulmonary disease, respiratory disease and malignant neoplasms are taken from International Futures (IFs) projections of cause-specific mortality, which are stratified by age group for each country[49-51]. We downloaded IFs projections from http://www.ifs.du.edu/ifs/index.aspx in July 2012, using IFs version 6.54 and the UNEPGEO Base Case scenario. Total population is shown in Table S4. We divide cause-specific mortality for population aged 30 and above by the population (also 30 and above) in each country to estimate the baseline mortality rates (Table S5). Baseline mortality rates for lung cancer were estimated using the ratio of lung cancer to total malignant neoplasms from WHO cause-specific mortality estimates in each country for 2000-2008, substituting regional rates for 2008 when country rates were not available[52,53]. This ratio was then assumed to be constant in the future and applied to the total malignant neoplasms in each country projected by IFs. Baseline mortality rates in each country for population aged 30 and above were gridded to 0.5°x0.5° resolution using ArcGIS10 geoprocessing tools, accounting for grid cells that span multiple nations, and were then regridded to the MOZART-4 modeling grid (2°x2.5°).

In Table S5, the global average respiratory mortality rates in the IFs more than double from the present to 2100, which contributes to higher ozone-related mortality than if we had used present-day mortality rates to 2100. Similarly, the cardiopulmonary mortality rates increase markedly to 2100, while small decreases are seen in lung cancer mortality rates.

For global population, we select IFs rather than the GCAM scenario for RCP4.5 (and REF), so that population is consistent with the baseline mortality rates, and because the IFs provide population and age distributions in each country that change in the future. As IFs population is greater than that for RCP4.5, differing by about 1 billion people in 2100 (Table S4), the estimated co-benefits of avoided mortality are greater than had we used the RCP4.5 population. Estimates of national population (30 and above) in 2030, 2050 and 2100 from IFs were used, and the LANDSCAN High Resolution Global Population Data Set[54] (www.ornl.gov/sci/landscan/) for the present day (2008) was used to provide the distribution of population within each nation. Similar GIS processing to that described above for the baseline mortality rates was used to produce the final population fields on the MOZART-4 atmospheric modeling grid. We assume that population aged 30 or above has the same spatial distribution as total population in each nation. Also, we do not account for future changes in population distribution within each nation; this is consistent with the emissions for REF and RCP4.5, which assume that anthropogenic emission distributions within each nation do not change in the future[8].

6. Methods for valuation of premature mortality

Valuation of avoided mortality follows the approach of the US Environmental Protection Agency[39], as reviewed by the US National Academy of Sciences[55], in which premature deaths within a society are valued equally. Accordingly, we do not attempt to value mortality based on the life-years lost.

We have previously argued that methane reductions benefit ozone air quality globally, and therefore methane reductions should be evaluated as a global policy. As such, we argued that a single value of a statistical life (VSL) should be applied globally, since for a global policy, it would be ethically problematic to use different VSLs for people in different countries[26,35]. For the present study, however, the majority of the mortality effects result from emissions within the same nation or world region. This is the case as most avoided deaths result from $PM_{2.5}$, which has a rather short atmospheric lifetime, as emissions of $PM_{2.5}$ and its precursors mainly influence mortality within the same world region[31]. Likewise, the influence of meteorology on air quality (via climate change) is significantly smaller than the influence via co-emitted air pollutants. Health benefits therefore reflect mainly domestic changes in emissions that occur within the same year. As such, it is appropriate here to use different VSLs for different regions, reflecting the different economic circumstances of each region, and willingness to pay to avoid health risks. Consequently, we value avoided mortality based on VSLs appropriate for each region to estimate monetized benefits within each region, and then combine to a global total. This approach is similar to that of Shindell et al.[37].

We value mortality in each of the 14 regions used in the GCAM global energy-economics model (Fig. S22), since we have economic growth projections for each region. Relative to a benchmark present-day (2005) VSL in a single region, 2005 VSLs in all other regions are calculated using their current GDP per capita values and an income elasticity of 0.5[56]. Similarly, regional VSLs in future years are calculated relative to the benchmark VSL, using the same elasticity. As a high estimate of the VSLs, we use as a benchmark the US EPA's suggested $7.4 million for the US[57]. The OECD[58] suggests a range of $1.8 million to $5.4 million for application to the EU-27 nations; we use $1.8 million for Western Europe as the benchmark low estimate. Resulting VSLs in each region and year are shown in Table S6. As a sensitivity exercise, we also value mortality using a uniform global VSL, given by the last row of Table S6. Monetized benefits using different VSLs can be obtained by simply scaling benefits to a different choice of 2005 VSL.

All monetary values in this study are in 2005 US dollars.

Marginal costs of the climate policy are simply the price of CO_2 reductions provided by a multi-model comparison study that included results from 13 models (including GCAM) for a 4.5 W m^{-2} radiative forcing target[59]. Since GCAM assumes (as do the other 12 models) that GHG reductions are achieved through a global GHG market, the same global carbon price applies in each world region in any year.

For marginal benefits, we divide the total monetized benefits of avoided deaths in a single year (2030, 2050 or 2100) by the total CO_2 reduction in that same year, in each of the 14 regions. We assume that the benefit curve with respect to CO_2 reductions is flat, such that the average benefit is equal to the marginal benefit. Since GCAM runs in 15-year increments, this requires interpolation or extrapolation to estimate VSLs and CO_2 reductions in 2030 and 2100, which we do by simple linear interpolation of the nearest time points. This approach of simply dividing benefits by emission reductions in a single year is justified by the fact that short-term co-benefits by co-emitted air pollutants dominate the total. This approach does not accurately reflect the long-term elements of the co-benefits – those via methane's effects on ozone, and through the second co-benefits mechanism of slowing the effects of climate change on air quality – since by these mechanisms, emissions reduced in a single year would create benefits spread over several years. Consequently, for 2030 (for example), we omit a small fraction of benefits of the 2030 emissions reductions occurring in future years, but we would also account for a small fraction of benefits that occur in 2030 from emission reductions in previous years. Because of this and because we have only modeled three years in the future, we do not attempt to discount future costs and benefits back to present-day net present values. For more on methods for dealing with the long-term components of co-benefits, see West et al.[26,35].

7. Results for health impacts analysis and valuation

Results for health impacts and valuation are shown in Figures S31-S34.

Figure 5 of the main paper shows monetized co-benefits for 9 world regions and the global average. Here we convert from the 14 world regions used by GCAM to 9 regions by combining regions as follows: N. America = Canada + USA; Europe = W. Europe + E. Europe; E. Asia = China + S. Korea + Japan; S. Asia = India + SE Asia. We combine these regions to avoid error in estimates of mortality within nation boundaries for small regions (e.g., S. Korea), and for the transparency of summarizing results for fewer regions. Premature deaths and monetized co-benefits were estimated for the 14 regions initially (using the VSL appropriate for each region) before combining together to 9 regions.

Table S7 show mortality results for ozone presented in the main paper, with no low-concentration threshold, and the sensitivity of the results to a low-concentration threshold of 33.3 ppb, which is the lowest measured level of ozone in the ACS study[22]. For $PM_{2.5}$, we evaluate the sensitivity of our results to a low-concentration threshold of 5.8 $\mu g\ m^{-3}$ (the lowest measured level in ACS[21]). Because the concentration-response function for $PM_{2.5}$ may flatten at higher concentrations[47,48], we also evaluate sensitivity for a log-linear function (using the function and risk coefficients for ACS reported by Evans et al.[60]), and for a high-concentration threshold of 30 $\mu g\ m^{-3}$ (Tables S8-S10).

For both ozone and $PM_{2.5}$, results with the low-concentration threshold are only modestly smaller in the global average, but are significantly smaller in some individual regions, including Canada, the US, Latin America, and Australia, especially in 2050 and 2100. These regions have less air pollution than the global average, and improvements in air quality in REF and RCP4.5 cause parts of these regions to have air pollutant concentrations below the thresholds. In contrast, applying a threshold has very little influence on estimated mortality in very polluted regions.

In Tables S8-S10, applying a high-concentration threshold significantly reduces $PM_{2.5}$ mortality in highly polluted regions. In the Middle East, the high-concentration threshold causes estimated mortality co-benefits to be zero, because the large influence of dust in this region causes $PM_{2.5}$ to be above the threshold. These results are highly dependent on the uncertainties involved in modeling dust contributions to $PM_{2.5}$. In 2030, global mortality co-benefits with a high-concentration threshold are 43% of the base case results, 55% in 2050, and 60% in 2100, as $PM_{2.5}$ concentrations decrease over the century. Using the log-linear function also decreases the mortality co-benefits to 73% of the base case results in 2030, 74% in 2050, and 84% in 2100. The log-linear function decreases estimated deaths in the most polluted regions, but increases deaths in less polluted regions, due to the shape of the function.

We do not assess the sensitivity of the results to the choice of other concentration-response functions, but premature deaths would change roughly proportionally to the value of β used in

Equation 1[33]. Results using the recent reanalysis of the Harvard Six Cities study for $PM_{2.5}$[46] would suggest more premature deaths than estimated here[39].

We also test sensitivity of the monetized co-benefits (Figure 5 of the main paper) to understand the importance of our assumptions of the growth of different parameters: population, baseline mortality rates, and VSLs. Tables S11-S13 show that monetized co-benefits are significantly smaller, particularly in 2100, if we assume no growth in these different parameters through time. Of these, we find that the growth of VSLs is most important globally, but the relative importance of these assumptions differ in specific world regions.

Figure S34 reproduces Figure 5 of the main paper, but applies uniform global VSLs in all world regions (increasing through time), given by the last row of Table S6. Relative to Figure 5, monetized co-benefits are substantially lower in high-income regions (N. America and Europe) and higher in low-income regions (Africa and S. Asia).

References

1. Clarke, L. *et al. Scenarios of Greenhouse Gas Emissions and Atmospheric Concentrations. Sub-report 2.1A of Synthesis and Assessment Product 2.1 by the U.S. Climate Change Science Program and the Subcommittee on Global Change Research* (Department of Energy, Office of Biological & Environmental Research, 2007).
2. Smith, S. J., West, J. J. & Kyle, P. Economically consistent long-term scenarios for air pollutant and greenhouse gas emissions. *Clim. Ch.* **108**, 619 (2011).
3. Smith, S. J. Income and pollutant emissions in the OBJECTS MiniCAM model *J. Environ. Develop.* **14** 175-96 (2005).
4. Smith, S. J., Pitcher, H. & Wigley, T. M. L. Future sulfur dioxide emissions. *Clim. Ch.* **73** 267-318 (2005).
5. Smith, S. J. & Wigley, T. M. L. Multi-gas forcing stabilization with Minicam. *Energy J.* **SI3**, *373*-91 (2006).
6. Smith, S. J. & Bond, T. C. Two hundred fifty years of aerosols and climate: the end of the age of aerosols, *Atmos. Chem. Phys. Discuss.* **13**, 6419-6453 (2013).
7. Streets, D. *et al.* Emission inventories and projections. In *Hemispheric Transport of Air Pollution 2010* (UNECE, Air Pollution Studies No. 17, 2010).
8. Thomson, A. M. *et al.* RCP4.5: a pathway for stabilization of radiative forcing by 2100. *Clim. Ch.* **109**, 77 (2011).
9. Van Vuuren, D. *et al.* The representative concentration pathways: an overview. *Clim. Ch.* **109**, 5-31 (2011).
10. Lamarque, J. F. *et al.* Historical (1850-2000) gridded anthropogenic and biomass burning emissions of reactive gases and aerosols: methodology and application. *Atmos. Chem. Phys.* **10**, 7017-7039 (2010).
11. Fry, M. M. *et al.* Net radiative forcing and air quality responses to regional CO emission reductions. *Atmos. Chem. Phys.* **13**, 5381-5399 (2013).
12. Bond, T. C. *et al.* Historical emissions of black and organic carbon aerosol from energy-related combustion, 1850-2000. *Glob. Biogeochem. Cyc.* **21**, GB2018 (2007).
13. Anenberg, S. C. *et al.* Impacts of global, regional, and sectoral black carbon emission reductions on surface air quality and human mortality. *Atmos. Chem. Phys.* **11**, 7253-7267 (2011).

14. Guenther, A. *et al.* Estimates of global terrestrial isoprene emissions using MEGAN (Model of Emissions of Gases and Aerosols from Nature). *Atmos. Chem. Phys.* **6**, 3181-3210 (2006).
15. Pfister, G. G. *et al.* Contribution of isoprene to chemical budgets: A model tracer study with the NCAR CTM MOZART-4. *J. Geophys. Res.* **113**, D05308 (2008).
16. Emmons, L. K. *et al.* Description and evaluation of the Model for Ozone and Related chemical Tracers, version 4 (MOZART-4). *Geosci. Model Develop.* **3**, 43 (2010).
17. Meinshausen, M. *et al.* The RCP Greenhouse Gas Concentrations and their Extensions from 1765 to 2500. *Clim. Change* **109**, 213-241 (2011).
18. Donner, L. J. *et al.* The dynamical core, physical parameterizations, and basic simulation characteristics of the atmospheric component AM3 of the GFDL global coupled model CM3. *J. Clim.* **24**, 3484-3519 (2011).
19. Lamarque, J. F. *et al.* The Atmospheric Chemistry and Climate Model Intercomparison Project (ACCMIP) overview and description of models, simulations and climate diagnostics. *Geosci. Model Develop.* **6**, 179-206 (2013).
20. Brauer, M. *et al.* Exposure assessment for estimation of the global burden of disease attributable to outdoor air pollution. *Environ. Sci. Tech.* **46**, 652-60 (2012).
21. Krewski, D. *et al. Extended Follow-up and Spatial Analysis of the American Cancer Society Study Linking Particulate Air Pollution and Mortality* (Health Effects Institute, 2009).
22. Jerrett, M., *et al.* Long-term ozone exposure and mortality. *N. Engl. J. Med.* **360**, 1085 (2009).
23. Tilmes, S. *et al.* Technical Note: Ozonesonde climatology between 1995 and 2011: description, evaluation and applications. *Atmos. Chem. Phys.* **12**, 7475-7497 (2012).
24. Fiore, A. M. *et al.* Global air quality and climate. *Chem. Soc. Rev.* **41**, 6663 (2012).
25. Luckow, P., Wise, M. A., Dooley, J. J. & Kim, S. H. Large-scale utilization of biomass energy and carbon dioxide capture and storage in the transport and electricity sectors under stringent CO2 concentration limit scenarios. *Intl. J. of Greenhouse Gas Control* **4**, 865–877 (2010).
26. West, J. J., Fiore, A. M., Horowitz, L. W. & Mauzerall, D. L. Global health benefits of mitigating ozone pollution with methane emission controls. *Proc. Natl. Acad. Sci. U. S. A.*, **103**, 3988 (2006).
27. West, J. J., Szopa, S. & Hauglustaine, D. A. Human mortality effects of future concentrations of tropospheric ozone. *Comptes rendus de l'Académie des sciences – Geoscience* **339**, 775-783 (2007).
28. Corbett, J. J. *et al.* Mortality from ship emissions: A global assessment. *Environ. Sci. Tech.* **41**, 8512 (2007).
29. Jacobson, M. Z. On the causal link between carbon dioxide and air pollution mortality. *Geophys. Res. Lett.* **35**, L03809 (2008).
30. West, J. J., Naik, V., Horowitz, L. W. & Fiore, A. M. Effect of regional precursor emission controls on long-range ozone transport: 2. Steady-state changes in ozone air quality and impacts on human mortality. *Atmos. Chem. Phys.*, **9,** 6095-6107 (2009).
31. Liu, J. F., Mauzerall, D. L. & Horowitz, L. W. Evaluating inter-continental transport of fine aerosols:(2) Global health impact. *Atmos. Environ.* **43**, 4339-4347 (2009).
32. Anenberg, S. C., *et al.* Intercontinental impacts of ozone pollution on human mortality. *Environ. Sci. Tech.* **43**, 6482-6487 (2009).

33. Anenberg, S. C., Horowitz, L. W., Tong, D. Q. & West, J. J. An estimate of the global burden of anthropogenic ozone and fine particulate matter on premature human mortality using atmospheric modeling. *Environ. Health Persp.* **118**, 1189 (2010).
34. Barrett, S. R. H., Britter, R. E. & Waitz, I. A. Global Mortality Attributable to Aircraft Cruise Emissions. *Environ. Sci. Tech.* **44**, 7736-7742 (2010).
35. West, J. J., Fiore, A. M. & Horowitz, L. W. Managing ozone air quality by reducing methane emissions: abatement costs and mortality benefits in scenarios to 2030, *Clim. Ch.* **114**, 441-461 (2012).
36. Anenberg, S. C. *et al.* Global air quality and health co-benefits of mitigating near-term climate change through methane and black carbon emission controls, *Environ. Health Persp.* **120**, 831-839 (2012).
37. Shindell, D. *et al.* Simultaneously Mitigating Near-Term Climate Change and Improving Human Health and Food Security. *Science* **335**,183-189 (2012).
38. Punger, E. M. & West, J. J. The effect of grid resolution on estimates of the burden of ozone and fine particulate matter on premature mortality in the United States. *Air Quality Atmos. Health* (in press).
39. US Environmental Protection Agency (2012) *Regulatory Impact Analysis for the Final Revisions to the National Ambient Air Quality Standards for Particulate Matter*, EPA-452/R-12-003, December, 2012, obtained from http://www.epa.gov/pm/2012/finalria.pdf.
40. Hoek, G., Brunekreef, B., Goldbohm, S., Fischer, P. & van den Brandt, P. A. Association between mortality and indicators of traffic-related air pollution in the Netherlands: a cohort study. *Lancet* **360**, 1203-1209 (2002).
41. Health Effects Institute International Scientific Oversight Committee *Health Effects of Outdoor Air Pollution in Developing Countries of Asia: A Literature Review* (Health Effects Institute, 2004).
42. Health Effects Institute Public Health and Air Pollution in Asia Program *Public Health and Air Pollution in Asia: Coordinated Studies of Short-Term Exposure to Air Pollution and Daily Mortality in Four Cities*. HEI Research Report 154. (Health Effects Institute, 2010).
43. Zanobetti, A., Schwartz, J. & Gold, D. Are there sensitive subgroups for the effects of airborne particles? *Environ Health Perspect* **108**, 841-845 (2000).
44. Krewski, D. et al. *Reanalysis of the Harvard Six Cities Study and the American Cancer Society Study of Particulate Air Pollution and Mortality* (Special report of the Institute's Particle Epidemiology Reanalysis Project, Health Effects Institute, 2000).
45. Schwartz, J. & Zanobetti, A. Using meta-smoothing to estimate dose-response trends across multiple studies, with application to air pollution and daily death. *Epidemiology* **11**, 666-672 (2000).
46. Lepeule, J., Laden, F., Dockery, D. & Schwartz, J. Chronic exposure to fine particles and mortality: an extended follow-up of the Harvard Six Cities Study from 1974 to 2009. *Environ. Health Perspect.* **120**, 965-970 (2012).
47. Pope, C. A. *et al.* Cardiovascular mortality and exposure to airborne fine particulate matter and cigarette smoke shape of the exposure-response relationship. *Circulation* **120**, 941-948 (2009).
48. Pope, C. A. *et al.* Lung cancer and cardiovascular disease mortality associated with ambient air pollution and cigarette smoke: shape of the exposure-response relationships. *Environ. Health Perspect.* **119**, 1616-1621 (2011).

49. Mathers, C. D. & Loncar, D. Projections of global mortality and burden of disease from 2002 to 2030. *PLoS Medicine* **3**, e442 (2006).
50. Hughes, B. B. *et al.* Projections of global health outcomes from 2005 to 2060 using the International Futures integrated forecasting model, *Bull. World Health Organ.* **89**, 478-486 (2011).
51. Hughes, B. B., Irfan, M. T., Moyer, J. D., Rothman, D. S. & Solorzano, J. R. Exploring future impacts of environmental constraints on human development, *Sustainability* **4**, 958-994 (2012).
52. World Health Organization, *WHO Statistical Information System (WHOSIS)*, download the detailed data files of the WHO Mortality Database, http://www.who.int/whosis/mort/download/en/index.html, data retrieved Sept. 2012.
53. World Health Organization *Cause-specific mortality: regional estimates for 2008*, http://www.who.int/healthinfo/global_burden_disease/estimates_regional/en/index, data retrieved Sept. 2012.
54. Dobson, J. E., Bright, E. A. , Coleman, P. R., Durfee, R. C. & Worley, B. A. LandScan: A global population database for estimating populations at risk. *Photogrammetric Engineering and Remote Sensing* **66**, 849-857 (2000).
55. US National Research Council, *Estimating Mortality Risk Reduction and Economic Benefits from Controlling Ozone Air Pollution* (National Academies Press, 2008).
56. Viscusi, W. K. & Aldy, J. E. The value of a statistical life: A critical review of market estimates throughout the world. *J. Risk and Uncertainty* **27**, 5-76 (2003).
57. US Environmental Protection Agency, Frequently asked questions on mortality risk valuation, http://yosemite.epa.gov/ee/epa/eed.nsf/pages/MortalityRiskValuation.html, accessed Dec. 17, 2012.
58. OECD (2012) *Mortality Risk Valuation in Environment, Health and Transport Policies*, ISBN: 978-92-64-13076-0, accessed Dec. 17, 2012 from http://www.oecd.org/env/environmentalpolicytoolsandevaluation/mortalityriskvaluationinenvironmenthealthandtransportpolicies.htm.
59. Clarke, L. *et al.* International climate policy architectures: Overview of the EMF 22 International Scenarios. *Energy Economics* **31**, S64 (2009).
60. Evans, J. *et al*. Estimates of global mortality attributable to particulate air pollution using satellite imagery, *Environmental Research* **120**, 33-43 (2013).
61. Van Vuuren, D. P. *et al.* Temperature increase of 21st century mitigation scenarios *Proc. Natl. Acad. Sci. U. S. A.* **105**, 15258-15262 (2008).

Table S1. Anthropogenic emissions and methane concentration in the 2000 simulation and future simulations under RCP4.5 and the GCAM reference case (in Tg yr^{-1}). Emissions totals for BC and OC are as reported by Lamarque et al.[10] for the RCP emissions, and do not include the factors (1.15 and 1.4) that we used to convert from PM_1 to $PM_{2.5}$ emissions.

		GCAM Reference (REF)			RCP4.5		
	2000	2030	2050	2100	2030	2050	2100
NO_x [1]	125.5	125.4	111.7	80.0	114.3	95.6	59.3
NMVOCs	210.8	239.6	233.8	165.1	204.1	190.6	140.0
CO	1069.0	1208.5	1103.4	556.7	996.3	872.7	477.3
SO_2	107.8	96.7	66.9	42.0	86.8	51.4	22.5
NH_3	48.5	58.6	62.6	59.2	55.0	56.5	52.9
OC	35.9	39.8	38.6	22.2	29.2	26.8	19.4
BC	7.8	9.0	8.2	5.3	7.3	6.2	3.9
CH_4 [2]	1766	2017	2267	2360	1829	1833	1576

[1] in Tg NO_2 yr^{-1}

[2] CH_4 concentrations in ppbv

Table S2. CO_2 emission reductions in RCP4.5 relative to REF, in Mton CO_2 yr^{-1}, in 14 world regions and globally. Values are shown to 3 significant figures.

	2030	2050	2100
Canada	333	439	569
United States	541	1,720	5,580
Western Europe	400	1,160	2,890
Eastern Europe	115	356	976
Former Soviet Union	400	934	2,190
China	1,700	5,210	15,800
S. Korea	44	121	318
Japan	111	285	600
Middle East	221	678	2,610
India	594	2,290	11,000
Africa	1,120	1,920	7,500
Southeast Asia	741	2,390	10,900
Latin America	567	1,220	4,530
Australia_NZ	56	151	295
Global	6,940	18,900	65,800

Table S3. Modeling scenarios.

Years	Emissions	Meteorology GFDL AM3	Name
2000	2000	2000	2000
2030, 2050, 2100	GCAM Reference	RCP8.5	REF
	RCP4.5	RCP4.5	RCP4.5
	GCAM Reference	RCP4.5	eREFm45
2050	RCP4.5	RCP8.5	e45m85

Table S4. Total global population in the International Futures dataset used in this project, and in the original RCP4.5 scenario (billion people). Population for RCP4.5 in 2030 was interpolated from reported values in 2020 and 2035, and the population in 2100 was extrapolated from reported 2080 and 2095 values.

	International Futures	RCP4.5
2030	8.293	8.071
2050	9.294	8.815
2100	9.716	8.664

Table S5. Population and baseline mortality rates for the adult population (30 and older), in 14 world regions and the global total or average. Baseline mortality rates are the adult population that dies of a given cause in a year, expressed per 1000 adult population. Future baseline mortality rates and population are based on IFs. Population and baseline mortality rates for the present day (2008) are not used in the calculation of mortality, but are shown here for comparison with projected future rates; present-day mortality rates are based on WHO[52,53] using rates for individual nations from 2008, or if not available, rates from the most recent year reported between 2000 and 2007, or if not available, estimated for each nation from regional rates.

	Population (millions)				Cardiopulmonary rate				Lung cancer rate				Respiratory rate			
	2008	2030	2050	2100	2008	2030	2050	2100	2008	2030	2050	2100	2008	2030	2050	2100
Canada	17	21	23	27	4.02	5.40	6.03	4.68	0.84	0.98	1.01	0.87	0.96	1.14	1.52	1.96
USA	190	238	274	331	5.25	5.57	5.90	4.82	0.83	0.92	0.93	0.83	1.26	1.23	1.56	2.07
W. Europe	304	339	347	316	5.31	7.23	8.31	7.00	0.67	0.84	0.90	0.80	1.07	1.14	1.65	2.43
E. Europe	79	88	83	60	8.01	10.2	11.9	10.7	0.75	0.91	1.00	0.97	0.76	0.81	1.22	2.21
FSU	176	201	208	189	11.9	11.9	13.2	12.6	0.48	0.29	0.31	0.25	0.79	0.69	0.99	1.58
China	825	1073	1081	806	6.14	7.96	10.7	10.8	0.61	0.80	1.00	0.91	1.96	2.56	4.43	7.03
S. Korea	16	18	17	10	2.80	5.31	6.99	6.00	0.53	0.93	1.23	1.14	0.75	1.12	2.00	2.90
Japan	87	85	75	49	5.11	6.71	7.05	5.88	0.70	0.99	1.12	1.09	1.83	1.33	1.82	2.69
Middle East	60	119	169	229	4.40	5.02	6.66	8.81	0.11	0.13	0.16	0.18	0.40	0.51	0.81	1.55
India	397	644	838	925	6.81	7.01	7.72	9.23	0.15	0.14	0.15	0.16	2.03	2.22	2.82	5.45
Africa	447	737	945	1098	5.79	6.45	7.84	8.80	0.21	0.23	0.26	0.26	1.45	1.58	2.17	3.71
SE Asia	258	398	486	495	3.92	4.66	5.70	6.80	0.22	0.28	0.33	0.37	1.01	0.90	1.36	2.68
Latin America	304	578	964	1893	6.03	5.93	6.32	7.96	0.08	0.09	0.09	0.08	1.19	0.96	1.06	1.78
Australia	15	20	23	28	3.91	4.92	5.61	4.67	0.53	0.70	0.76	0.68	0.80	0.94	1.27	1.77
Global	3177	4558	5533	6456	6.12	6.94	8.06	8.49	0.42	0.46	0.47	0.35	1.47	1.62	2.27	3.40

Table S6. Projected regional per capita income (GDP, in 2005 US thousand dollars) and value of a statistical life in 2005, 2030, 2050, and 2100 under low and high VSL assumptions (in 2005 US million dollars). VSLs in 2005 are not used in the valuation, and here show how present-day values are translated into other regions and into the future. The values on which all VSLs are based are shown in bold red, for the low and high assumptions. Per capita GDP values correspond with Figure S1.

	Per capita GDP				Low VSL				High VSL			
	2005	2030	2050	2100	2005	2030	2050	2100	2005	2030	2050	2100
Canada	28.6	41.6	53.4	101.6	2.0	2.5	2.8	3.8	6.1	7.4	8.4	11.6
USA	41.6	57.5	73.1	141.2	2.5	2.9	3.3	4.5	**7.4**	8.7	9.8	13.6
W. Europe	22.4	30.2	38.1	73.1	**1.8**	2.1	2.3	3.3	5.4	6.3	7.1	9.8
E. Europe	4.7	10.6	18.7	70.2	0.8	1.2	1.6	3.2	2.5	3.7	5.0	9.6
FSU	2.1	4.8	8.4	30.7	0.5	0.8	1.1	2.1	1.7	2.5	3.3	6.4
China	1.5	7.2	15.0	57.3	0.5	1.0	1.5	2.9	1.4	3.1	4.4	8.7
S. Korea	14.8	21.3	30.0	69.5	1.5	1.8	2.1	3.2	4.4	5.3	6.3	9.6
Japan	44.0	58.0	74.1	141.2	2.5	2.9	3.3	4.5	7.6	8.7	9.9	13.6
Middle East	4.7	7.5	10.2	24.4	0.8	1.0	1.2	1.9	2.5	3.1	3.7	5.7
India	0.7	2.3	5.2	27.3	0.3	0.6	0.9	2.0	0.9	1.8	2.6	6.0
Africa	0.9	1.4	1.8	8.7	0.4	0.4	0.5	1.1	1.1	1.3	1.6	3.4
SE Asia	1.9	5.3	10.2	44.9	0.5	0.9	1.2	2.5	1.6	2.6	3.7	7.7
Latin America	4.6	6.3	8.8	33.0	0.8	1.0	1.1	2.2	2.5	2.9	3.4	6.6
Australia	24.3	33.7	43.2	78.3	1.9	2.2	2.5	3.4	5.7	6.7	7.5	10.2
Global	6.3	9.7	14.3	42.6	1.0	1.2	1.4	2.5	2.9	3.6	4.3	7.5

Table S7. Co-benefit of reduced premature respiratory mortality due to changes in ozone (REF-RCP4.5) in deaths yr^{-1}, shown to three significant figures. Results with no threshold correspond to Figure 3 of the main paper and Figures S31-S33. Also shown are mortality co-benefits when a low-concentration threshold of 33.3 ppb is applied.

	No threshold			Low-concentration threshold		
	2030	2050	2100	2030	2050	2100
Canada	368	792	1180	368	792	1050
United States	2,440	7,550	24,800	2,440	7,550	24,700
Western Europe	4,130	9,100	21,600	4,130	9,100	21,500
Eastern Europe	649	1,590	4,160	649	1,590	4,150
Former Soviet Union	1,440	3,650	6,400	1,440	3,650	6,000
China	36,800	83,000	184,000	36,800	83,000	184,000
S. Korea	255	558	946	255	558	946
Japan	1,630	2,260	4,000	1,630	2,260	4,000
Middle East	321	2,177	9,350	321	2,177	9,350
India	19,500	35,500	191,500	19,500	35,500	191,500
Africa	5,040	15,800	99,100	5,000	15,500	96,300
Southeast Asia	15,500	30,300	141,000	15,200	29,900	137,000
Latin America	2,600	9,320	30,000	2,210	8,440	21,700
Australia_NZ	53	197	577	1	0	4
Global	90,700	202,000	719,000	89,900	200,000	702,000

Table S8. Co-benefit of reduced premature cardiopulmonary and lung cancer mortality due to changes in $PM_{2.5}$ (REF-RCP4.5) in 2030 in deaths yr^{-1}, shown to three significant figures. Results with no threshold correspond to Figure 3 of the main paper and Figures S31-S33. Also shown are mortality co-benefits when a low-concentration threshold (LCT) of 5.8 $\mu g\ m^{-3}$ is applied, a log-linear concentration-response function, and a high-concentration threshold (HCT) of 30 $\mu g\ m^{-3}$.

	No threshold	LCT	Log-Linear	HCT
Canada	4,270	1,810	10,000	4,270
United States	19,300	16,500	38,700	19,300
Western Europe	23,700	23,000	30,000	23,200
Eastern Europe	5,390	5,390	7,600	5,390
Former Soviet Union	27,700	27,100	33,000	23,900
China	304,000	304,000	124,000	50,700
S. Korea	2,090	2,090	1,500	2,090
Japan	4,360	4,360	4,970	4,360
Middle East	2,100	2,100	460	0
India	-20,100	-20,100	-2,680	-1,440
Africa	33,200	32,500	26,400	22,800
Southeast Asia	23,700	22,800	26,900	23,800
Latin America	10,100	7,080	20,200	10,100
Australia_NZ	39	35	73	40
Global	440,000	429,000	321,000	189,000

Table S9. As Table S8, but for 2050.

	No threshold	LCT	Log-Linear	HCT
Canada	5,750	2,220	14,100	5,750
United States	29,500	14,200	70,000	29,500
Western Europe	32,200	31,700	41,800	31,000
Eastern Europe	8,220	8,220	12,600	8,220
Former Soviet Union	54,100	51,900	65,600	44,400
China	430,000	430,000	337,000	351,000
S. Korea	3,180	3,180	3,320	3,180
Japan	9,190	9,190	12,700	9,190
Middle East	8,260	8,260	2,270	0
India	235,000	235,000	77,000	31,700
Africa	81,600	79,600	48,600	37,600
Southeast Asia	204,000	202,000	99,900	46,300
Latin America	25,100	18,100	48,300	25,100
Australia_NZ	222	205	402	220
Global	1,130,000	1,090,000	834,000	623,000

Table S10. As Table S8, but for 2100.

	No threshold	LCT	Log-Linear	HCT
Canada	2,880	128	10,200	2,880
United States	35,400	3,340	102,000	35,400
Western Europe	41,700	40,000	55,900	39,800
Eastern Europe	15,400	12,700	25,300	15,400
Former Soviet Union	42,000	35,700	48,400	35,200
China	381,000	373,000	397,000	380,000
S. Korea	2,010	2,010	2,600	2,010
Japan	6,580	6,570	10,700	6,580
Middle East	27,700	27,700	7,090	0
India	356,000	356,000	150,000	75,900
Africa	206,000	196,600	130,000	86,000
Southeast Asia	364,000	352,000	249,000	193,000
Latin America	37,400	19,300	89,000	37,300
Australia_NZ	463	324	924	460
Global	1,520,000	1,420,000	1,280,000	910,000

Table S11. Estimated sensitivity of the 2030 monetized co-benefits to alternative demographic and valuation assumptions, using the high valuation estimate for illustration. Base values correspond to the central estimates for high valuation in Figure 5 of the main paper (in $ / ton CO_2), once these 14 regions are combined to 9 regions. Alternative assumptions include: No population growth (assume constant 2008 population), no change in baseline mortality rates (assume constant 2008 rates), and no change in valuation (assume constant 2005 VSLs from Table S6).

	Base	No population growth	No change in baseline mortality rates	No change in valuation
Canada	103	82	80	85
United States	349	279	329	297
Western Europe	439	402	343	378
Eastern Europe	197	180	151	131
Former Soviet Union	184	166	190	120
China	617	478	471	285
S. Korea	284	243	150	237
Japan	471	481	434	410
Middle East	34	18	30	27
India	-2	-1	-6	-1
Africa	46	23	51	38
Southeast Asia	140	90	117	84
Latin America	65	41	58	55
Australia_NZ	11	8	9	9
Global	260	205	212	156

Table S12. As Table S11, but for 2050.

	Base	No population growth	No change in baseline mortality rates	No change in valuation
Canada	125	90	85	91
United States	212	147	184	160
Western Europe	252	225	158	193
Eastern Europe	137	128	85	68
Former Soviet Union	206	175	171	102
China	437	338	241	140
S. Korea	194	180	74	137
Japan	396	461	305	305
Middle East	56	22	36	38
India	310	146	268	110
Africa	79	25	76	56
Southeast Asia	358	168	283	155
Latin America	96	49	67	69
Australia_NZ	21	14	14	16
Global	278	188	192	124

Table S13. As Table S11, but for 2100.

	Base	No population growth	No change in baseline mortality rates	No change in valuation
Canada	82	50	63	44
United States	147	84	130	80
Western Europe	215	200	131	119
Eastern Europe	192	242	115	50
Former Soviet Union	141	111	100	36
China	311	327	148	51
S. Korea	89	138	34	41
Japan	240	430	186	134
Middle East	80	21	39	35
India	299	128	183	46
Africa	137	27	96	45
Southeast Asia	355	142	224	73
Latin America	98	50	46	37
Australia_NZ	36	19	22	20
Global	242	159	143	57

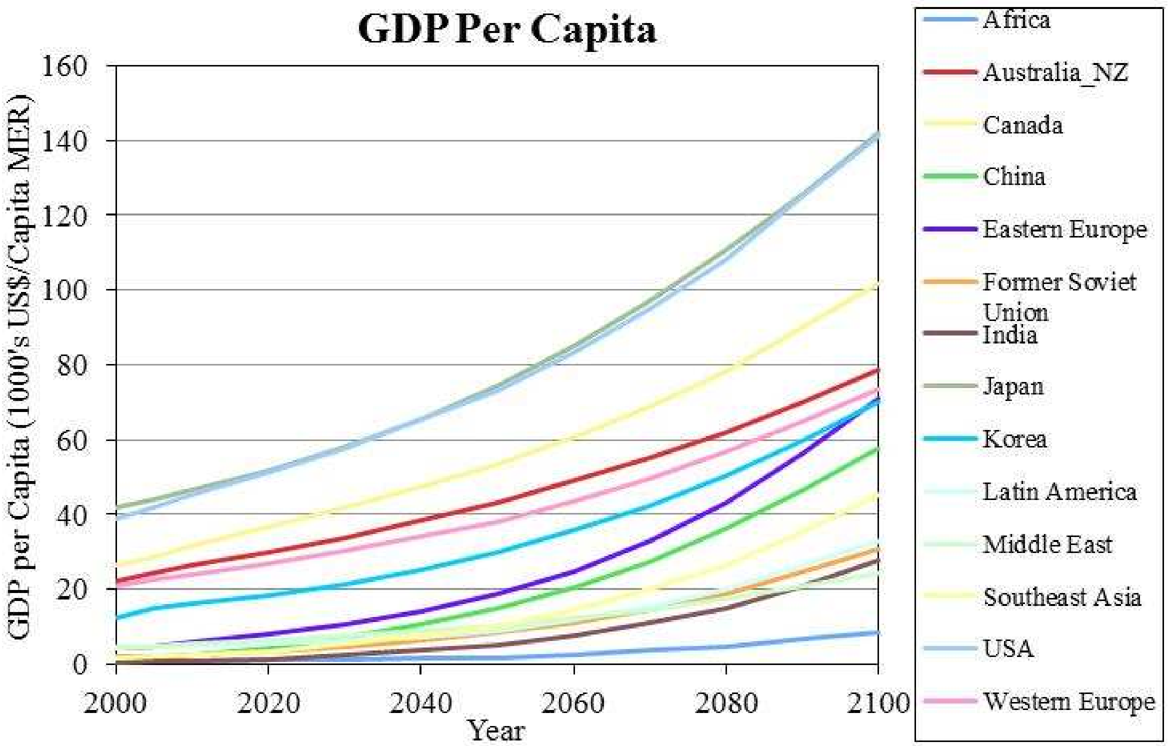

Figure S1. GDP per capita for the 14 GCAM world regions in year 2005 $US at a Market Exchange Rate basis.

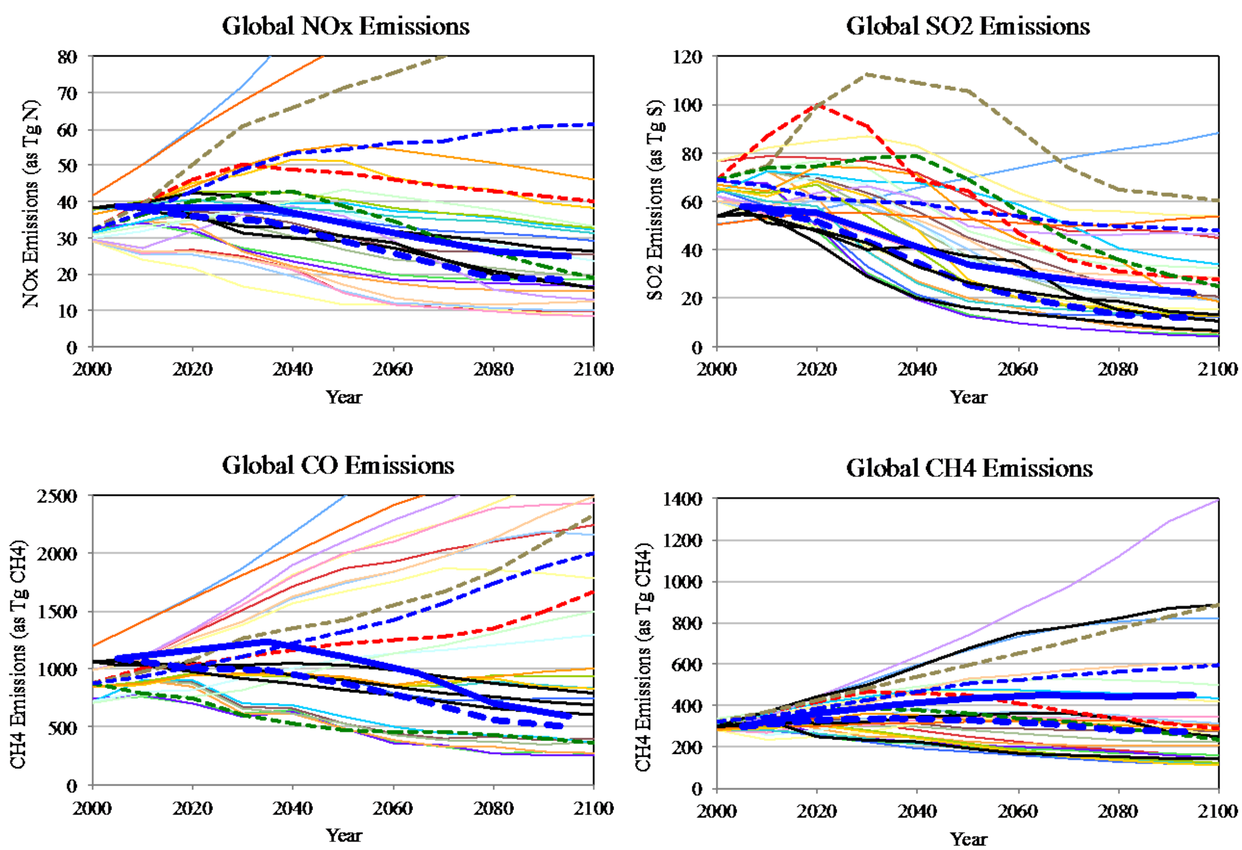

Figure S2. GCAM REF (thick solid blue line) and RCP4.5 (thick dashed blue line) emissions from 2005 - 2095 as compared to: emissions from the literature[61] as thin colored lines, the other RCP scenarios (solid black lines), and older estimates from the SRES scenarios (dotted lines). In a few cases, the maximum on the vertical scale has been adjusted so that the two GCAM scenarios are discernable. These figures (without GCAM highlighted) are also available in Streets et al.[7].

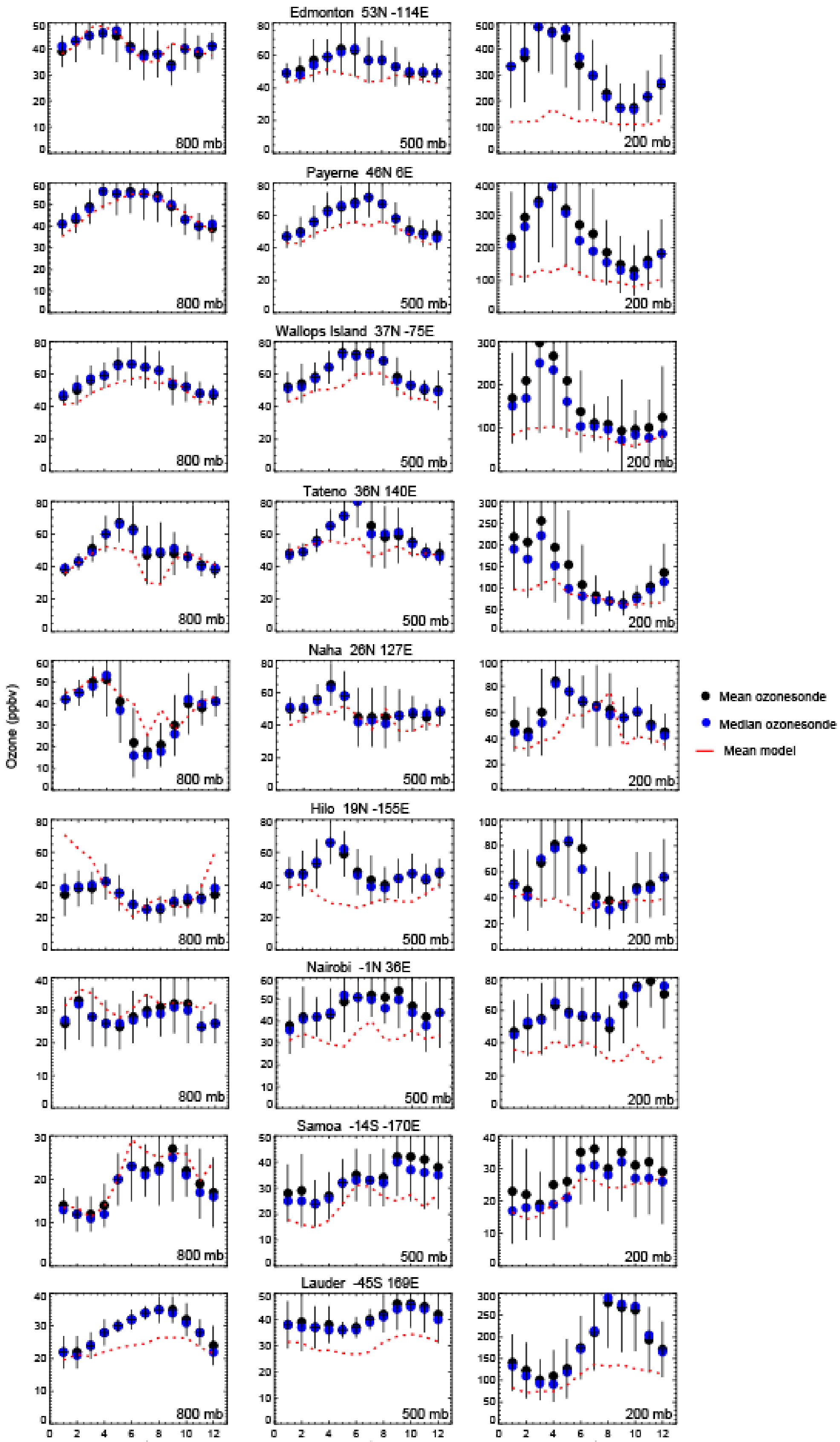

Figure S3. Comparison of modeled monthly mean ozone with ozonesonde observations, which are the monthly mean and median observations from 1990-2009[23]. Model results are for year 2000 emissions, and are the average of four model years representative of climate in 2000. Nine stations are shown here as a representative sample.

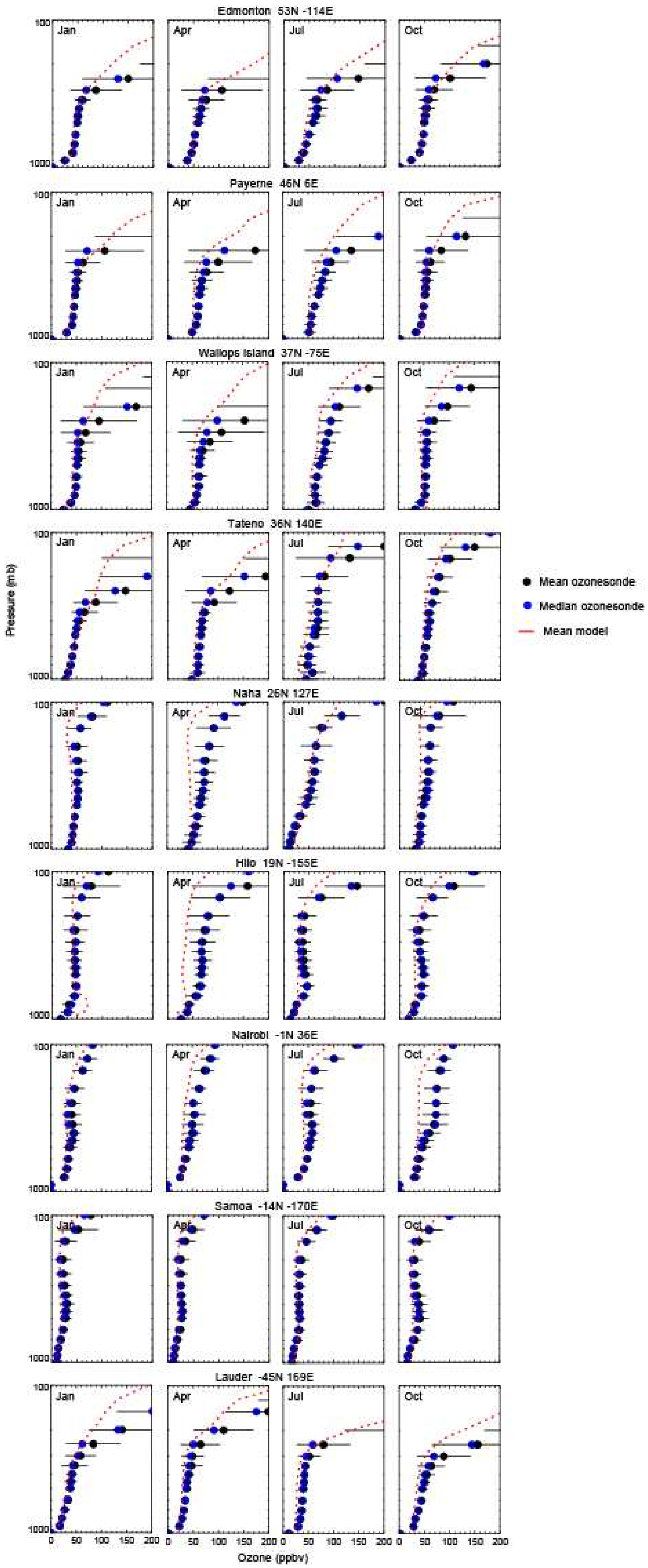

Figure S4. Comparison of modeled monthly mean ozone with vertical profiles of ozonesonde observations, which are the monthly mean and median observations from 1990-2009[23]. Model results are for year 2000 emissions, and are the average of four model years representative of climate in 2000.

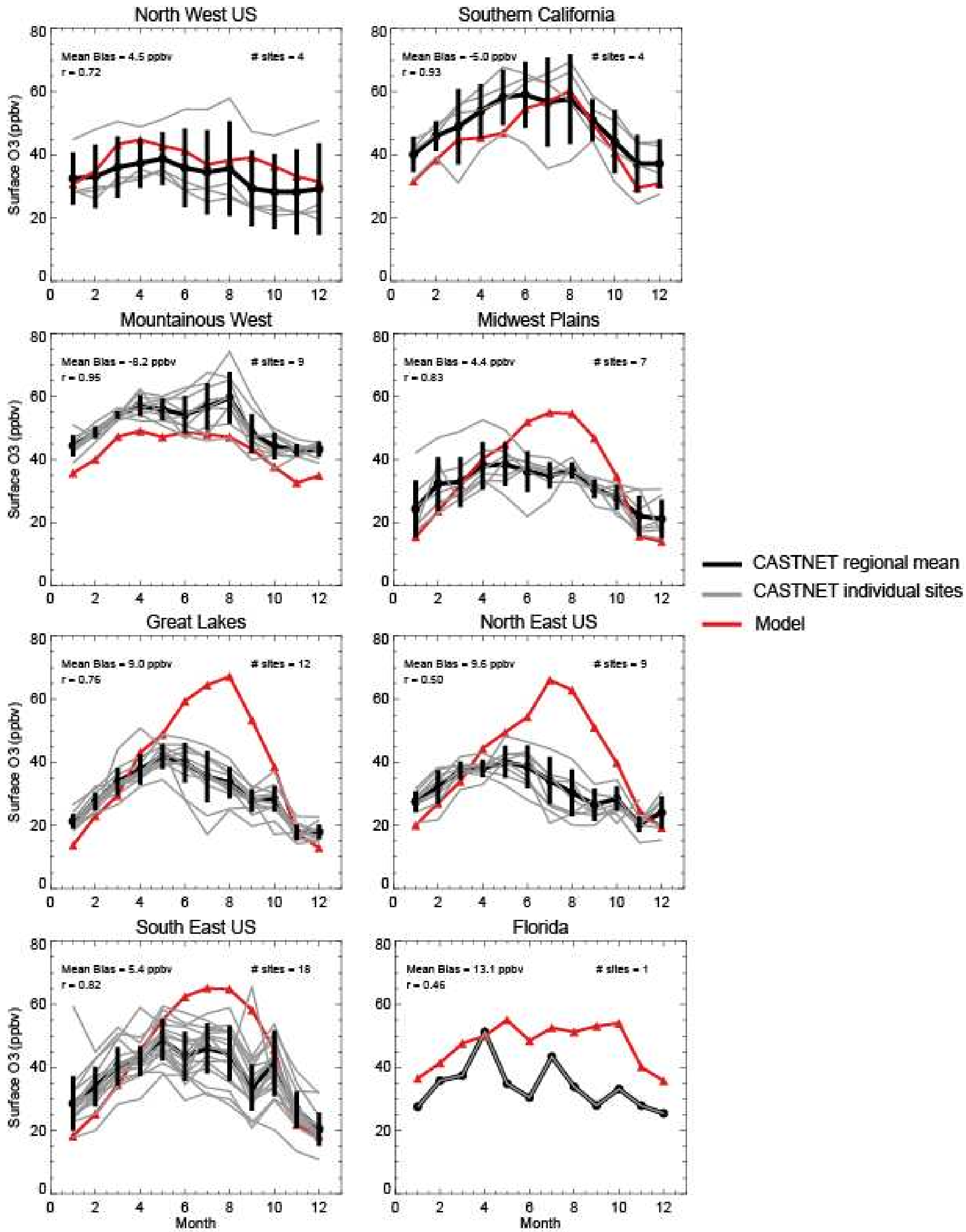

Figure S5. Comparison of modeled ozone with surface ozone measurements in the US at CASTNET stations. Observations are from 2005. The model is for year 2000 emissions and is the average of four meteorological years representative of 2000.

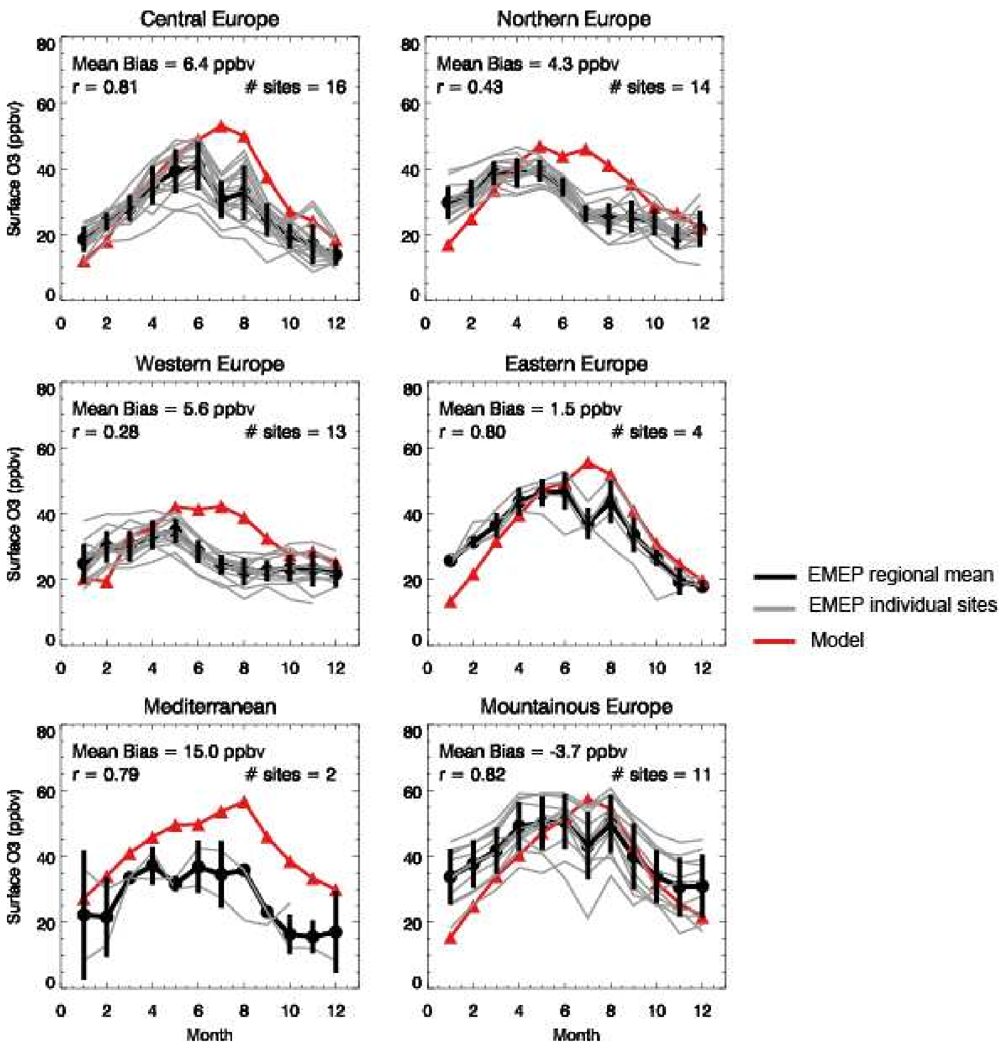

Figure S6. Comparison of modeled ozone with surface ozone measurements in Europe at EMEP stations. Observations are from 2005. The model is for year 2000 emissions and is the average of four meteorological years representative of 2000.

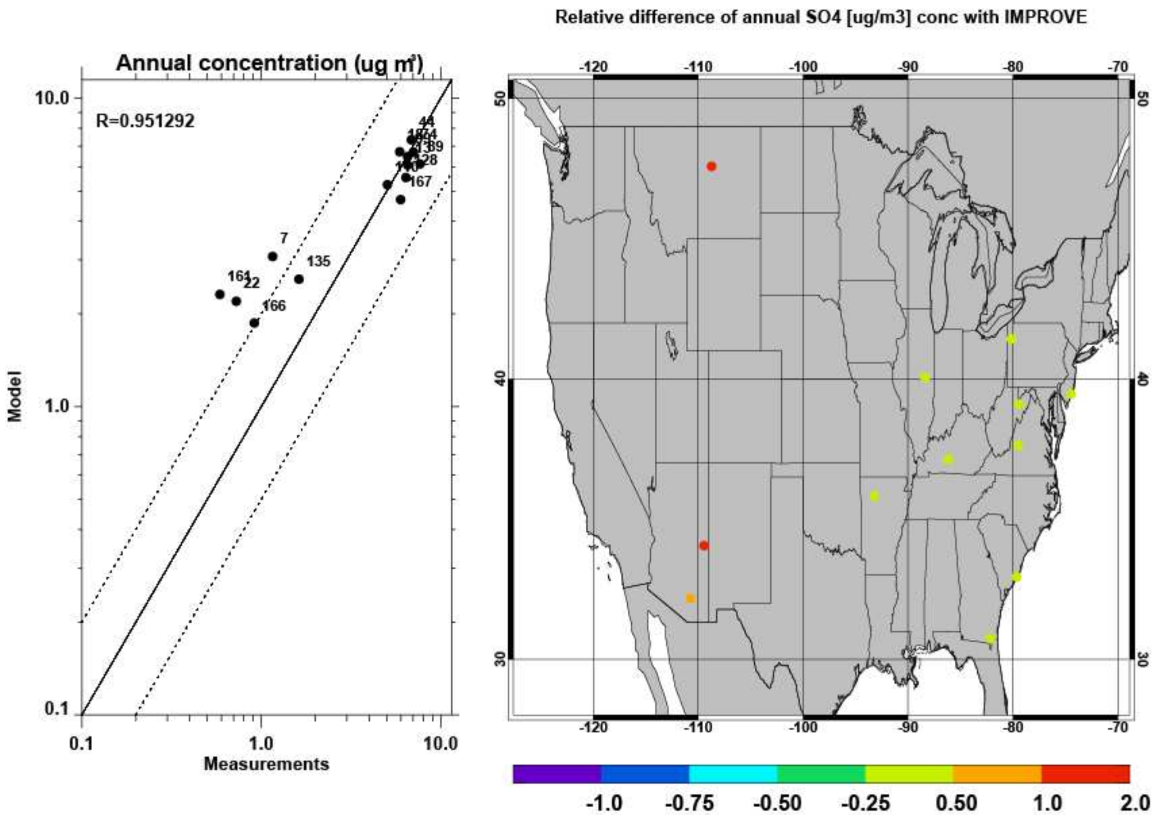

Figure S7. Comparison of modeled and measured surface sulfate in the US at IMPROVE stations. Observations are from 2005. The model is for year 2000 emissions and is the average of four meteorological years representative of 2000.

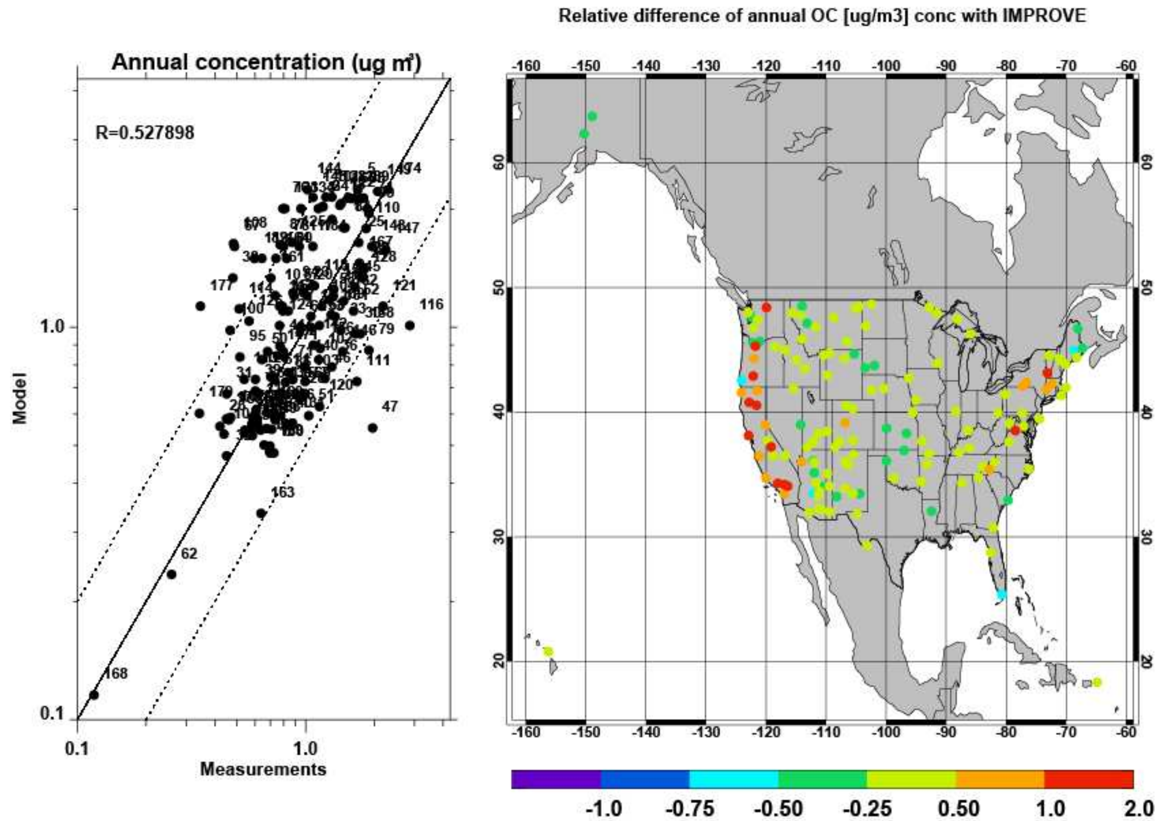

Figure S8. Comparison of modeled and measured surface organic carbon in the US at IMPROVE stations. Observations are from 2005. The model is for year 2000 emissions and is the average of four meteorological years representative of 2000.

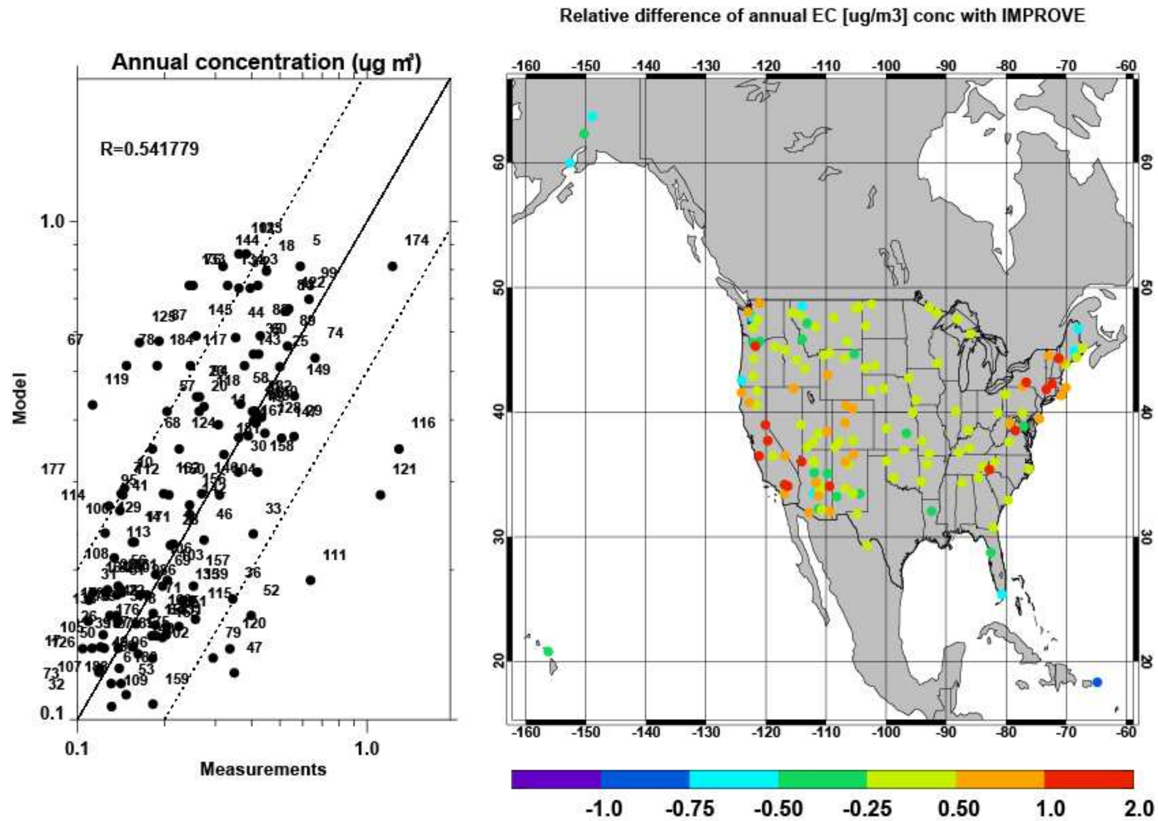

Figure S9. Comparison of modeled and measured surface elemental carbon in the US at IMPROVE stations. Observations are from 2005. The model is for year 2000 emissions and is the average of four meteorological years representative of 2000.

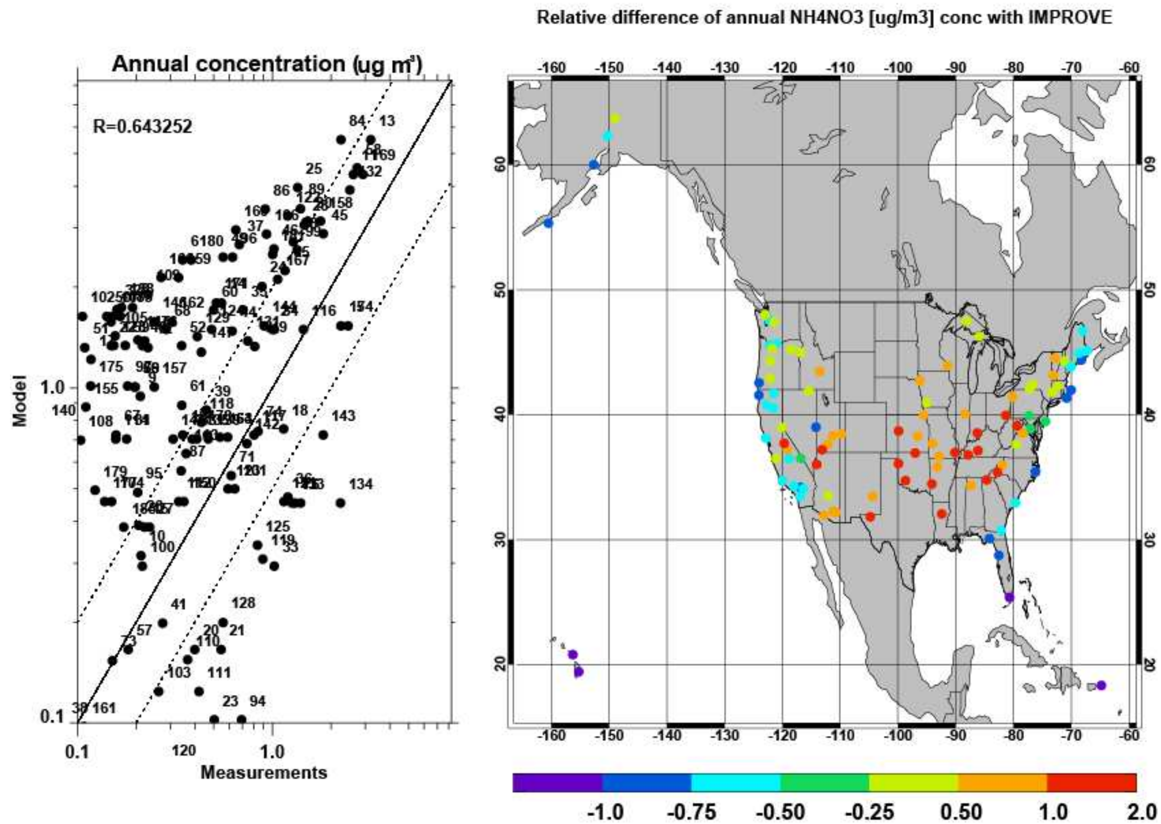

Figure S10. Comparison of modeled and measured surface ammonium nitrate in the US at IMPROVE stations. Observations are from 2005. The model is for year 2000 emissions and is the average of four meteorological years representative of 2000.

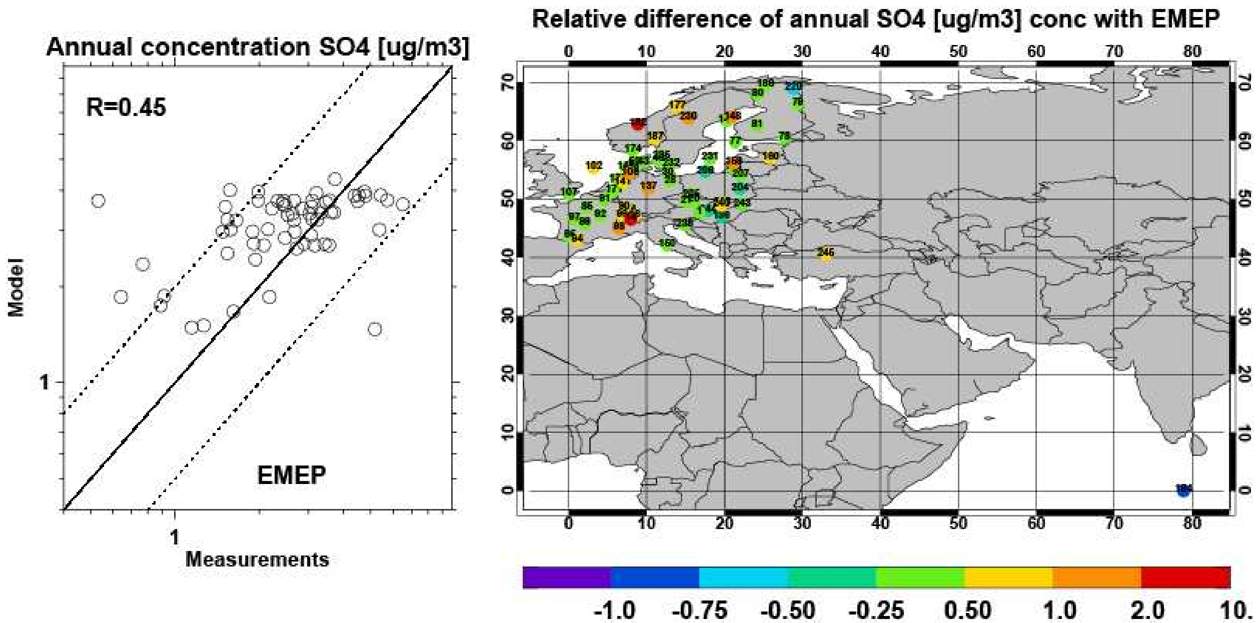

Figure S11. Comparison of modeled and measured surface sulfate in Europe at EMEP stations. Observations are from 2005. The model is for year 2000 emissions and is the average of four meteorological years representative of 2000.

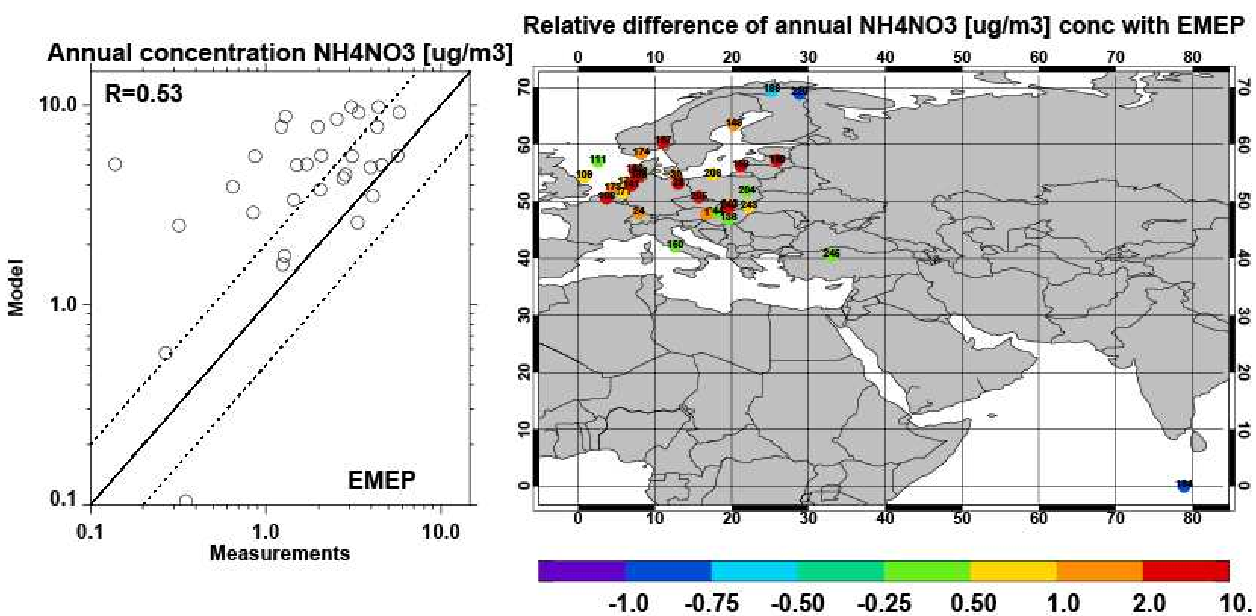

Figure S12. Comparison of modeled and measured surface ammonium nitrate in Europe at EMEP stations. Observations are from 2005. The model is for year 2000 emissions and is the average of four meteorological years representative of 2000.

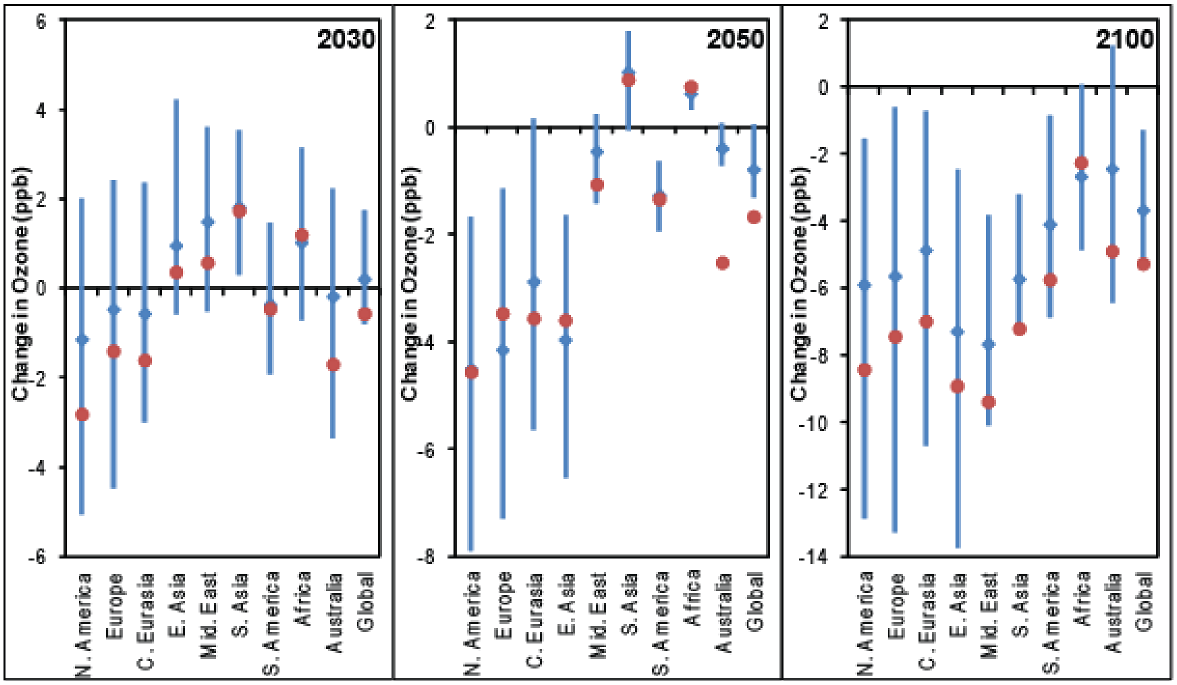

Figure S13. Comparison of RCP4.5 annual average (area-weighted) ozone surface concentration changes relative to 2000, in this study (red), and the mean and multi-model range from the ACCMIP ensemble of models (blue), for the global average and 9 world regions defined by Fiore et al.[24]. Results are shown as changes relative to the 2000 simulation, and are the average of four model years for MOZART-4, and multi-year averages for ACCMIP models varying from 1 year to 10 years depending on the data reported by each model. For ACCMIP, results are the average of 9 models that report ozone in 2030 and 2100, and 3 models in 2050.

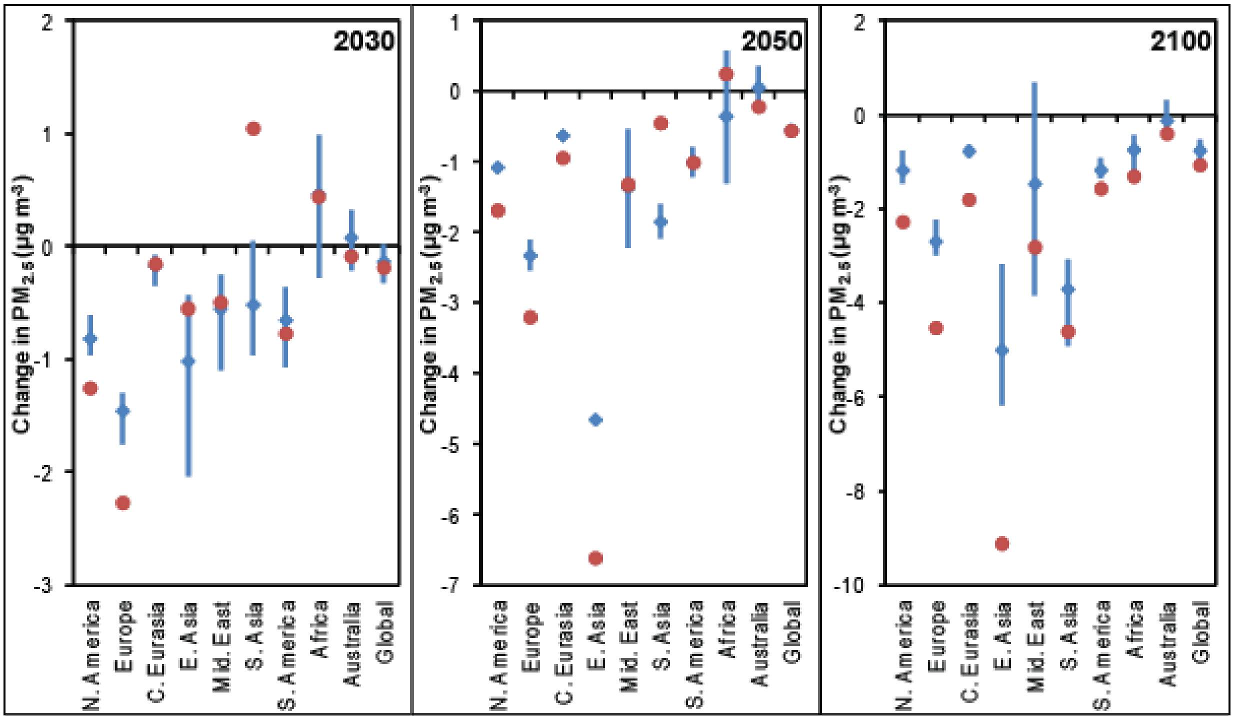

Figure S14. Comparison of RCP4.5 annual average (area-weighted) $PM_{2.5}$ surface concentration changes relative to 2000, in this study (red), and the mean and multi-model range from the ACCMIP ensemble of models (blue), for the global average and 9 world regions defined by Fiore et al.[24]. Results are shown as changes relative to the 2000 simulation, and are the average of four model years for MOZART-4, and multi-year averages for ACCMIP models varying from 1 year to 10 years depending on the data reported by each model. For ACCMIP, results are the average of 3 models that report $PM_{2.5}$ in 2030 and 2100, and 2 models in 2050, selecting only those models that report an indicator of $PM_{2.5}$.

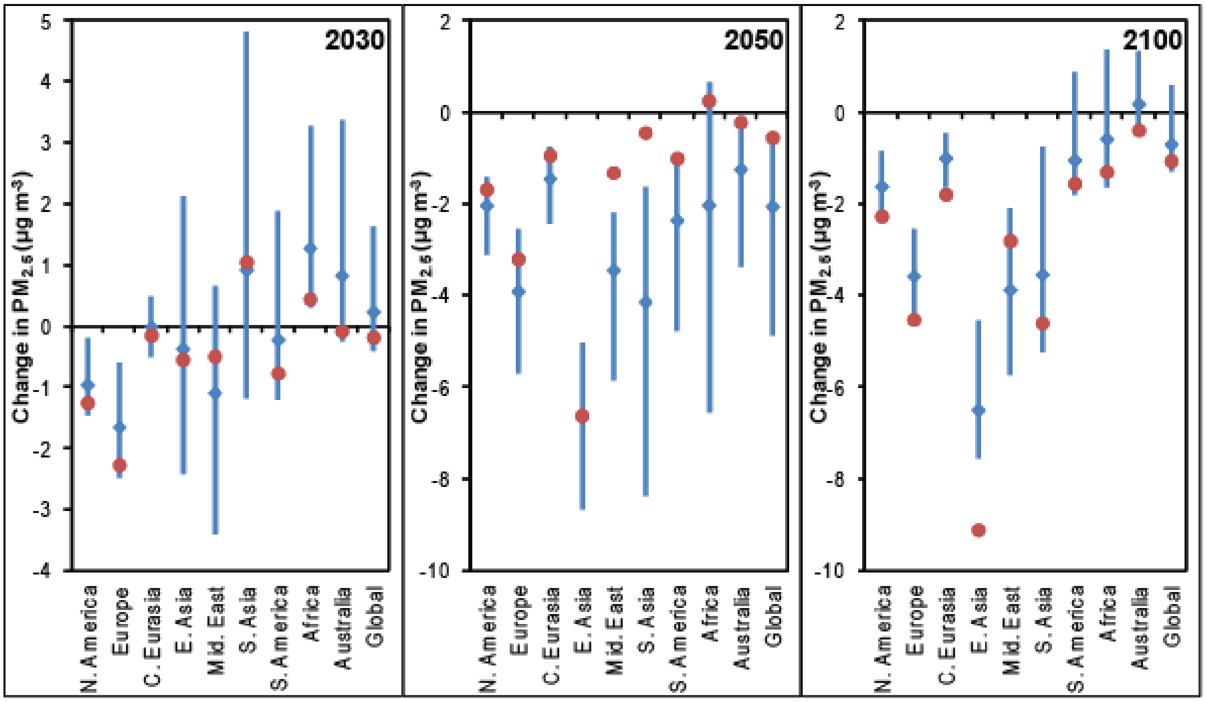

Figure S15. As Figure S14 but for $PM_{2.5}$ estimated as a sum of species (BC+OA+SOA+SO4+NO3+NH4+0.25*SeaSalt+0.1*Dust, this formula was modified for individual models based on differences in how results were reported), following Fiore et al.[24], for the average and range of 5 ACCMIP models in 2030 and 2100, and 3 models in 2050.

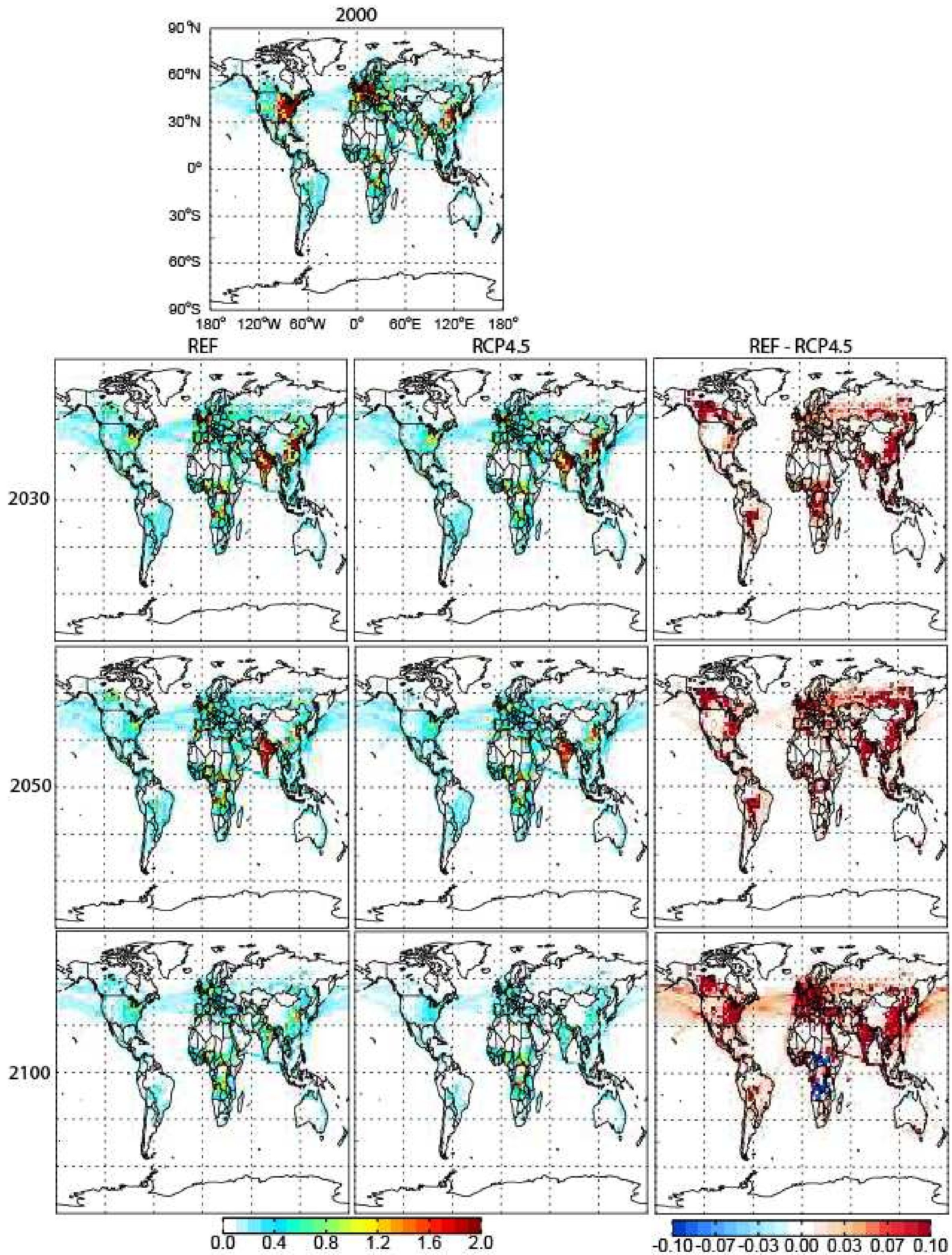

Figure S16. Emissions of NO_x (as NO, in tons yr^{-1} km^{-2}) in 2000, and in 2030, 2050 and 2100 under the REF and RCP4.5 scenarios, and the difference between the REF and RCP4.5 scenarios (red indicates that RCP4.5 has lower emission than REF).

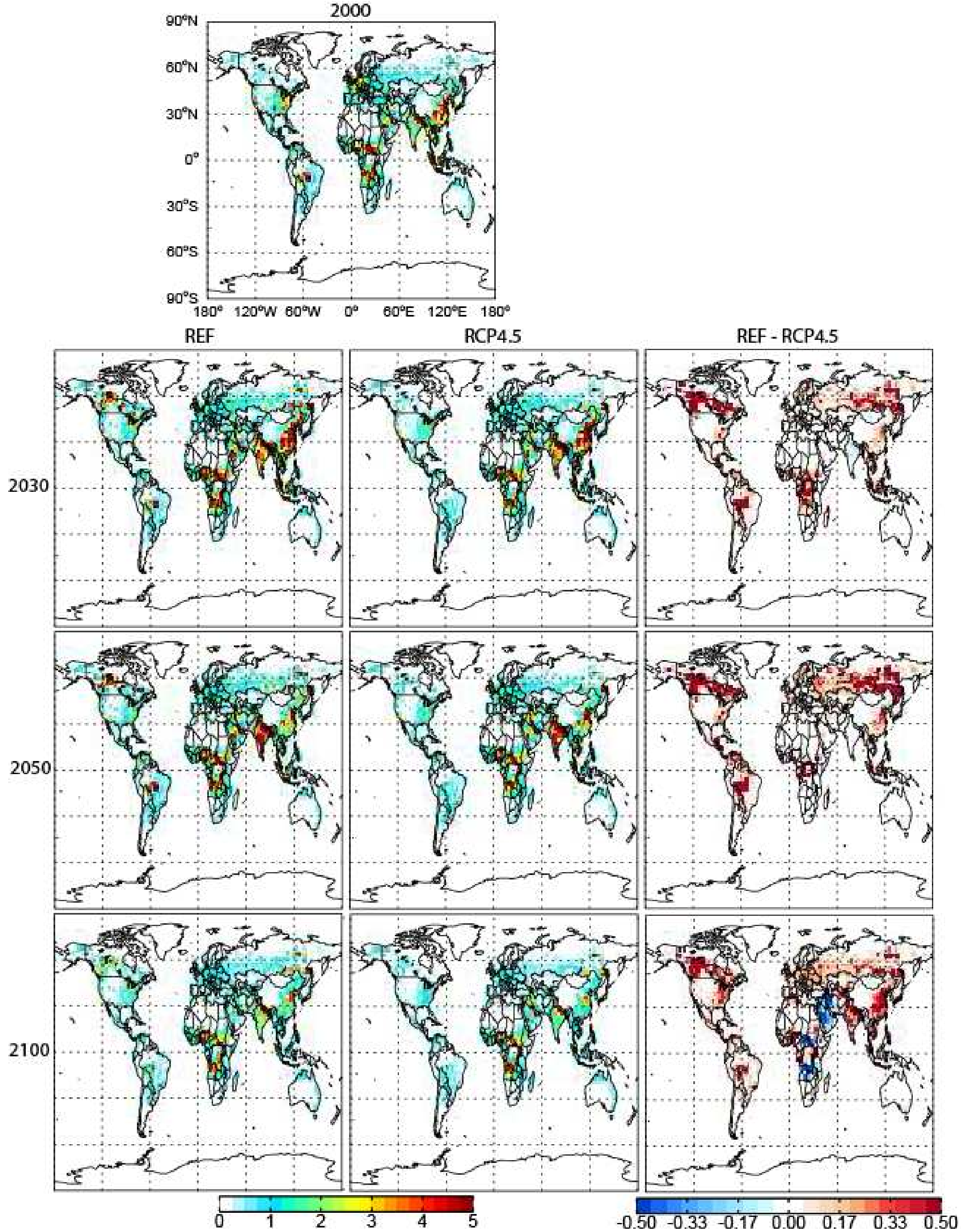

Figure S17. Emissions of NMVOCs (in tons yr^{-1} km^{-2}) in 2000, and in 2030, 2050 and 2100 under the REF and RCP4.5 scenarios, and the difference between the REF and RCP4.5 scenarios (red indicates that RCP4.5 has lower emission than REF).

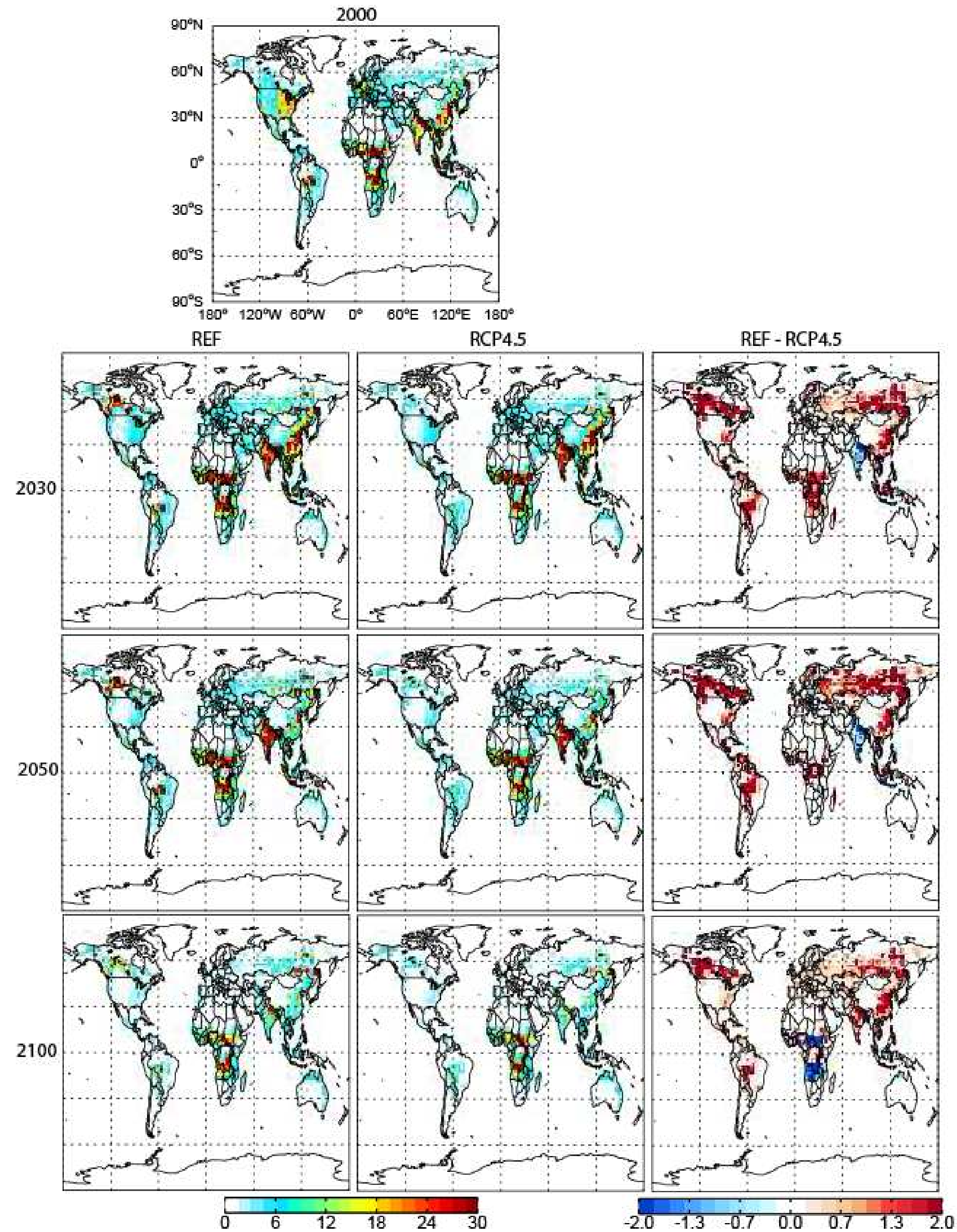

Figure S18. Emissions of CO (in tons yr^{-1} km^{-2}) in 2000, and in 2030, 2050 and 2100 under the REF and RCP4.5 scenarios, and the difference between the REF and RCP4.5 scenarios (red indicates that RCP4.5 has lower emission than REF).

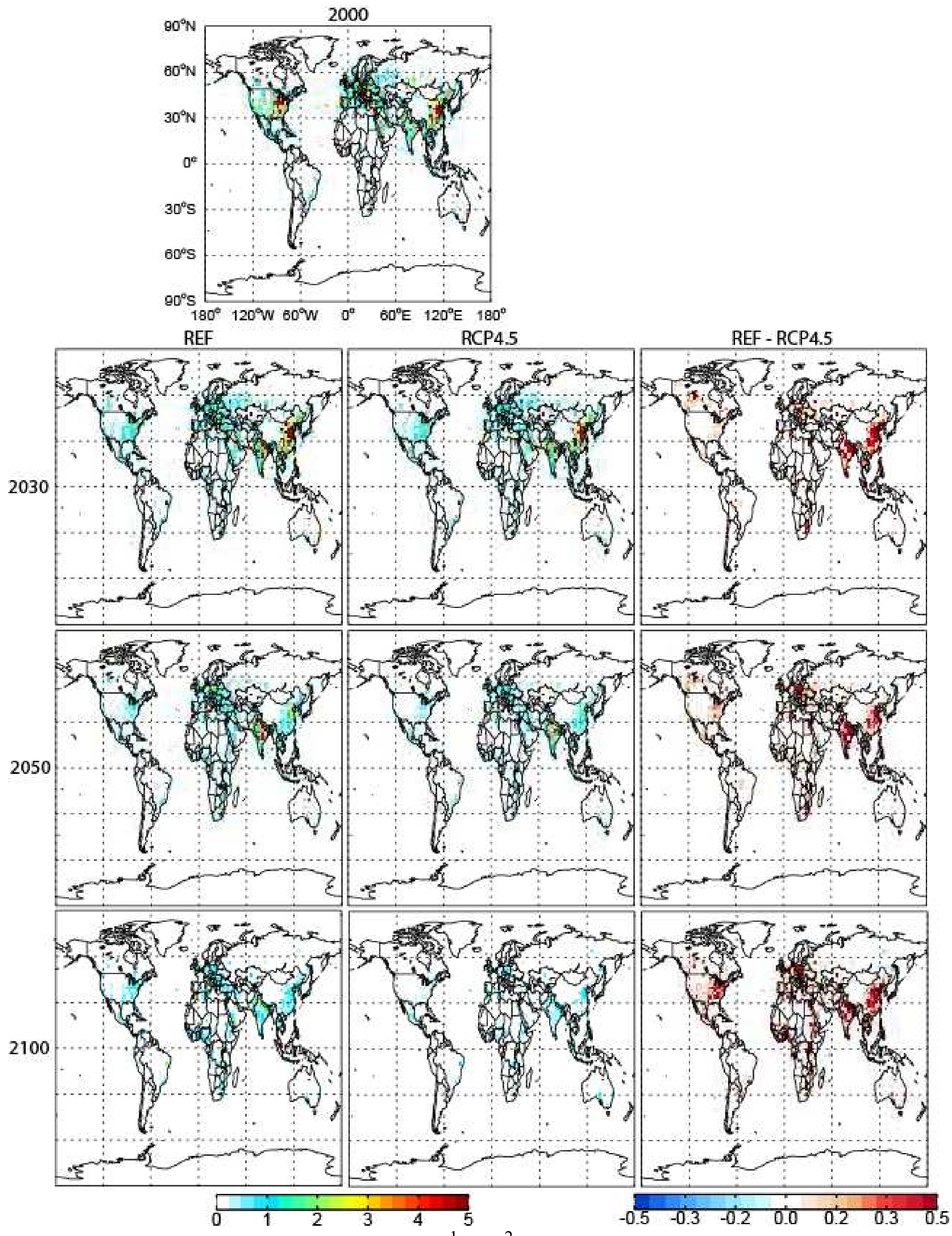

Figure S19. Emissions of SO_2 (in tons yr^{-1} km^{-2}) in 2000, and in 2030, 2050 and 2100 under the REF and RCP4.5 scenarios, and the difference between the REF and RCP4.5 scenarios (red indicates that RCP4.5 has lower emission than REF).

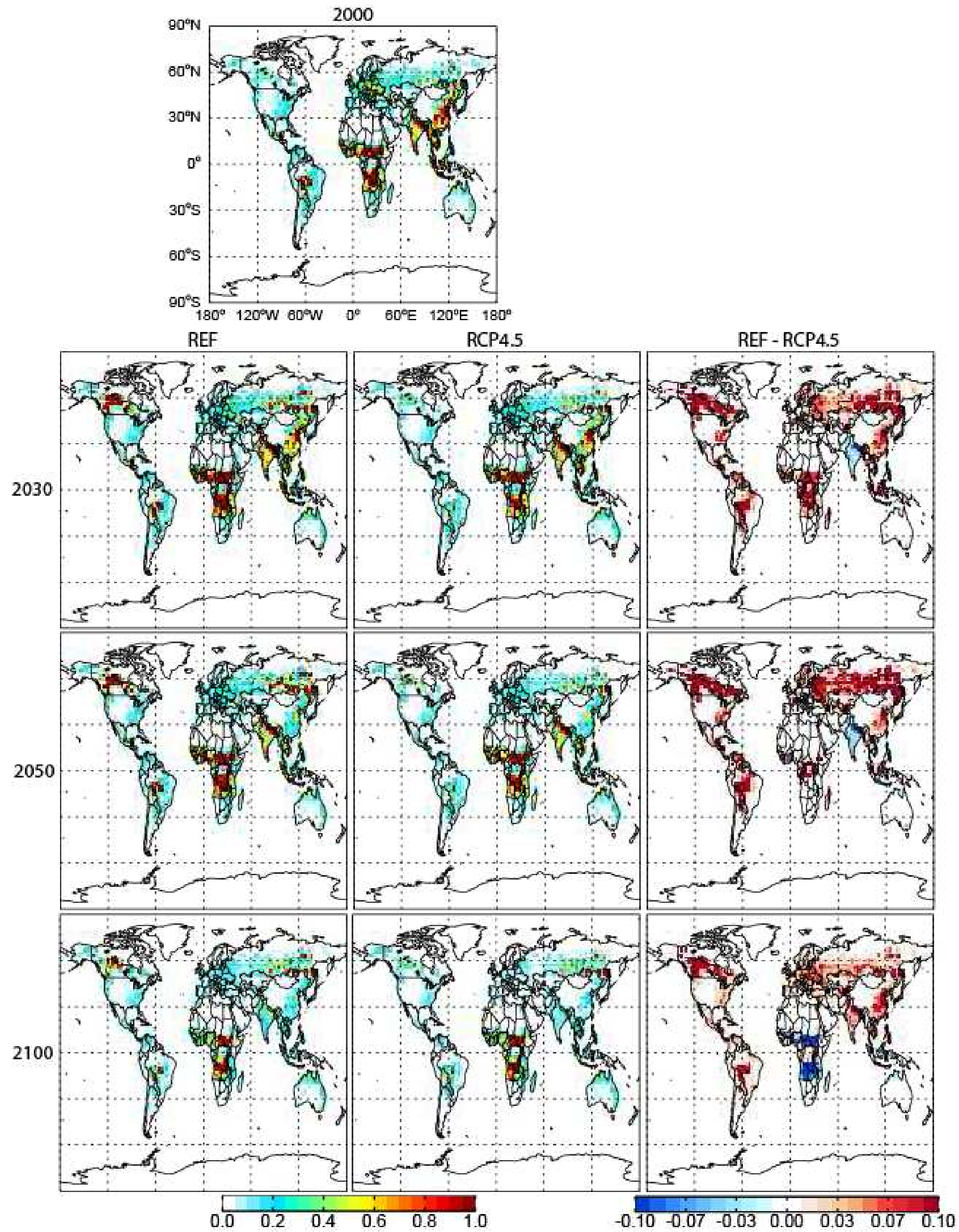

Figure S20. Emissions of OC (in tons yr^{-1} km^{-2}) in 2000, and in 2030, 2050 and 2100 under the REF and RCP4.5 scenarios, and the difference between the REF and RCP4.5 scenarios (red indicates that RCP4.5 has lower emission than REF).

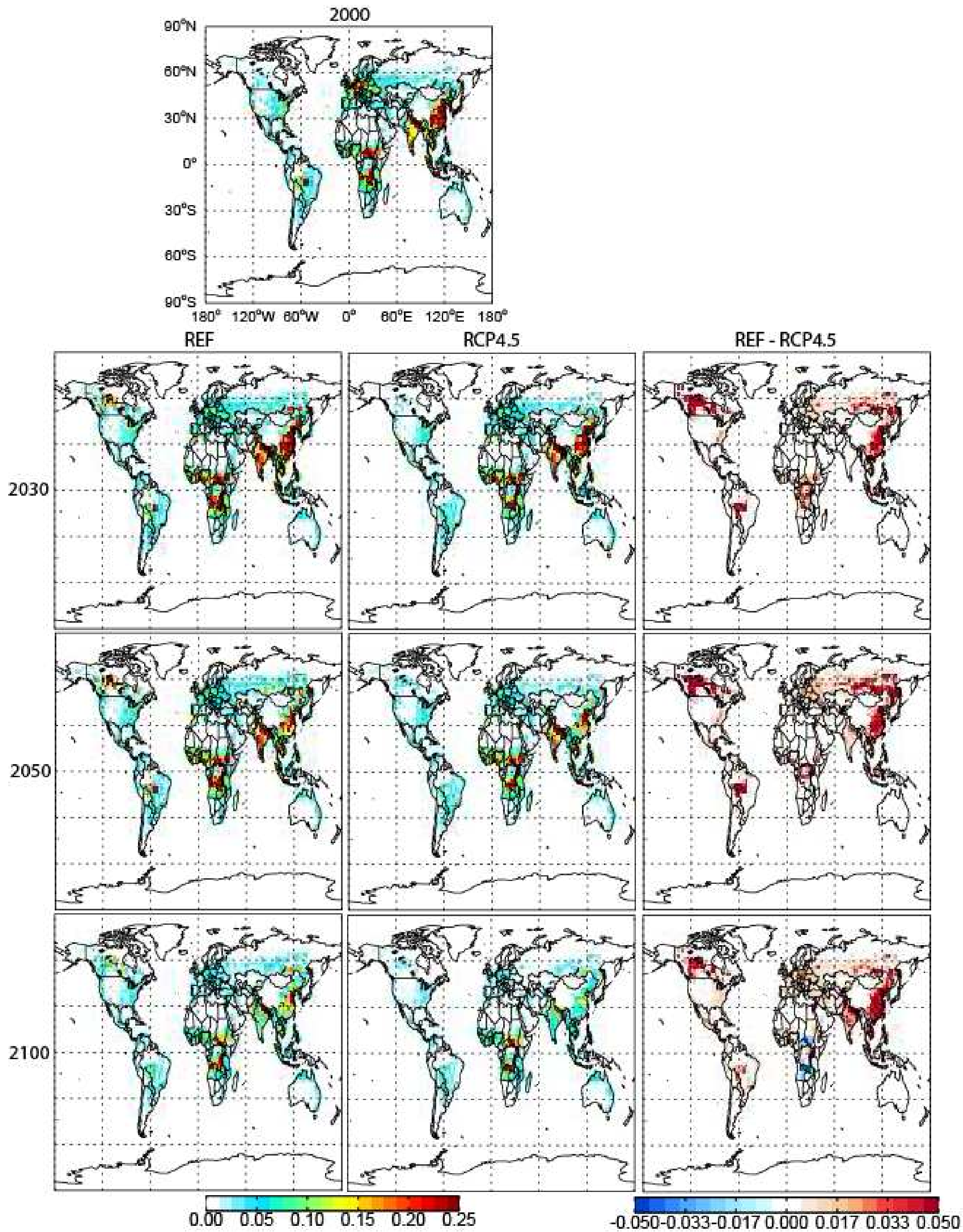

Figure S21. Emissions of BC (in tons yr^{-1} km^{-2}) in 2000, and in 2030, 2050 and 2100 under the REF and RCP4.5 scenarios, and the difference between the REF and RCP4.5 scenarios (red indicates that RCP4.5 has lower emission than REF).

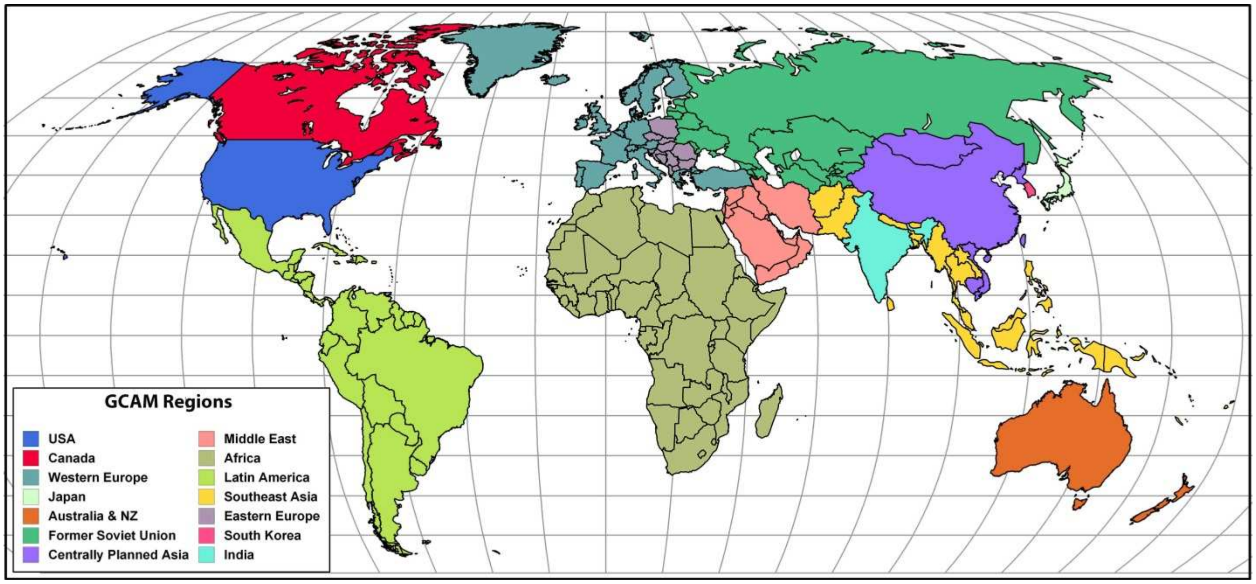

Figure S22. 14 world regions used in the GCAM model and used here to present results for air pollutant concentrations and premature mortality.

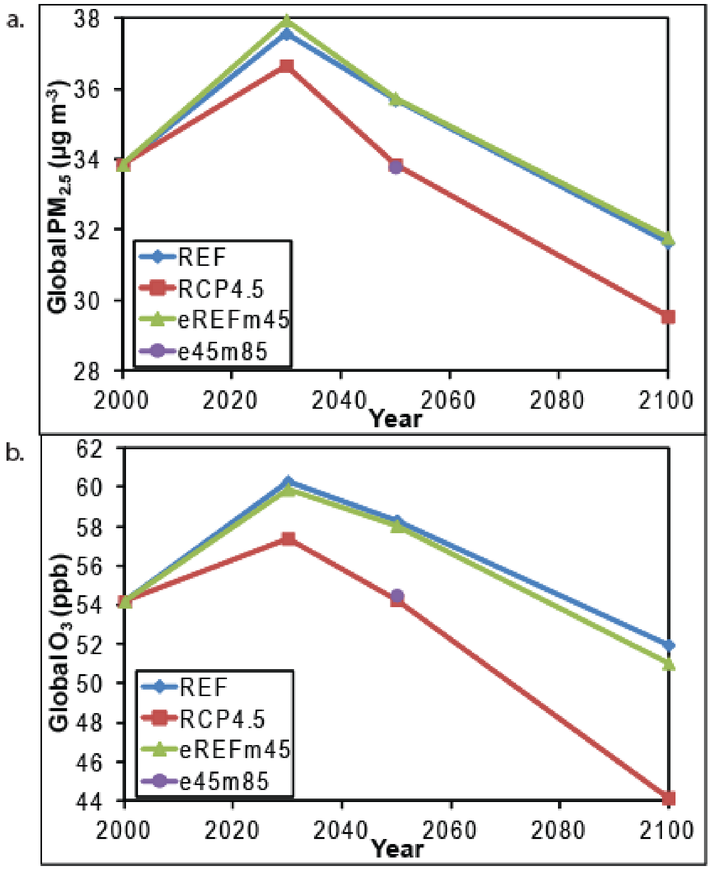

Figure S23. As Figure 1 of the main paper, but including e45m85 in 2050.

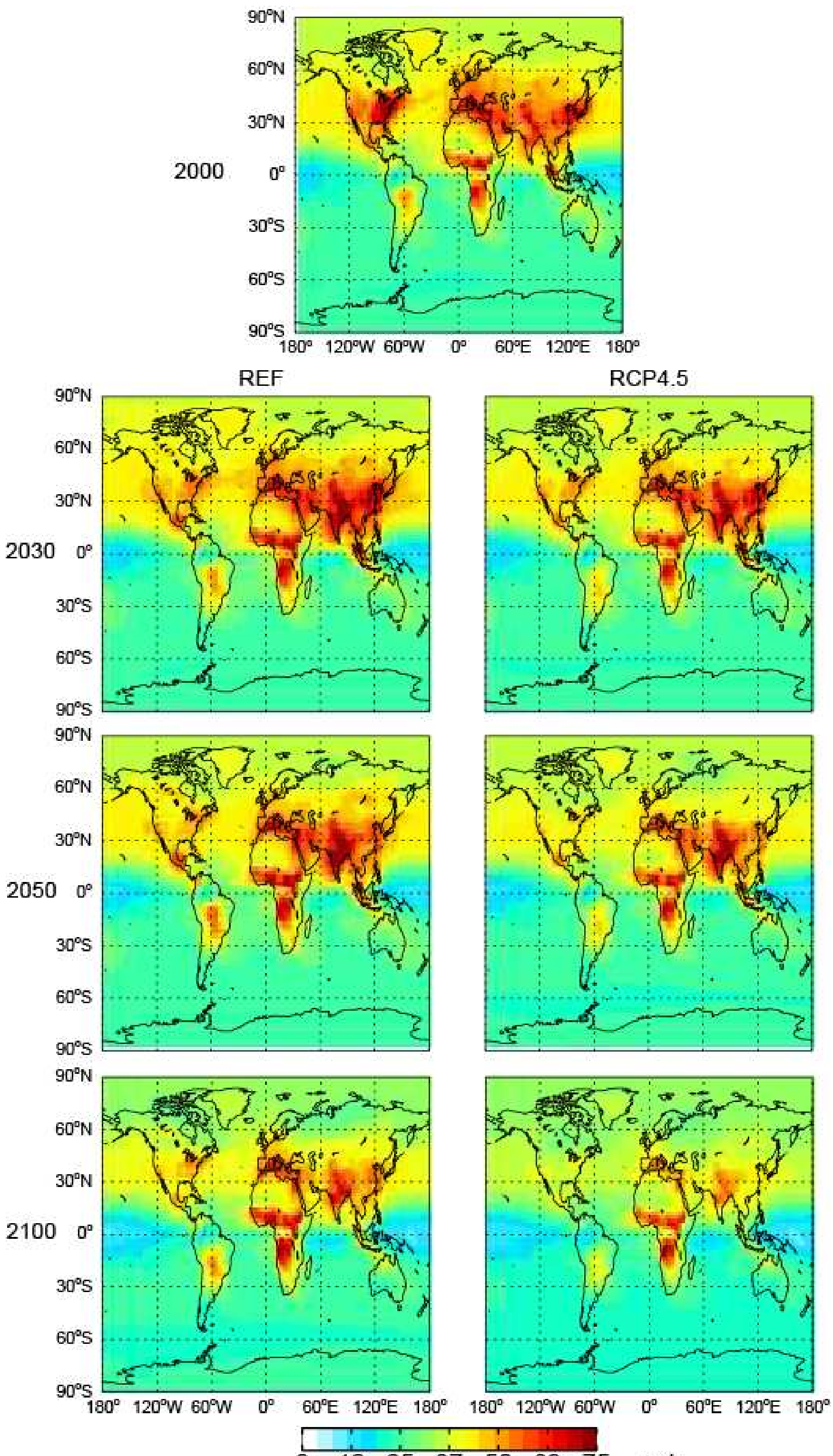

Figure S24. Modeled ozone concentrations (ppbv), for the six-month ozone season average of 1-hr. daily maximum ozone, in 2000, and in 2030, 2050, and 2100 for the REF and RCP4.5 scenarios.

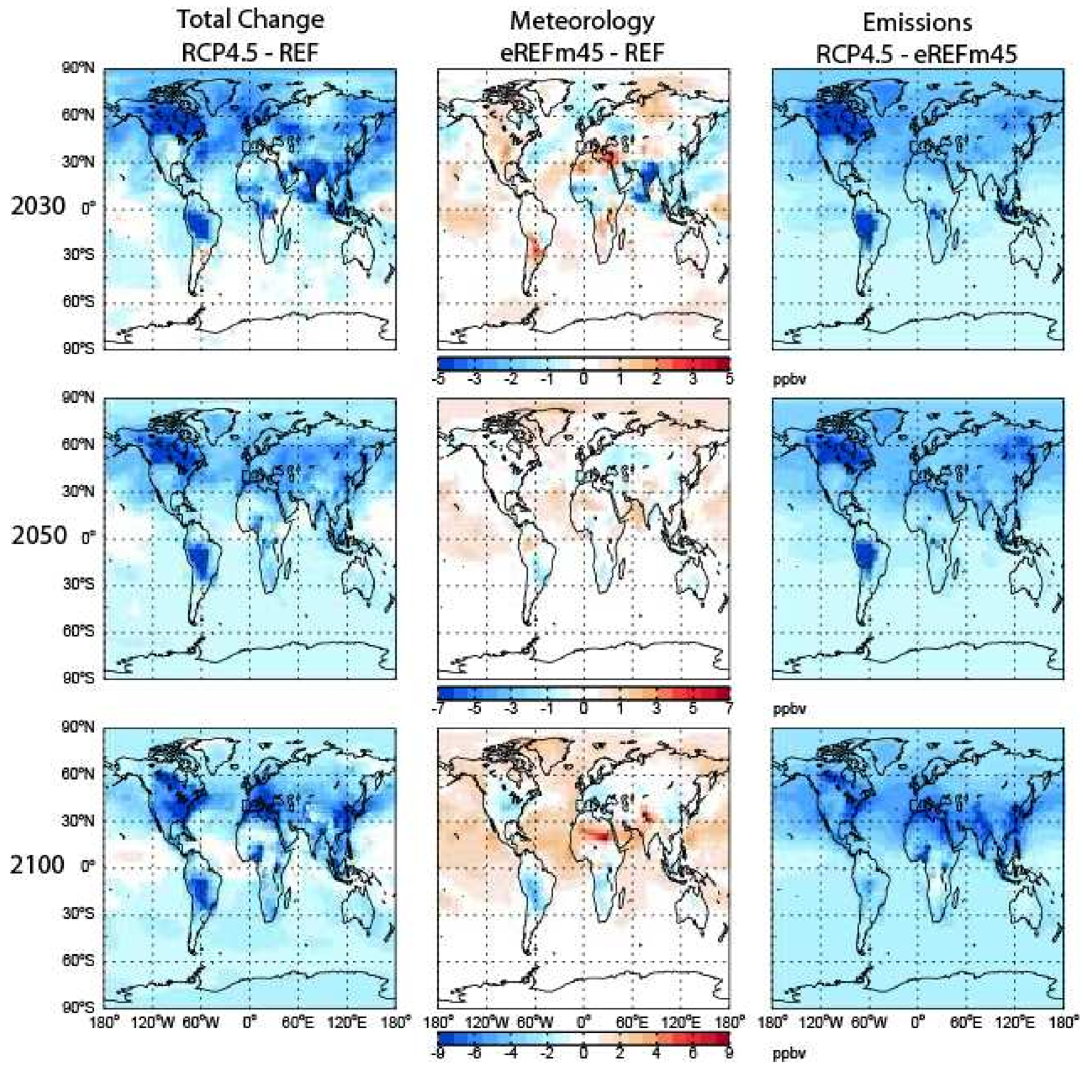

Figure S25. Ozone concentration change resulting as from the GHG emission reductions in RCP4.5, for the 6-month ozone season average of 1-hr. daily maximum ozone. Results are shown for the total ozone change (left, RCP4.5-REF), the change resulting from slowing climate change (center, eREFm45-REF), and the change from co-emitted air pollutants (right, RCP4.5-eREFm45), in 2030, 2050, and 2100. Note that different scales are used in different years. Results for 2100 are also shown in Figure 2 of the main paper.

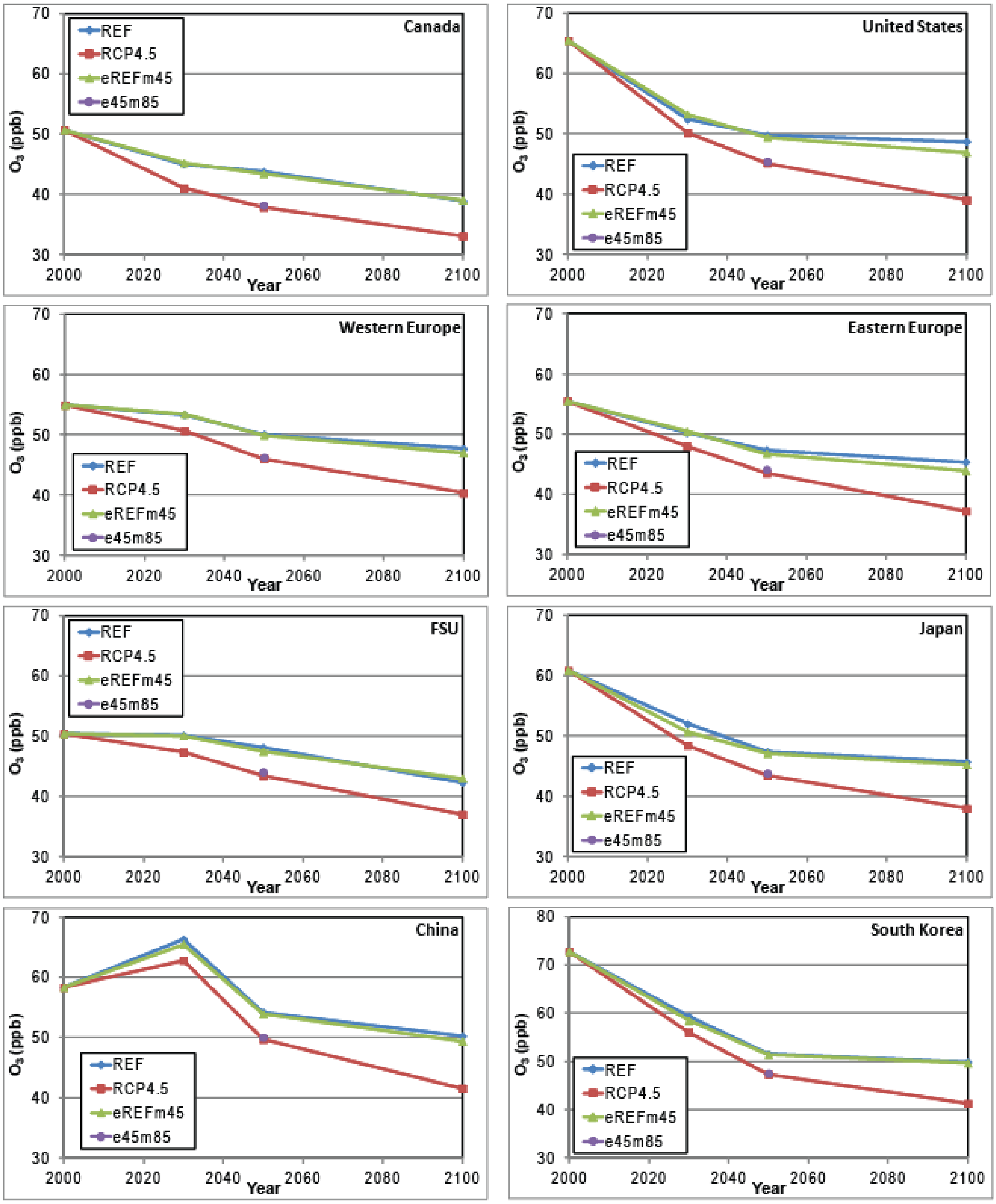

Figure S26. Regional population-weighted ozone concentrations for 4 scenarios, and for the 6-month ozone season average of 1-hr. daily maximum ozone.

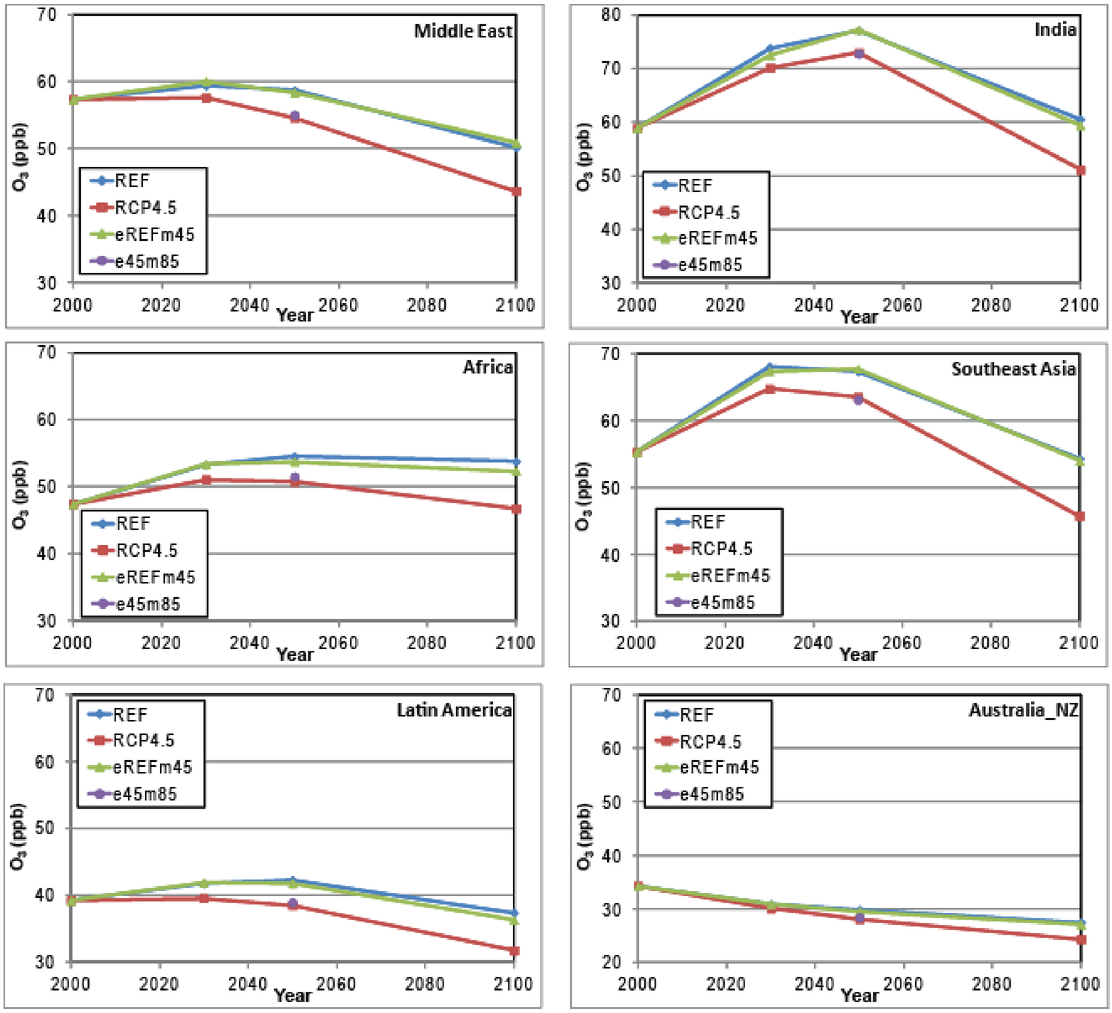

Figure S26. continued

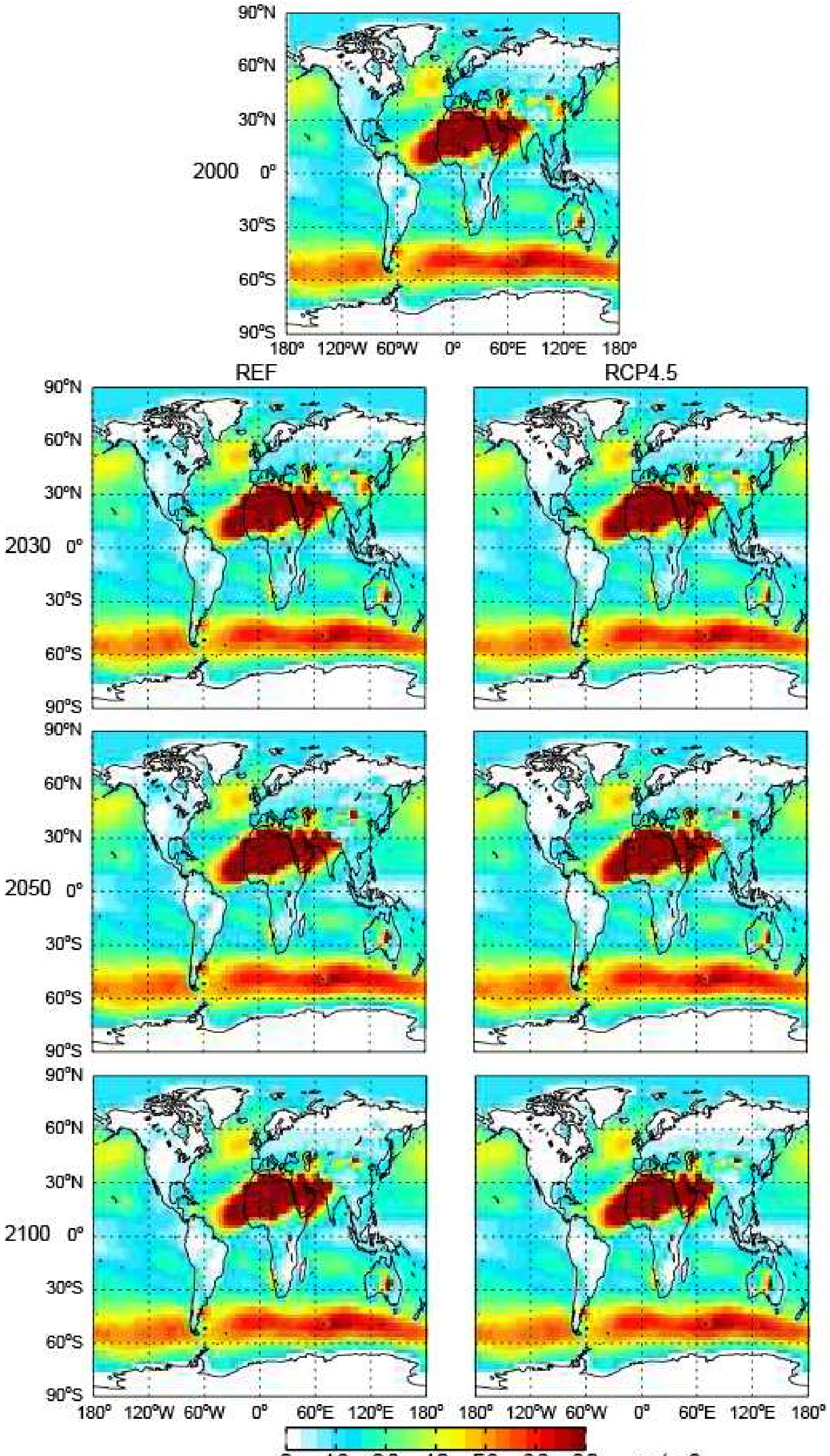

Figure S27. Modeled annual average $PM_{2.5}$ concentrations ($\mu g\ m^{-3}$), in 2000, and in 2030, 2050, and 2100 for the REF and RCP4.5 scenarios.

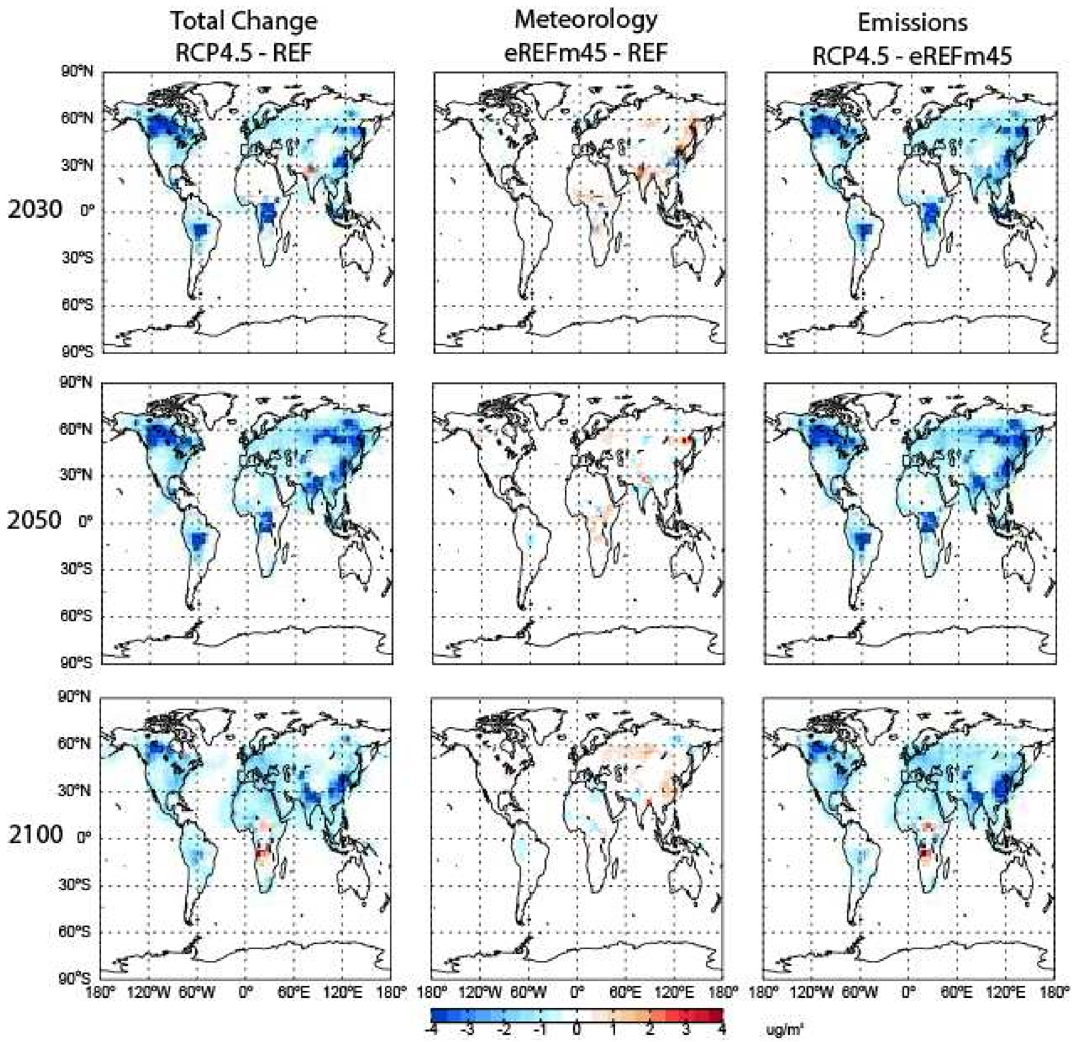

Figure S28. Annual average $PM_{2.5}$ concentration change resulting as from the GHG emission reductions in RCP4.5. Results are shown for the total ozone change (left, RCP4.5-REF), the change resulting from slowing climate change (center, eREFm45-REF), and the change from co-emitted air pollutants (right, RCP4.5- eREFm45), in 2030, 2050, and 2100. Results for 2100 are also shown in Figure 2 of the main paper.

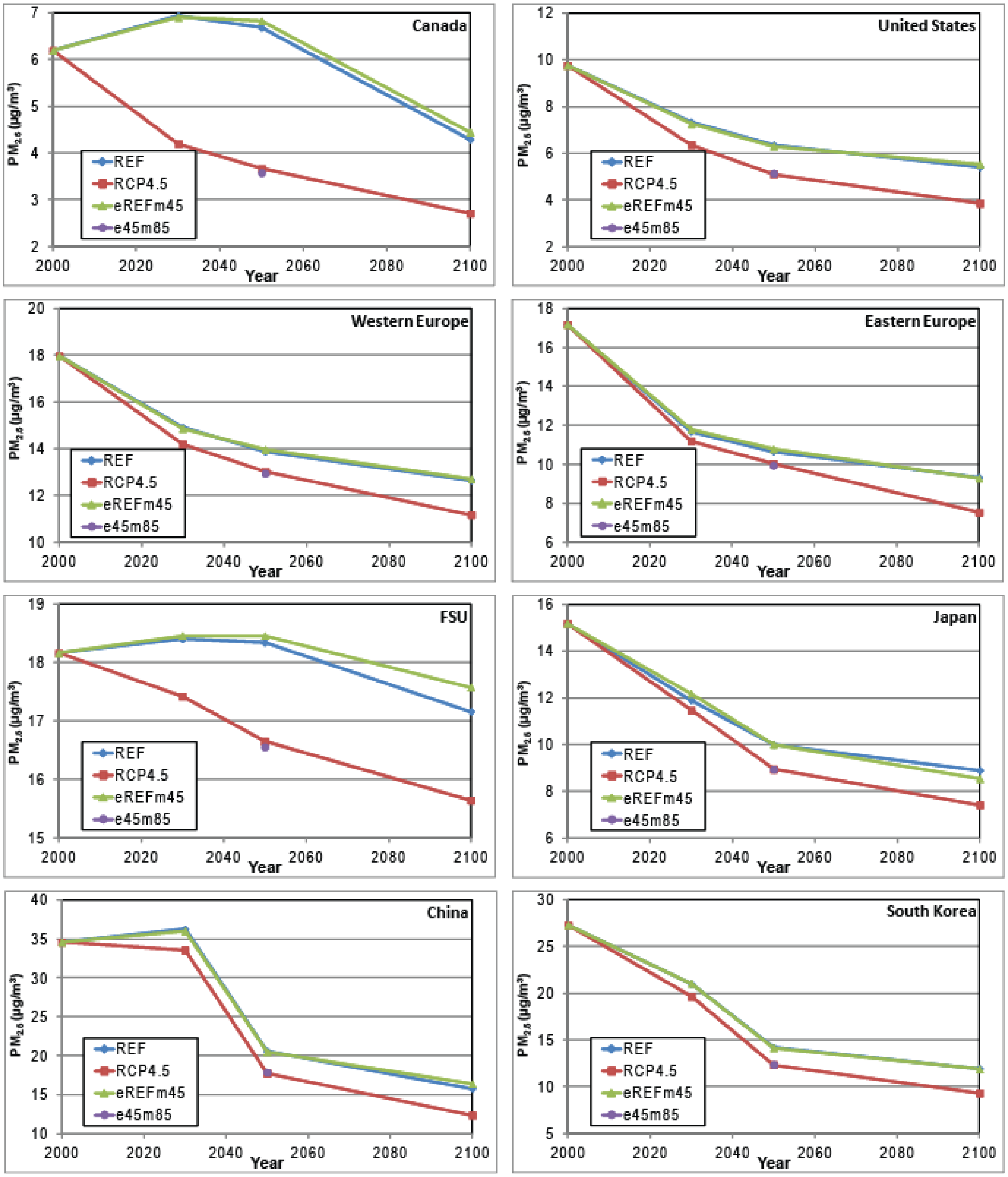

Figure S29. Regional population-weighted $PM_{2.5}$ concentrations for 4 scenarios, and for the annual average $PM_{2.5}$.

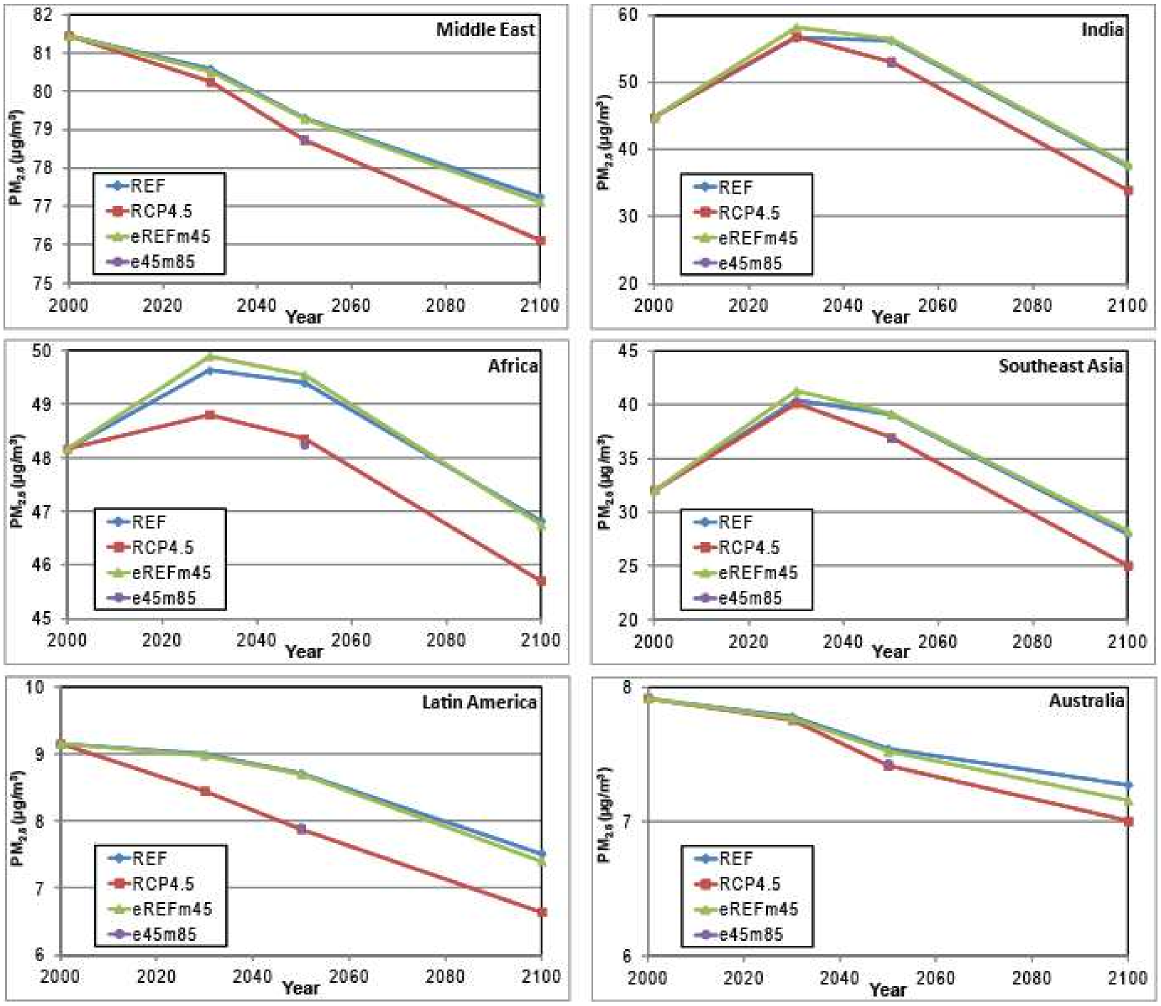

Figure S29. continued

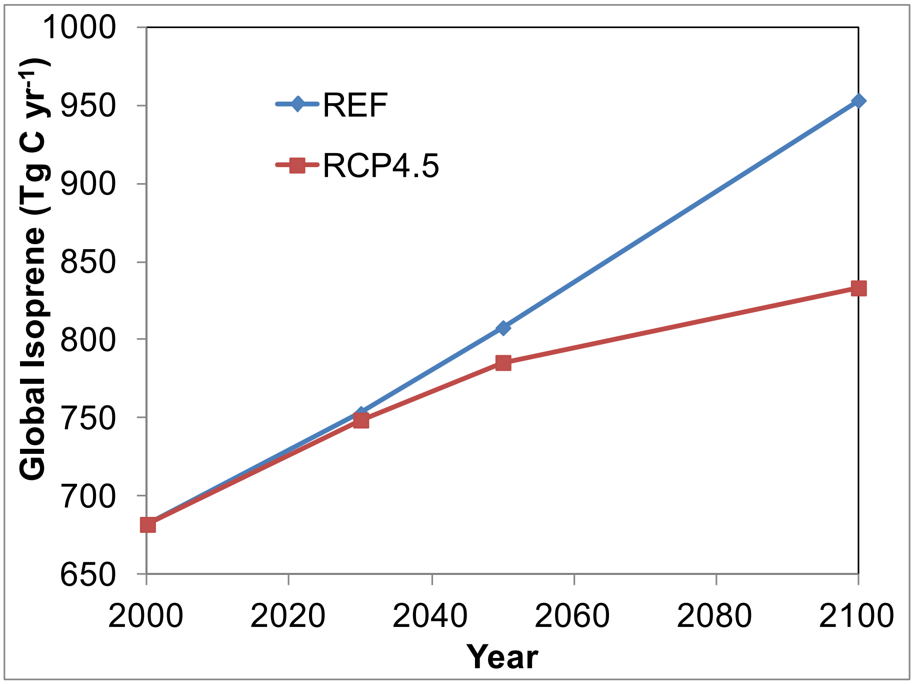

Figure S30. Global emissions of isoprene responding to changes in climate in REF (driven by RCP8.5 meteorology) and RCP4.5.

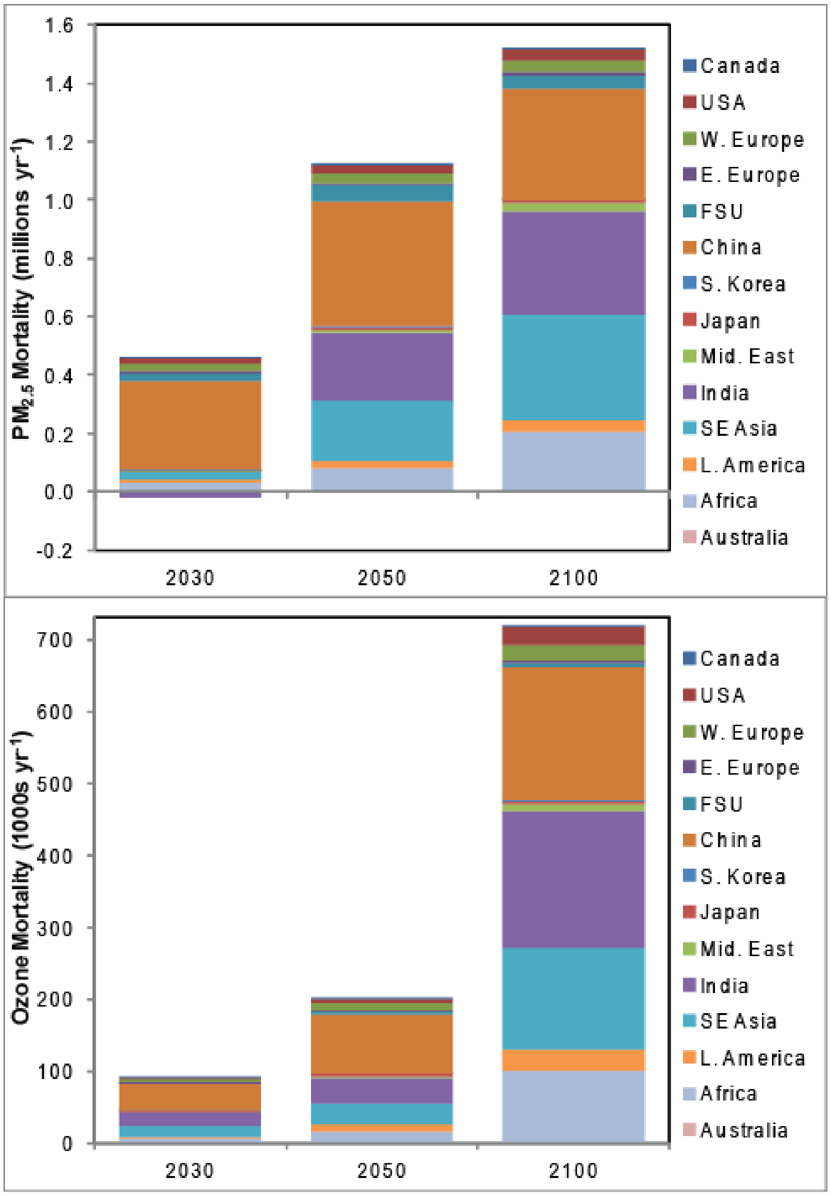

Figure S31. Co-benefit of GHG mitigation (REF relative to RCP4.5) on reduced premature mortality from $PM_{2.5}$ (cardiopulmonary and lung cancer) and ozone (respiratory), among 14 world regions from GCAM.

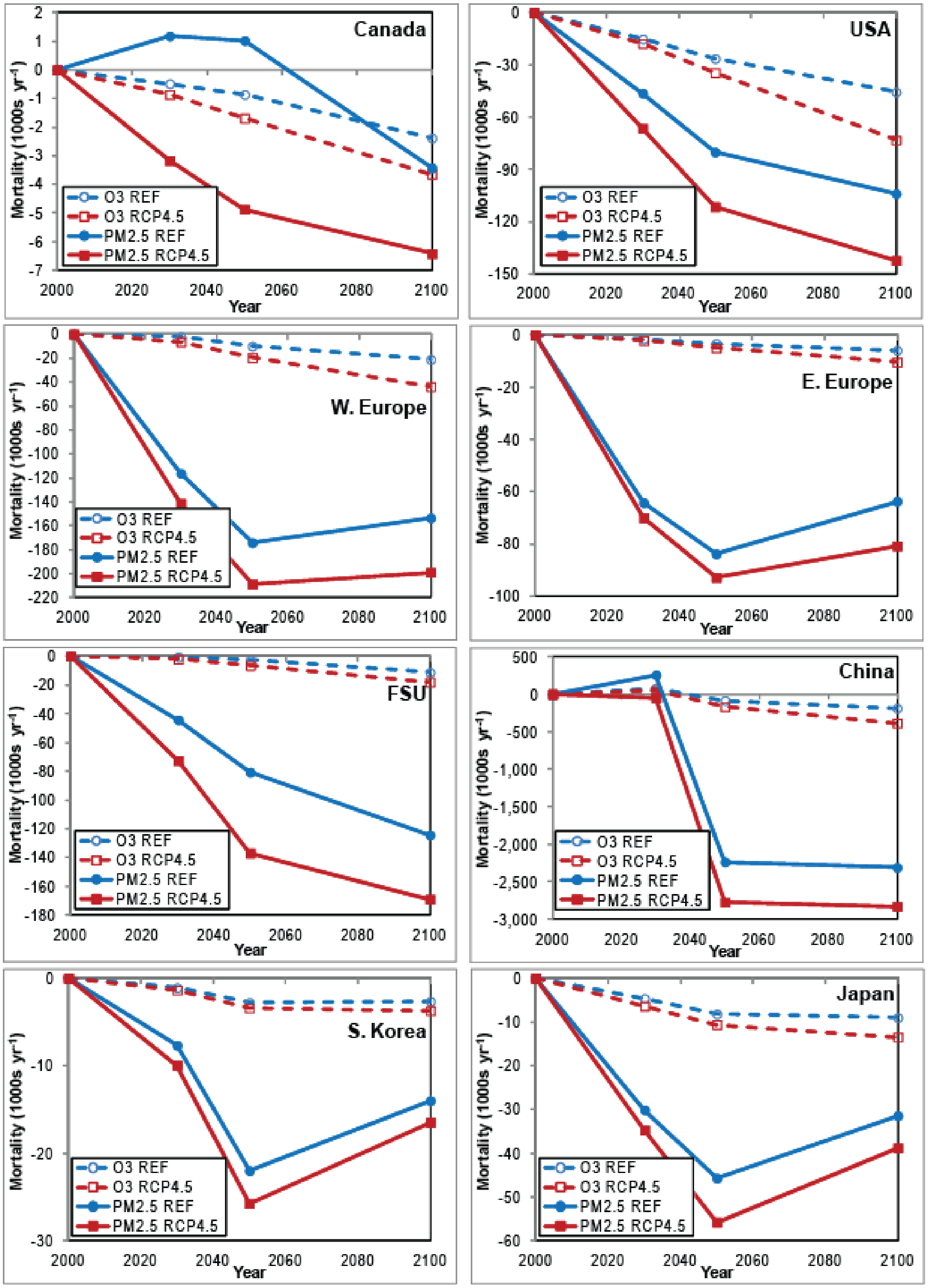

Figure S32. Premature mortality attributed to changes in ozone (respiratory) and $PM_{2.5}$ (cardiopulmonary and lung cancer) in each region. Mortality is evaluated for changes in concentration with respect to year 2000. The global mortality and 5 regions from this figure are presented in Figure 3 of the main paper.

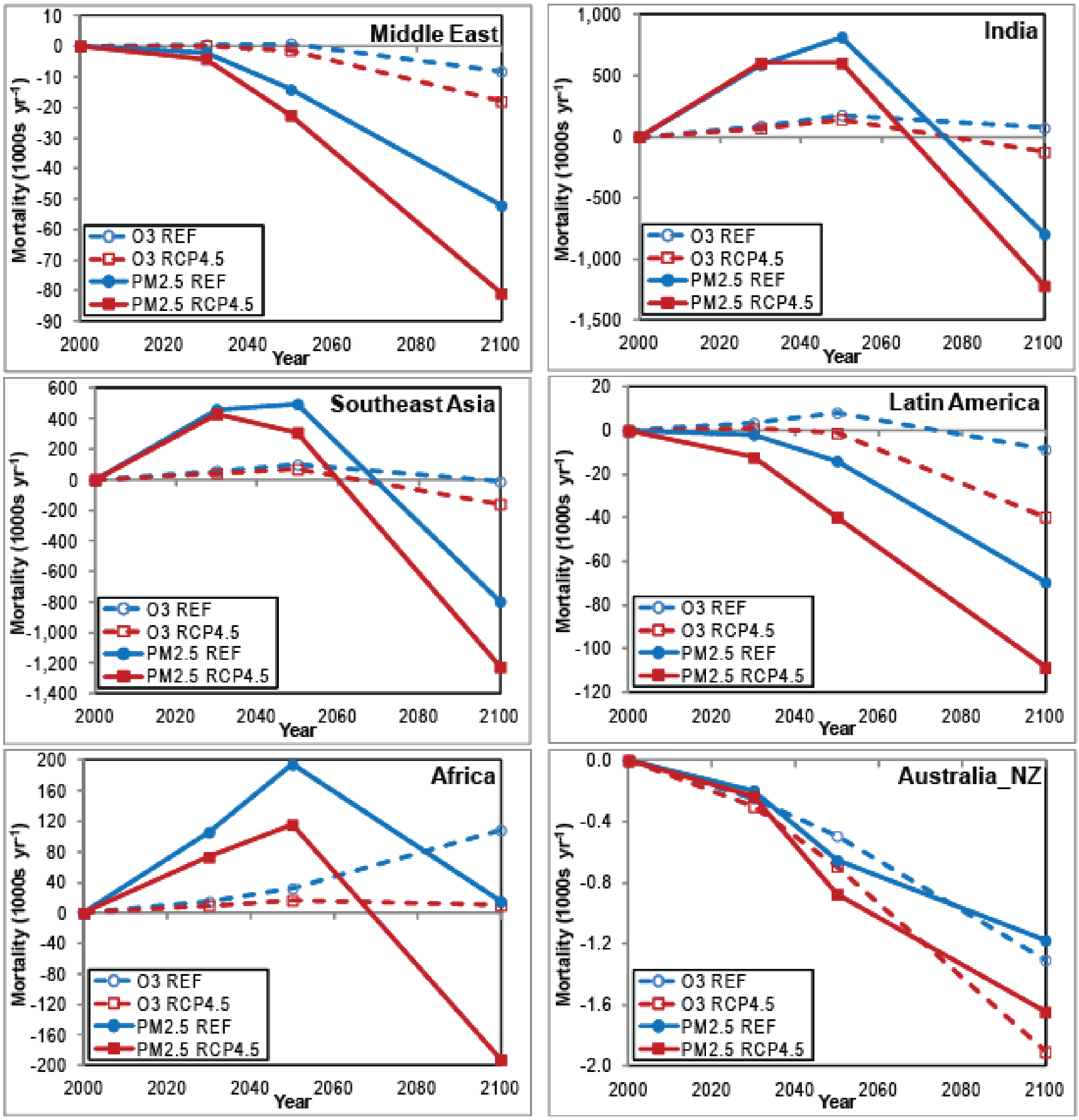

Figure S32. continued.

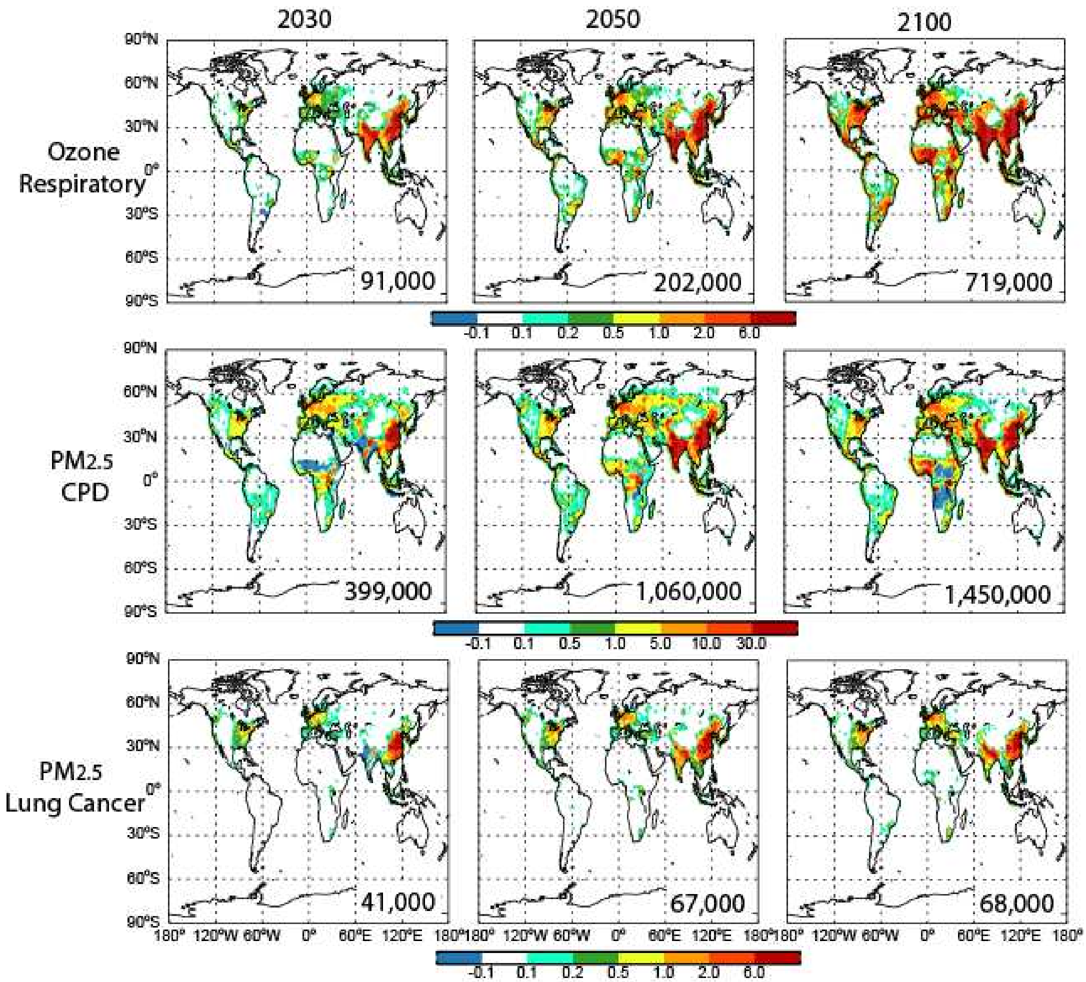

Figure S33. Avoided mortality from the co-benefits of GHG mitigation (REF minus RCP4.5) in deaths per year per 1000 km^2, for ozone respiratory, $PM_{2.5}$ cardiopulmonary disease (CPD), and $PM_{2.5}$ lung cancer. Note that $PM_{2.5}$ CPD has a different color scale. Global total premature deaths in each year shown are in the bottom right of each panel. The sum of ozone respiratory mortality, $PM_{2.5}$ cardiopulmonary disease (CPD) mortality, and $PM_{2.5}$ lung cancer mortality gives the total mortality plotted in Figure 4 of the main paper.

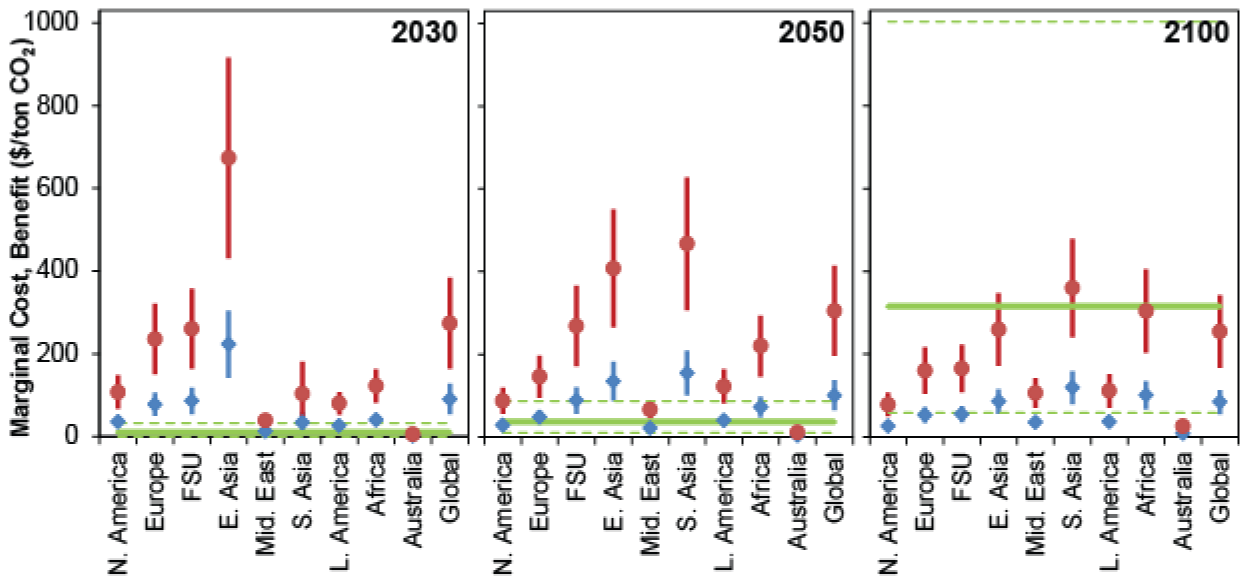

Figure S34. As Figure 5 of the main paper, but using a globally uniform VSL in each year.